DOCTORAATSPROEFSCHRIFT

2007 | Faculteit Wetenschappen

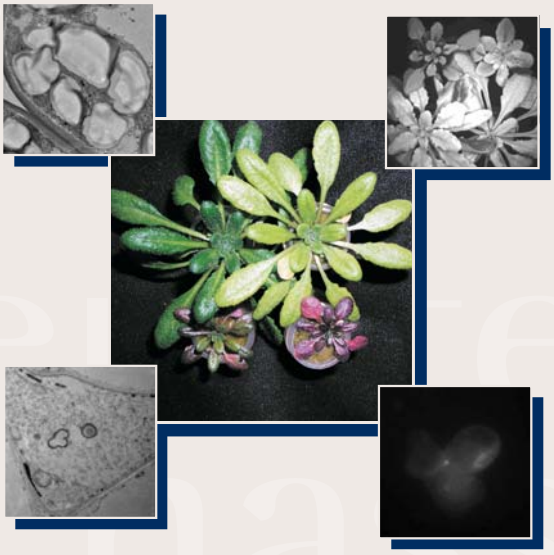

Cadmium responses in *Arabidopsis thaliana*: a study focusing on subcellular localization, effects on the cellular ultrastructure and photosynthesis in relation to oxidative stress

Proefschrift voorgelegd tot het behalen van de graad van
Doctor in de Wetenschappen, richting Biologie, te verdedigen door:

Frank VAN BELLEGHEM

Promotor: prof. dr. R. Valcke
Copromotor: dr. Ann Cuypers

universiteit hasselt
CENTRUM
VOOR MILIEUKUNDE

DOCTORAATSPROEFSCHRIFT

2007 | Faculteit Wetenschappen

Cadmium responses in *Arabidopsis thaliana*: a study focusing on subcellular localization, effects on the cellular ultrastructure and photosynthesis in relation to oxidative stress

Proefschrift voorgelegd tot het behalen van de graad van
Doctor in de Wetenschappen, richting Biologie, te verdedigen door:

Frank VAN BELLEGHEM

Promotor: prof. dr. R. Valcke
Copromotor: dr. Ann Cuypers

universiteit hasselt
CENTRUM
VOOR MILIEUKUNDE

D/2007/2451/26

PhD thesis presented on the 29th of May 2007 at Hasselt University

Members of the Jury

Prof. dr. E. Nauwelaerts, Universiteit Hasselt, Diepenbeek, BELGIUM, Chair
Prof. dr. R. Valcke, Universiteit Hasselt, Diepenbeek, BELGIUM, Promotor
Dr. A. Cuypers, Universiteit Hasselt, Diepenbeek, BELGIUM, Co-promotor
Prof. dr. J. Vangronsveld, Universiteit Hasselt, Diepenbeek, BELGIUM
Prof. dr. F. Franck, Université de Liège, Liège, BELGIUM
Prof. dr. Y. Guisez, Universiteit Antwerpen, Antwerpen, BELGIUM
Dr. É. Hideg, University of Szeged, Szeged, HUNGARY
Dr. M. Wójcik, Maria Curie-Sklodowska University, Lublin, POLAND
Dr. M. Ciscato, Hoeilaart, BELGIUM

Discovery consists of seeing what everyone else has seen and thinking what no-one else has thought.

Albert von Szent-Györgyi (1893-1986)
The Hungarian scientist who noted the anti-scorbutic activity of ascorbic acid and discovered that paprika (*Capsicum annuum*) was a rich source of vitamin C (Nobel Prize in 1937).

Woord vooraf

Met dit werk is niets minder dan een droom in vervulling is gegaan. Toen ik als groentje in 1996 aan de Onderzoeksgroep Dierkunde begon te werken had ik nog weinig besef van wetenschappelijk onderzoek. Daar kwam snel verandering in toen ik werd ingeschakeld in het onderzoek van lic. Mischa Indeherberg naar de toxiciteit van zware metalen op de platworm *Polycelis tenuis*. Ik had de microbe te pakken en wou zelf aan de slag, alleen moest ik nog een academisch diploma behalen. Daarvoor ben ik gaan aankloppen bij de Open Universiteit Nederland en mede door de flexibiliteit die ik op het voormalige LUC genoot heb ik de opleiding Voeding en Toxicologie in 2003 kunnen afronden. Daarna ben ik kunnen starten met dit doctoraatsonderzoek.

In de eerste plaats wil ik mijn Promotor prof. dr. Roland Valcke bedanken omdat hij mij de mogelijkheid heeft gegeven me te verdiepen in dit onderzoeksdomein en me heeft ingewijd in de wondere wereld van de chlorofyl *a* fluorescentie en fotosynthese. Daarnaast gaat mijn oprechte dank uit naar mijn Copromotor dr. Ann Cuypers om haar niet aflatende steun in de soms lastige momenten die eigen zijn aan een doctoraat en haar scherpe en kritische kijk op het oxidatieve stress avontuur. Verder wil ik prof. dr. Jaco Vangronsveld bedanken, niet alleen omdat hij mij de nodige plantkundige inzichten heeft bijgebracht omtrent cadmiumtoxiciteit maar ook omdat hij als steunpilaar van het CMK voor mij al vele jaren een vaste waarde is. Ook wil ik prof. dr. Emmy Van Kerkhove bedanken voor het kritisch luisteren en meedenken tijdens de BOF-meetings en voor het verzorgen van de contacten met dr. Andreas Ziegler. Eveneens wil ik hier dr. Brahim Semane en dr. Sandy Thijssen vermelden, die als companen in het groot BOF-project, in hetzelfde schuitje zaten.

Ik heb tijdens dit onderzoek het geluk gehad met heel wat mensen te mogen samen werken. Ik wil vooreerst Natascha Steffani bedanken voor het minutieus prepareren van de elektronenmicroscopische coupes. Verder ben ik Myriam Claeys van de Universiteit Gent dankbaar voor het deskundig cryofixeren en cryosubstitueren van het weefsel en prof. dr. Gaetan Borgonie omdat ik van deze faciliteiten gebruik mocht maken. Dr. Jan d' Haen heeft mij de kneepjes van de elektronenmicroscopie bijgebracht en mij de tijd en de ruimte op het IMO geboden om dit monnikenwerk tot een goed einde te brengen. Tevens wil ik

Dany Polus bedanken voor de technische assistentie. Em. prof. dr. Herman Clijsters ben ik erkentelijk voor het kritisch nalezen van de allereerste versie van het lokalisatieartikel.

Ik wil dra. Karen Smeets hartelijk bedanken voor haar onmisbare inbreng in de genexpressie-analyse, al moest ik daarvoor af en toe rondspattende koffie ontwijken. Ook heb ik kunnen rekenen op dra. Kelly Opdenakker, Ing. Carine Put en Ann Wijgaerts voor het verwerken en analyseren van de stalen. Dr. Lieve Quanten, dra. Michelle Plusquin en dr. Ann Ruttens waren een grote steun bij de statistische analyse met SAS.

I am very grateful to dr. Éva Hideg, for letting me work and develop the singlet oxygen detection method with fluorescent probe DanePy at her lab at the Biological Research Centre in Szeged, Hungary. It was both a very useful and pleasant stay. Ook wil ik dr. Nele Horemans en dr. Tine Raeymaekers van de Universiteit Antwerpen bedanken voor het ter beschikking stellen van de *Arabidopis thaliana* celcultuur en het geven van de o zo belangrijke 'insider' informatie. Greet Clerx wil ik bedanken voor het in leven houden van diezelfde celcultuur en voor het assisteren bij de pigment analyse. Martin Van De Ven wil ik bedanken voor het assisteren bij de opnamen met de fluorescentiemicroscoop. I would like to thank prof. dr. Fabrice Franck from the Université de Liège for the HPLC pigment analysis and for being a member of the Jury. Many thanks to dr. Massimo Ciscato for solving software problems on the Fluorescence Imaging System and also for being a member of the Jury. Thanks also go out to prof. dr Yves Guisez and dr. Malgorzata Wójick for being a member of the Jury and to prof. dr. Erna Nauwelaerts, for being the Chair of the Jury.

Van de Onderzoeksgroep Dierkunde wil ik em. prof. dr. Ernest R. Schockaert bedanken voor zijn goede raad en prof. dr. Tom Artois omdat ik in zijn lab alle faciliteiten mocht gebruiken en voor onze jarenlange vriendschap.

Verder wil ik alle medewerkers en studenten van diverse pluimage bij de 'Biologie' bedanken voor de prettige sfeer.

Mijn schoonouders, dr. Michel Asperges en lic. Maria Van den Wijngaert, wil ik bedanken voor hun plantkundige advies en om altijd klaar te staan voor om het even wat.

Ma, bedankt omdat je me altijd hebt gesteund in alles wat ik deed, ook was dat niet altijd evident.

Tenslotte wil ik mijn vrouwtje Els bedanken voor al die jaren geduld zowel bij tijdens de studie bij de OU als bij het doctoraat, we hebben heel wat in te halen. Pieter en Joris, omdat het zo'n fantastische kereltjes zijn, opgewekt en vol levenslust. En, Ja, ja Pieter, ik heb het beloofd, als ik klaar ben gaan we naar de dierentuin….

Summary

Cadmium (Cd), which is known to be very toxic to plants, animals and humans, is a relatively rare element. However, since the 19th century, industrial activities have contaminated extensive areas with cadmium, which presents a considerable environmental threat. Also in Belgium there are several locations with Cd contamination. For instance, in the north east of Belgium, an area as large as 280 km^2 has become contaminated with Zn, Cd and Pb, because of the historic presence of several zinc smelters. Cross-sectional population studies in that area have demonstrated a positive correlation between the high Cd concentrations in various crops and an increased body burden, which was further correlated with several clinical symptoms on the kidney and skeleton, and with an increased risk of cancer. In addition, there is the potential danger to animals that depend upon the plants for survival and to the predators feeding on them, which can have a negative influence on the biodiversity. Therefore, fundamental knowledge concerning the sequestration and toxicity of Cd in plants is important to obtain a more complete picture of the impact of Cd on the environment.

The aim of this thesis was to investigate the effects of low to intermediate external Cd concentrations on the wild-type of *Arabidopsis thaliana* (ecotype Columbia), a well-known and intensively used model plant in toxicological studies. In this work, we tried to gain knowledge concerning transport and sequestration of Cd in the root and the leaves, and to investigate the Cd-induced physiological, morphological and photosynthetic effects in relation to oxidative stress. In addition, a fluorimetric method was developed to measure the singlet oxygen production in an *Arabidopsis thaliana* cell culture.

The subcellular cadmium (Cd) localization in roots and leaves, described in **chapter 3**, was performed with energy-dispersive X-ray microanalysis (EDXMA) on high-pressure frozen and freeze-substituted tissues from plants exposed for 21 days to 0, 1, 5 and 50 µM Cd. It was found that in the root cortex, Cd was associated with phosphorus (Cd/P) in the apoplast and sulfur (Cd/S) in the symplast, suggesting phosphate and phytochelatin sequestration, respectively. In the endodermis, sequestration of Cd/S was present as fine granular deposits in the vacuole and as large granular deposits in the remaining cytoplasm. In the central cylinder, symplastic accumulation followed a distinct pattern illustrating the importance of passage cells for the uptake of Cd. In the

apoplast of the pericycle, a shift of Cd/S granular deposits from the middle lamella towards the plasmalemma was observed. Large amounts of precipitated Cd in the phloem suggested retranslocation from the shoot. In leaves, Cd was detected in tracheids but not in the mesophyll tissue. Extensive symplastic and apoplastic sequestration in the root parenchyma combined with retranslocation via the phloem confirmed the excluder strategy of *Arabidopsis thaliana*.

The next part of the thesis was dedicated to the investigation of toxic effects inflicted by Cd on *Arabidopsis thaliana*. Therefore, the Cd-induced effects on the leaf morphology, ultrastructure and physiology, described in **chapter 4**, was studied in relation to the gene expression of ROS producing (LOX1/2 and RBOHD/F/C) and ROS scavenging enzymes (CAT, CuZn-SOD, Fe-SOD and Mn-SOD). Although low to moderate external concentrations were used, this study revealed tremendous inhibitory effects on growth and photosynthetic activity and a decreased water content in plants exposed to Cd. Cd also decreased the cell size of spongy parenchyma cells and changed the cell shape of palisade parenchyma cells. On the ultrastructural level, increasing Cd exposure concentrations resulted in increasingly severe membrane damage. These structural alterations might be attributed to Cd-induced oxidative stress. Nevertheless, application of different Cd concentrations emphasized a different role for the cellular redox state in response to external stress factors. The rise in the foliar H_2O_2 content of 1 µM Cd exposed plants was most likely the result of the induction of NADPH-oxidases and could be designated as a signaling response, most likely in relation with Cd-induced disturbance of the water balance. However, at 1 µM the plant was apparently able to adapt to this mild stress without fully activating the extensive range of antioxidative protection mechanisms. In 5 µM Cd exposed plants, the increased expression of NADPH-oxidase and lipoxygenase genes represented an additional source of oxidative stress giving rise to the disorganization of thylakoid membranes. The highly toxic 50 µM Cd concentration, inducing severe water stress and plastidial ultrastructural damage, imposed an impairment of the cellular redox state and a decrease of the plastidial antioxidative enzyme mRNA expression. Therefore, the increased plastidial ultrastructural damage was most likely caused by ROS because of the inhibition of antioxidative defence system indicating the

decreased ability of the plant to respond to the high oxidative stress levels in that organelle.

As Cd induced a reduction of the photosynthesis rate at all concentrations, the next step in this thesis was a profound analysis of the Cd-induced effects on photosynthesis. Therefore, the effect of Cd on the photosynthetic efficiency (more specifically on the stress sensitive photosystem II), described in **chapter 5**, was studied using chlorophyll *a* fluorescence transient analysis, fluorescence imaging analysis and HPLC pigment analysis. The results revealed no irreversible damage to photosystem II, not even at the highest exposure concentration (50 µM Cd). This was related to the downregulation (photoinhibition) of photosystem II (formation of silent reaction centres) and the protection by an induced xanthophyll cycle through increased thermal dissipation in the antennae. The protective action was confirmed by the apparently unharmed electron transport in the photochemically active reaction centres. At 5 µM Cd, photosynthesis had the tendency to perform better than at the less polluting 1 µM Cd concentration, which was most likely related to increased induction of several protective processes between 1 and 5 µM Cd. At 50 µM however, the increased Cd-toxicity caused a further decline in photosynthetic efficiency.

Singlet oxygen is considered to be a crucial factor for the downregulation of photosystem II. Therefore the final part of this thesis was dedicated to study the effect of Cd on the generation of singlet oxygen. **Chapter 6** is the description of the pilot study, which had the purpose of developing a fluorimetric analysis method using the fluorescent sensor DanePy, to study the Cd-induced generation of singlet oxygen in a cell culture of *Arabidopsis thaliana*. After optimization and verification of the method, experiments revealed an instantaneous singlet oxygen signal upon addition of Cd to the cell culture. The instantaneous singlet oxygen signal was not related to high light stress, precluding a chlorophyll-mediated generation. Additional tests indicated no direct involvement of NADPH-oxidases but a role for both Ca and superoxide in the singlet oxygen burst. It was therefore hypothesised that the observed singlet oxygen burst should possibly be seen as a very early signaling process dependent on both the disruption of the Ca^{2+} balance and a superoxide burst. However, additional research is necessary to confirm this hypothesis.

It can be concluded that much of the morphological and ultrastructural effects, caused by mild to high Cd toxicity, were most likely related to the disturbance of the water balance. At the highest Cd concentration, however, the inhibition of the antioxidative defence system seemed to be increasingly more important. Although Cd toxicity inflicted a great deal of oxidative stress causing substantial membrane damage, there was no irreversible damage to photosystem II. This illustrates the adaptive ability of the nontolerant *Arabidopsis thaliana* to Cd stress and is almost certainly attributable to activation of an extensive range of protective mechanisms of which the excluder strategy is an important first line of defence.

Samenvatting

Cadmium (Cd) is een toxisch element voor zowel planten, dieren als mensen en komt onder natuurlijke omstandigheden in zeer lage concentraties voor. Echter, door de industriële evolutie vormt Cd-vervuiling vanaf de 19de eeuw op verscheidene plaatsen een substantiële bedreiging voor het milieu. Ook in België zijn verscheidene locaties met Cd vervuild. In de Noorderkempen, bijvoorbeeld, is een gebied van 280 km^2 vervuild met Zn, Cd en Pb door historische aanwezigheid van zinksmelters. Cross-sectionele populatiestudies hebben voor dat gebied een positieve correlatie aangetoond tussen de verhoogde Cd-concentraties in gewassen en een verhoogde lichaamsbelasting van de inwoners. Deze verhoogde lichaamsbelasting werd verder in verband gebracht met verscheidene klinische symptomen in de nier en het skelet en met een verhoogd kankerrisico. Bovendien vormen met Cd gecontamineerde planten een potentieel gevaar voor herbivoren en hun predatoren wat de biodiversiteit negatief kan beïnvloeden. Om een algemeen beeld van de impact van Cd op het milieu te kunnen schetsen is het bijgevolg van belang om fundamentele kennis te verwerven betreffende de sekwestratie en toxiciteit van Cd in planten.

Het voornaamste doel van dit werk betrof het onderzoeken van de effecten van laag tot gematigde blootstellingconcentraties van Cd op het wildtype van *Arabidopsis thaliana* (ecotype Columbia), een welbekende en veelvuldig gebruikte plantensoort in toxiciteitstudies. Met dit werk hebben wij vooreerst getracht een nauwkeuriger beeld te vormen van het Cd transport en sekwestrering in wortel en blad en vervolgens de relatie onderzocht van Cd-geïnduceerde effecten op de fysiologie, morfologie en fotosynthese met oxidatieve stress. Tenslotte werd een fluorimetrische analysemethode ontwikkeld om de singlet zuurstof generatie te detecteren in een *Arabidopsis thaliana* celcultuur.

De lokalisering van Cd op subcellulair niveau in wortel en blad, beschreven in **hoofdstuk 3**, werd uitgevoerd met Energie Dispersieve X-stralen Microanalyse (EDXMA) op gecryofixeerde en cryogesubstitueerde weefsels van planten die gedurende 21 dagen werden blootgesteld aan 0, 1, 5 en 50 µM Cd. De analyses wezen uit dat in de wortelschors Cd voornamelijk was geassocieerd met fosfor (Cd/P) in de apoplast en met zwavel (Cd/S) in de symplast, wat een indicatie is voor een respectievelijk fosfaat en fytochelatine geassocieerde sekwestratie. In de endodermis, was Cd/S gesekwestreerd in fijne granulaire

deposities in de vacuole en in grote granulaire deposities in de rest van het cytoplasma. Het specifieke patroon van de symplastische accumulatie in de centrale cilinder gaf een duidelijke aanwijzing dat doorlaatcellen belangrijk zijn voor de opname van Cd in de centrale cilinder. In de pericykel apoplast werd een markante relocatie geobserveerd van Cd/S granulaire deposities van de middenlamella naar de plasmalemma toe. De grote hoeveelheden geprecipiteerd Cd in het floeem suggereerde retranslocatie vanuit het bovengrondse gedeelte. In het blad werd Cd gedetecteerd in de tracheïden maar niet in het mesofiele weefsel. Alles samengenomen kunnen we besluiten dat de extensieve symplastische en apoplastische accumulatie in het wortelparenchym in combinatie met de retranslocatie via het floeem de excluder strategie van *Arabidopsis thaliana* bevestigd.

Hoofdstuk 4 beschrijft het onderzoek naar verscheidene toxische effecten van Cd op *Arabidopsis thaliana*. Hierbij werden de Cd-geïnduceerde effecten of bladmorfologie, -ultrastructuur en -fysiologie bestudeerd in relatie met de genexpressie van ROS producerende (LOX1/2 en RBOHD/F/C) en antioxidative enzymen (CAT, CuZn-SOD, Fe-SOD en Mn-SOD). Hoewel in dit onderzoek lage tot middelmatige blootstellingconcentraties werden gebruikt, was de vermindering in groei en fotosynthese-activiteit aanzienlijk en was het vochtgehalte duidelijk verlaagd. Cd verminderde ook de celoppervlakte van het sponsparenchym en veranderde de vorm van de pallisadeparenchymcellen. Op het ultrastructurele niveau resulteerde blootstelling aan Cd in ernstige membraanschade. Deze structurele veranderingen werden toegeschreven aan Cd-geïnduceerde oxidatieve stress. Het blootstellen aan verschillende Cd-concentraties bracht bovendien een gedifferentieerd responspatroon aan het licht voor de cellulaire redox status. Daarbij was bij de laagste blootstellingconcentratie (1 µM Cd) het verhoogde H_2O_2 gehalte in het blad van planten blootgesteld voor het grootste gedeelte het gevolg van de inductie van NADPH-oxidases. Het betrof hier vermoedelijk om een signaalmechanisme dat gerelateerd was aan een verstoring van de waterbalans door Cd. *Arabidopsis thaliana* was echter in staat om zich aan de milde stress aan te passen zonder daarbij hun extensief arsenaal van antioxidatieve beschermingsmechanismen te induceren. Planten blootgesteld aan 5 µM Cd vertoonden een sterk verhoogde expressie van NADPH-oxidase en lipoxygenase genen wat aanzien wordt als een

additionele bron van oxidatieve stress. De verhoogde oxidatieve stress bleek ook duidelijk uit de geobserveerde desorganisatie van the thylakoidmembranen. De hoogste Cd-dosis (50 µM) veroorzaakte ernstige droogtestress en een aanzienlijke membraanschade in de chloroplast. De ultrastructurele schade in de chloroplast werd daarbij niet zozeer in verband gebracht met de activering van NADPH-oxidases en lipoxygenases maar eerder door een verminderde expressie van antioxidatief systeem. Dit was een duidelijke indicatie voor het gereduceerde vermogen van de plant om te reageren tegen de Cd-geïnduceerde oxidatieve stress in de chloroplast.

Omdat uit deze studie bleek dat zelfs de laagste Cd-dosis een sterke vermindering van fotosynthese-activiteit veroorzaakte, werd een grondige analyse uitgevoerd naar de effecten van Cd op de fotosynthese. Daarbij werd het effect van Cd op de fotosynthese-efficiëntie (meer specifiek op het stressgevoelige fotosysteem II), zoals beschreven in **hoofdstuk 5**, bestudeerd aan de hand van chlorofyl-*a* fluorescentieanalyse, fluorescentie-imaging analyse (meerbepaald een fluorescentie-quenching analyse) en pigmentanalyse met HPLC (high pressure liquid chromatography). Uit de resultaten bleek dat er geen onomkeerbare schade was aan fotosysteem II, zelfs niet bij de hoogste dosis (50 µM). Dit feit kon worden toegeschreven aan de downregulatie (foto-inhibitie) van fotosysteem II door de vorming van fotochemisch inactieve reactiecentra en door de thermische dissipatie van de excitatie-energie in de antennes door de inductie van de xanthofylcyclus. Het beschermend effect van deze processen werd verder bevestigd door het feit dat zelfs bij blootstelling aan hoge dosissen Cd het elektronentransport intact bleef in de fotochemisch actieve reactiecentra. Erg opvallend was het feit dat planten die werden blootgesteld aan 5 µM Cd een hogere fotosynthese-efficiëntie vertoonden dan planten die werden blootgesteld aan de laagste dosis (1 µM Cd). Dit heeft naar alle waarschijnlijkheid te maken met een verhoogde inductie van verscheidene beschermende processen (tussen 1 en 5 µM Cd). Bij de hoogste Cd-dosis (50 µM) was de fotosynthese-efficiëntie echter sterk verlaagd.

Singlet zuurstof wordt algemeen aanzien als een cruciale factor in de bovenvermelde downregulatie van fotosysteem II. Daarom werd een onderzoek uitgevoerd naar de effecten van Cd op de generatie van singlet zuurstof. In **hoofdstuk 6** wordt de pilootstudie beschreven die tot doel had om een

fluorimetrische analysemethode te ontwikkelen gebruikmakende van de fluorescente merker DanePy. Met deze methode werd vervolgens de Cd-geïnduceerde generatie van singlet zuurstof onderzocht in een celcultuur van *Arabidopsis thaliana*. Na het ontwikkelen, optimaliseren en verifiëren van de methode, bleek uit de tests dat de additie van Cd aan de celcultuur een instantaan singlet zuurstof signaal veroorzaakte. Dit signaal werd echter niet beïnvloed door het blootstellen van de celcultuur aan een hoge lichtintensiteit wat de betrokkenheid van chlorofyl uitsloot. Ook NADPH oxidases bleken geen directe invloed te hebben op het signaal, dit in tegenstelling tot zowel Ca als superoxide die blijkbaar wel betrokken waren in de singlet zuurstof productie. Als voorlopige hypothese werd dan ook vooropgesteld dat de instantane singlet zuurstof vorming waarschijnlijk kan worden gezien als een vroeg signaalproces dat gerelateerd is aan de verstoring van de Ca^{2+} balans en een instantane superoxide productie. Uiteraard is verder onderzoek noodzakelijk ter ondersteuning van deze hypothese.

Samengevat kon uit dit werk worden geconcludeerd dat bij milde tot hoge Cd stress de morfologische en ultrastructurele effecten hoogstwaarschijnlijk waren gerelateerd aan de verstoring van de waterbalans. Bij de hoogste Cd concentratie echter, bleek de inhibitie van het antioxidatieve defensiemechanisme aan belang te winnen. Niettegenstaande Cd toxiciteit in erge mate oxidatieve stress veroorzaakte met aanzienlijke membraanschade tot gevolg, resulteerde dit echter niet in een onomkeerbare schade aan fotosysteem II. Deze resultaten illustreren het opmerkelijk adaptieve vermogen van de niet-tolerante *Arabidopsis thaliana* tegen Cd stress, wat hoogstwaarschijnlijk kan worden toegeschreven aan de activering van een extensief geheel van beschermingsmechanismen waarvan de excluderstrategie een belangrijke eerste lijn van defensie vormt.

Table of contents

Abbreviations

ABA	abscisic acid
A	antheraxanthin
ABC	ATP-binding cassette
ABS	absorption flux
ACT2	Actin2 gene
ANOVA	analysis of variance
AOX	alternative oxidases
APx	ascorbate peroxidase (EC 1.11.1.11)
AsA	ascorbate (reduced)
ATP	adenosine triphosphate
CadmiBel	Cadmium in Belgium study
car	carotene
CAT	catalase (EC 1.11.1.6)
CAT	catalase gene
Cd	cadmium
cDNA	complementary DNA
chl	chlorophyll
cPTIO	2-(4-carboxyphenyl)-4,4,5,5-tetramethylimidazoline-1-oxyl-3 oxide
CS	cross section
CSD	CuZn-superoxide dismutase gene
D1, D2	reaction centre-binding protein of photosystem II
DHA	dehydroascorbate
DHAR	dehydroascorbate reductase (E.C. 1.8.5.1)
DI	dissipated excitation energy flux
DPI	diphenyleneiodonium
e^-	electron
EDXMA	energy-dispersive X-ray microanalysis
ET	electron transport flux
EXAFS	Extended X-ray Absorption Fine Structure
FD	ferredoxin
FIS	fluorescence imaging system
FNR	ferredoxin NADPH reductase (EC 1.18.1.2)
FSD	Fe-superoxide dismutase gene
GLM	General Linear Model
GLR	glutaredoxin
GPOD	guaiacol peroxidase (EC 1.1.11.7)
GPx	glutathione peroxidase (EC 1.1.11.9)
GR	glutathione reductase (EC 1.6.4.2)
GSH	glutathione (reduced)
GSSG	glutathione disulfide (oxidized)
H_2O_2	hydrogen peroxide
HEPES	4-(2-hydroxyethyl)-1-piperazineethanesulfonic acid
HMA	heavy metal ATPase

HMW	high-molecular-weight
HPLC	high performance liquid chromatography
IARC	International Agency for Research on Cancer
IRT	iron-regulated transporter
JA	jasmonic acid
LHCII	peripheral light-harvesting antenna complex of photosystem II
LMW	low-molecular-weight
LOX	lipoxygenase (EC 1.11.71.12)
LTP	lipid transfer proteins
MDHA	monodehydroascorbate
MDHAR	monodehydroascorbate reductase (EC 1.6.5.4)
MeJA	methyl jasmonate
MES	β-morpholino-ethanesulfonic acid
mRNA	messenger RNA
MSD	Mn-superoxide dismutase gene
MT	metallothionein
NADPH	nicotinamide-adenine dinucleotide phosphate
$NO^{\cdot}$	nitroxide
NOX	NADPH oxidase (EC 1.6.1.7)
NPQ	nonphotochemical quenching (energy dissipation by heat)
Nramp	natural resistance-associated macrophage protein
$^1O_2$	singlet oxygen
O_2	(di)oxygen
$O_2^{\cdot -}$	superoxide
OEC	oxygen evolving complex
^-OH	hydroxyl anion
$^{\cdot}OH$	hydroxyl radical
$ONOO^-$	peroxynitrite
P	phosphorus
P680	primary electron donor of photosystem II
PAR	photoactive radiation
PC	phytochelatin
PCR	polymerase chain reaction
PCS	phytochelatin synthase (EC 2.3.2.15)
PEA	plant efficiency analyser
PheeCad	Public Health and Environmental Exposure to Cadmium study
PI	performance index
PQ	plastoquinone
PQH_2	plastohydroquinone
Prx	peroxiredoxin (EC 1.11.1.5)
PSI	photosystem I
PSII	photosystem II
PTI	Photon Technology International

Q_A	primary plastoquinone electron acceptor of photosystem II
Q_B	secondary plastoquinone electron acceptor of photosystem II
RBOH	respiratory burst oxidase homolog
RC	reaction centre
RCII	reaction centre of photosystem II
RNA	ribonucleic acid
Rnase	ribonuclease
ROS	reactive oxygen species
Rubisco	Ribulose-1,5-bisphosphate carboxylase oxygenase
S	sulfur
SOD	superoxide dismutase
S_i (i=0,1,2,3)	S-states or redox states of the oxygen evolving complex
TEM	transmission electron microscopy
TR	trapping flux
Trx	thioredoxin
V	violaxanthin
Yz	tyrosine
Z	zeaxanthin
ZIP	Zrt-like, Irt-like protein
ZNT	zinc transporter
ZRT	zinc-regulated transporter

Chapter 1

Introduction

1.1 General information on cadmium

1.1.1 History

Cadmium (the chemical symbol = Cd) was discovered in Germany in 1817 by Friedrich Strohmeyer as an impurity in calamine (zinc carbonate ($ZnCO_3$) Fig. 1.1a). The name is derived from the Latin cadmia and the Greek kadmeia meaning "calamine", which was exploited near the ancient city of Thebes (founded by the Phoenician Kadmos).

(a)

(b)

(c)

Fig. 1.1 *Photographs of different forms of Cd, with (a) the ore calamine ($ZnCO_3$) (source: www.mindat.org/min-8129.html), (b) purified metallic cadmium (source: U.S. Geological Survey) and (c) greenockite (dark yellow crystal (CdS)) (collection: Museum Edinburgh, Great Britain. Photo:Rainer Bode, Haltern).*

1.1.2 Chemical and physical properties

Cadmium is an element of group IIb with an atomic number of 48 and an atomic mass of 112.41. Eight naturally occurring isotopes of cadmium exist: ^{114}Cd (28.73%), ^{112}Cd (24.13%), ^{111}Cd (12.8%), ^{110}Cd (12.49%), ^{113}Cd (12.22%), ^{116}Cd (7.49%), ^{106}Cd (1.25%), ^{108}Cd (0.89%). In addition, 34 other isotopes and isomers are now known and recognized. Cadmium reacts slowly with oxygen in moist air at room temperature forming cadmium oxide (CdO). It does not react with water, but it does react with most acids.

Cd is a shiny metal with a bluish cast (Fig. 1.1b). It is very soft and can be cut with a knife. Its melting point is 594.22 K (321 °C) and its boiling point is 1040 K (765 °C). The density of cadmium is 8.65 g cm^{-3}. When cadmium is used in alloys, it tends to lower the melting point of the alloy.

1.1.3 Occurrence, production and use

Cadmium is relatively rare in the Earth's crust with an estimated abundance of *c.* 0.1 - 0.2 parts per million. The only important ore of cadmium is greenockite (Fig. 1.1c), or cadmium sulfide (CdS) that is nearly always associated with sphalerite (ZnS).

Consequently, cadmium is produced mainly as a byproduct from mining, smelting, and refining sulfide ores of zinc, and to a lesser degree, lead and copper. Historically, cadmium was isolated from melted zinc by vacuum distillation. Nowadays, cadmium sulfate is precipitated out of a electrolysis solution. In 2004, the worldwide cadmium production was *c.* 17800 tons/year.

Most of the produced cadmium is used in Ni-Cd batteries (79 %) and pigments such as cadmium sulfide (yellow) and cadmium selenide (red) (12 %). Other applications are in coatings and plating (7 %), and as stabilizers for polyvinylchloride (2 %). Other uses (1 %) are the application in low melting alloys and bearing alloys and in some semiconductors such as cadmium sulfide, cadmium selenide and cadmium telluride, which can be used for light detection or solar cells (Buckingham & Plachy, 2004).

1.2 Contaminations and toxicological risks

The element Cd is of great concern in the environment, because of its toxicity to plants, animals and humans. As a consequence, various studies have been conducted to investigate the effects of acute and chronic exposure to humans, animals, invertebrates, plants and micro-organisms to establish acceptable limits of exposure for organisms.

Anthropogenic pathways by which Cd enters the environment mainly consist of the industrial waste from the above described processes including electroplating, manufacturing of plastics, mining, paint pigments, alloy preparation, and batteries that contain cadmium (Adriano, 2001). Worldwide, large amounts of Cd have also been released into the environment through the burning of refuse materials (*i.e.* discarded food) that contain Cd and through the use of Cd-contaminated sludge and phosphate salts as fertilizers (ATSDR, 1999).

Cadmium toxicity affects humans in particular, because of their longevity and its accumulation in their organs because of the low excretion rate of cadmium (half-life as long as 15–20 years) (Jin *et al.*, 1998). Human intoxication results mainly from cigarette smoking because of high concentrations of cadmium in cigarettes but also from water, food and air contaminations (reviewed by Jarup *et al.*, 1998). Elevated levels of Cd in humans can cause kidney damage (Fig. 1.2a), and low levels of Cd in the diet are linked to renal dysfunction. Other diseases associated with Cd exposure are pulmonary emphysema, diabetic and renal complications, deregulated blood pressure, immune-suppression and bone disorders (the Itai–Itai disease) (Fig. 1.2b) (IARC, 1993; Jarup *et al.*, 1998).

The International Agency for Research on Cancer (IARC) has classified cadmium as a carcinogen of category 1 (IARC, 1993). Cadmium has primarily been linked to lung cancer (by occupational cadmium exposure), and also to human prostate and renal cancer (although this linkage is weaker than for lung cancer). Other target sites of cadmium carcinogenesis in humans, such as liver, pancreas and stomach, are considered equivocal (reviewed by Waalkes, 2003).

Although the potential mechanisms of Cd carcinogenesis are unknown, Cd mainly interferes with DNA repair processes, and enhances the mutagenicity

induced by other DNA damaging agents. The genotoxic effects of cadmium on animal and plants cells and tissues has recently been reviewed by Deckert (2005), Hartwig and Schwerdtle (2002), Waalkes (2003) and Waisberg *et al.* (2003).

(a) 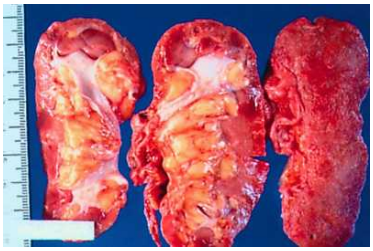 (b) 

Fig. 1.2 *Two examples of detrimental effects on human health under high Cd exposure, (a) picture showing damage to the kidney leading to atrophy; (b) a pelvic roentgenogram showing a case of osteomalacia bone disease. The zones pointed with a black and white arrow are "looser zones" (increased osteoid tissue) of bilateral femoral bones (source: http://www.kanazawa-med.ac.jp/~pubhealt/cadmium2/itaiitai-e/itai01.html).*

1.3 Uptake and transport in plants

1.3.1 Long distance transport

The degree to which higher plants are able to take up Cd is reviewed by Sanità di Toppi and Gabbrielli (1999) and depends on its concentration in the soil and its bioavailability, modulated by the presence of organic matter, pH, redox potential, temperature and concentrations of other elements (K, Ca, Mg, Fe, Mn, Cu, Zn, Ni). In addition, Cd uptake is dependent on the presence of mycorrhizas, the binding properties of the cell wall and root exudates (Das *et al.*, 1997; Hall, 2002). Cadmium is characterized by a high mobility in the soil, especially in poor and acidic soils, and is easily taken up by the root (Barceló & Poschenrieder, 1990).

Cd enters the root via the apoplast, comprising the cell wall continuum and intercellular spaces of the root cells (Fig. 1.3). This movement is a non-metabolic, passive process driven by mass flow (Marschner, 1995). The apoplastic space provides a site for the accumulation of positively charged ions, particularly divalent or polyvalent cations. The negatively charged carboxyl groups of the

apoplast provide sites for cation exchange, increasing the concentration of cations in the vicinity of the active uptake sites of the plasma membrane (Marschner, 1995). The apoplast provides a continuum from the external solution, through the cortex of the root to the endodermis, so entrance into the symplast is not essential. However, apart from Cd leakage in the cells via Ca, Fe and Zn uptake systems (Perfus-Barbeoch *et al.*, 2002; Connolly *et al.*, 2002) energy-dependent transport of Cd from the apoplast into the symplast has been described by Heber *et al.* (2002), as a means to prevent solute accumulation in the apoplast.

Once at the endodermis, the apoplastic movement is blocked by the Casparian bands on the anticlinal (transverse and radial longitudinal) cell walls and ions are routed towards the symplast (Fig. 1.3 (inset)). In the central cylinder, ions are transported primarily through the apoplast towards the xylem (reviewed by Ma & Peterson, 2003). However, transport of Cd from the apoplast into the symplast of stelar cells has been reported by Seregin and Ivanov (2001).

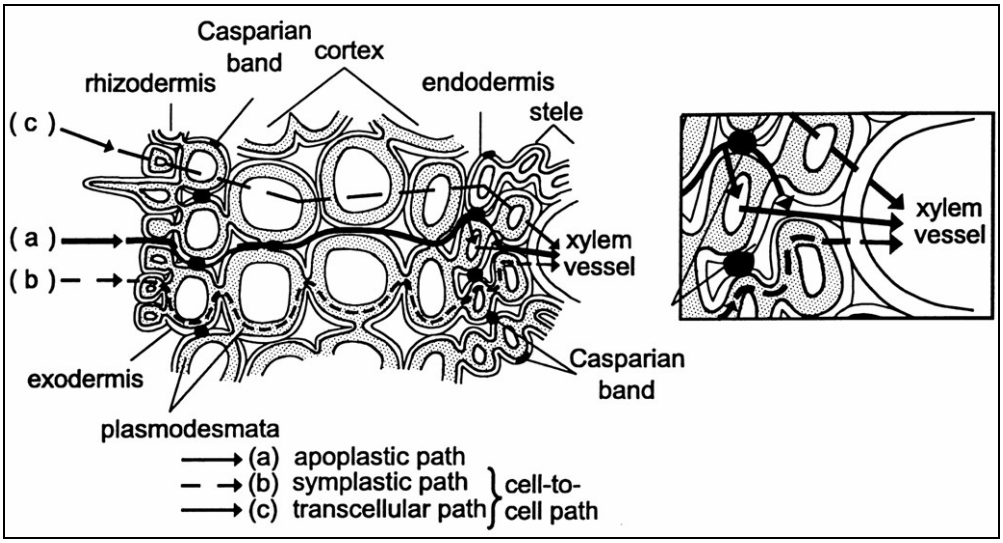

Fig. 1.3 *A drawing illustrating the different routes of radial transport across the root and into the xylem vessels (source: Steudle, 2000). The apoplastic flow runs along the continuum of cell walls around the protoplasts. The symplastic flow runs along the cytoplasmic continuum (formed by plasmodesmata, which bridge the cell walls between adjacent cells). During the passage along the apoplast (and symplast), no membranes have to be crossed. In the endodermis (and if present, also the exodermis) the apoplastic flow is modified by the Casparian bands (suberin lamellae), which are considered as impermeable for water and solutes (inset).*

Transfer from the cortical cells to the xylem in roots may be a passive process as ions move down an electropotential gradient. However, the final step of xylem loading is suggested to be an active process (Marschner, 1995), most likely mediated by the efflux pump HMA 4 from the P_{IB}-ATPases subfamily of P-type ATPases (see section 1.3.2 and Fig. 1.4). Cd can be transported as a free Cd ion in the xylem (Leita *et al.*, 1996) but also organic acids (citrate), amino acids (e.g. histidine) and nicotianamine are considered to be involved in metal transport (Cataldo *et al.*, 1988; Krämer *et al.*, 1996; Pich & Scholz, 1996).

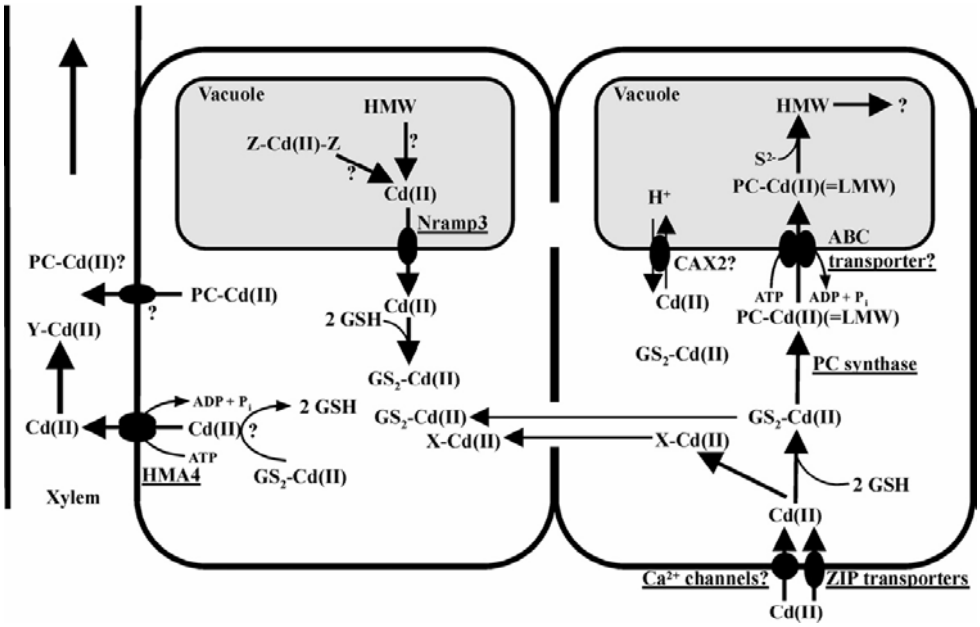

Fig. 1.4 *A schematic representation of processes involved in the uptake, sequestration and (symplastic) translocation of Cd in plant roots (source: Clemens, 2006). Two root cells are depicted: one is facing the rhizosphere (right), one is adjacent to the xylem (left). Cd^{2+} ions are most likely taken up by Fe^{2+}/Zn^{2+} ZIP transporters and by Ca^{2+} channels. In the cytosol Cd^{2+} ions are chelated with GSH (bisglutathionato–Cd complexes, GS_2–Cd(II)) and potentially other unknown molecules (X-Cd(II)). GS_2–Cd(II) interacts with PCS resulting in the activation of PC synthesis. PC–Cd(II) complexes (=LMW complexes) are hypothesized to be transported into the vacuole by an ABC-type transporter (HMT1). Inside the vacuole HMW complexes are formed that contain sulfide. A second pathway of vacuolar sequestration could be Cd^{2+}/H^+ antiport (CAX2). At least a fraction of the vacuolar bound Cd can apparently be mobilized back into the cytosol by AtNramp3. Symplastic transfer requires the availability of (GS_2–Cd(II), X–Cd(II)). Loading of the xylem is dependent on efflux pumps, most likely AtHMA4. An efflux of PC-Cd(II) complexes has also been proposed. In the acidic xylem, transport as a free Cd(II) ion is possible besides transport of PC Cd(II) complexes and Cd(II) associated with citrate, histidine or nicotianamine.*

The pH of the phloem is typically higher than 8, which is higher than the xylem and largely precludes the free ionic activity of all cationic metals in the phloem, instead they would be complexed with other compounds (Welch, 1995) but this mechanism of transport of metals is still poorly documented (Briat & Lebrun, 1999). Nicotiniamine is the sole molecule that has been identified in the phloem sap as a potential phloem metal transporter (Stephan & Scholz, 1993). However, other unknown metal chelators have been postulated for the phloem but the chemical identity and the role of these complexes in the phloem metal-transport needs to be clarified (Briat & Lebrun, 1999).

1.3.2 Cellular transport mechanisms

Although, the mechanism(s) by which Cd is transported across the plasma membrane of higher plants are still elusive, some hypotheses have been postulated.

Cd transport has been related to the presence of nonselective cation channels, a diverse group of metal transport channels that are ubiquitous in plant tissues. These cation channels are active in the plasma membrane and tonoplast and exhibit broad substrate specificity (thus a low discrimination between many essential and toxic cations). Members of this group are likely to function in low-affinity nutrient uptake, in distribution of cations within and between cells, and as plant Ca^{2+} channels (Fig. 1.4) (see the review by Demidchik *et al.*, 2002). As Cd has many physical characteristics similar to Ca, it has been proposed that Cd^{2+} may enter the cell via a Ca^{2+} channel in place of Ca^{2+} (White, 2000). Indeed, a strong indication for the uptake of Cd via Ca ion channels has been delivered by Perfus-Barbeoch *et al.* (2002). By the application of putative calcium channel inhibitors, which suppressed the inhibitory effect of Cd^{2+} in epidermal strip experiments, they have shown that Cd could enter the guard cells through calcium channels.

Various members of the ZIP (Zrt-like, Irt-like protein) family are known to be able to transport Fe, Zn, Mn, and Cd (Guerinot, 2000). By complementation of a yeast Zn-transport defective mutant with a *Thlaspi caerulescens* cDNA library, Lasat *et al.* (2000) cloned the ZNT1 cDNA, which encodes a high affinity Zn transporter. However, ZNT1 can also mediate low affinity Cd transport (Lasat *et al.*, 2000; Pence *et al.*, 2000). Further analysis

revealed that *ZNT1* is a member of the micronutrient transport gene family, which includes the *Arabidopsis* IRT1 (iron-regulated transporter) and the ZIP Zn transporters (Pence *et al.*, 2000). Additional studies in yeast showed that IRT1, an iron transporter belonging to the ZIP family, has a broad substrate range and also transports Zn and possibly Cd (Fig. 1.4) (Korshunova *et al.*, 1999; Clemens, 2001, 2006).

A part of the natural resistance-associated macrophage protein (Nramp) family (*i.e.* AtNramp1, AtNramp3, and AtNramp4) has been reported to transport Mn and Fe and plays a role in the iron homeostasis (Curie *et al.*, 2000; Thomine *et al.*, 2000). Thomine *et al.* (2000) further revealed that Nramp proteins also play a role in Cd uptake. This was illustrated by the fact that disruption of an *AtNramps3* gene slightly increased Cd resistance, whereas overexpression resulted in Cd hypersensitivity in *Arabidopsis*.

P_{IB}-ATPases, a subfamily of P-type ATPases (initial named CPx-ATPases by Solioz and Vulpe (1996)), transport essential (Cu, Zn) as well as potentially toxic elements (Cd and Pb) across cell membranes (Argüello, 2003; Eren & Argüello, 2004; Williams *et al.*, 2000). These enzymes have been identified in a wide range of organisms and are regarded as essential for the absorption, distribution, and bioaccumulation of metal micronutrients by higher organisms (Solioz & Vulpe, 1996). Recently the heavy metal ATPase HMA2 (a P_{IB}-ATPase present in *Arabidopsis thaliana*) was cloned and functionally characterized after heterologous expression in yeast (*Saccharomyces cerevisiae*), which revealed a high affinity interaction of HMA2 with Zn^{2+} and Cd^{2+} (Eren & Argüello, 2004). Zn^{2+} transport determinations indicated that the enzyme drives the outward transport of metals from the cell cytoplasm and is therefore responsible for the Zn^{2+} efflux from the cytoplasm. Analysis of HMA2 mRNA suggested that the enzyme is present in all plant organs and removal of the HMA2 full-length transcript resulted in Zn^{2+} accumulation in plant tissues but also in Cd^{2+} accumulation when the *hma2* mutant plants were exposed to this element (Eren & Argüello, 2004). In addition, HMA4 (Fig. 1.4) seems to be involved as an efflux pump in the xylem loading of Cd (reviewed by Clemens, 2006).

1.3.3 Complexation and sequestration mechanisms

A general mechanism for detoxification of Cd is the chelation by a ligand and, in some cases, the subsequent compartmentalization of the ligand-metal complex. In this way the phytotoxic ionic form of Cd is converted into a non-toxic non-ionic Cd complex and removed from metabolic sites.

Precipitation of Cd in the cell walls (apoplast) has been proposed as an avoidance mechanism at lower concentrations (Wagner *et al.*, 1993) and it has been found associated with phosphates (Küpper *et al.*, 2000; Sela *et al.*, 1990). In the cytoplasm (symplast), the free Cd^{2+} concentration is reduced by intracellular metal ligands such as phytochelatins, metallothioneins, and organic acids (Clemens, 2001, 2006; Cobbett & Goldsbrough, 2002).

Complexation with phytochelatins followed by compartmentalization into the vacuole (Fig. 1.4) (Clemens, 2006; Cobbett & Goldsbrough, 2002; Sanità di Toppi & Gabbrielli, 1999) or possible precipitation in the cytoplasm (Rauser & Ackerley, 1987; van Steveninck *et al.*, 1990) is probably the most important chelation pathway. For a more in-depth discussion concerning the mechanism of phytochelatins complexation, vacuolar sequestration and cytoplasmic precipitation, see chapter 3.

Metallothioneins are a second group of metal ligands. Although metallothioneins are structurally similar to phytochelatins, they are encoded by genes while phytochelatins are synthesized enzymatically. Metallothioneins have an important detoxification function for Cu toxicity but are considered of secondary importance for Cd toxicity in plants (Cobbett & Goldsbrough, 2002; Sanità di Toppi & Gabbrielli, 1999). However, since the knowledge of the function of metallothioneins in metal tolerance is still fragmentary, the involvement of metallothioneins in Cd detoxification should not be excluded immediately.

In addition, organic acids such as citrate and malate have been hypothesised to be ligands of free Cd^{2+} (Senden *et al.*, 1992; Wagner, 1993).

Another way of reducing intracellular Cd^{2+} concentrations in higher plants could be through efflux pumping as suggested by Costa and Morel (1993). However, although the presence of a cation efflux system that excludes Cd from

the bacteria *Alcaligenes eutrophus* has been revealed by Nies and Silver (1989), its function in plants is still speculative.

1.4 Cd phytotoxicity

1.4.1 General

Leaf roll, chlorosis and inhibited growth, both in roots and in stems are the most prominent visual symptoms of Cd toxicity (Sanità di Toppi & Gabbrielli, 1999). The effects of Cd at the physiological level are extensively reviewed by Benavides *et al.* (2005) and Deckert (2005). Cd affects the uptake, transport and use of several nutritional elements (Fe, Mn, Ca, Mg, P, Cu, Ni and K), nitrate and water (see the review by Benavides *et al.*, 2005 and Clemens, 2006), and inhibits nitrogen fixation and ammonium assimilation (Balestrasse *et al.*, 2003). It affects photosynthesis (see chapter 5), respiration (Burzynski & Klobus, 2004), transpiration, plasma membrane integrity (Skórzyńska-Polit *et al.*, 2006) and the water balance (Barceló & Pochenrieder, 1990; Vitória *et al.*, 2003). Also inhibition of cell division and changes in gene expression are observed (Foyer & Noctor, 2003; Scandalios, 2005). Finally, cadmium induces oxidative stress resulting in lipid peroxidation (see section 1.5).

Many toxic effects of the non-essential element Cd on the plant metabolism are caused by the high affinity for and reactivity with sulfhydryl groups (SH-groups) and carboxyl groups (Nieboer & Richardson, 1980). Cd has been suggested to be involved in the inhibition of enzymes like for example malate dehydrogenase and NADPH-oxidoreductase (at the reducing side photosystem I) (reviewed by Vangronsveld & Clijsters, 1994).

Furthermore, Cd can be responsible for DNA strands breaks and mutagenic effects (Fojtová & Kovarik, 2000; Gichner *et al.,* 2004).

The substitution of essential metals in metallo-enzymes by Cd is also an important factor of phytotoxicity. For instance, the substitution of Mg has an influence on chlorophyll and Rubisco (Stiborova *et al.*, 1986) whereas the substitution of Mn and/or Ca has an influence on the oxygen evolving complex (Faller *et al.*, 2005; Kriedemann *et al.*, 1985; Mallick & Mohn, 2003; Sayed, 1998).

1.4.2 Specific effects on photosynthesis

Inhibition of photosynthesis, a common symptom of adverse conditions, is reported to cause an increased sensitivity to photoinhibition because of an imbalance between light capture, CO_2 assimilation and carbohydrate utilization (Foyer & Noctor, 2000; Long *et al.*, 1994). In other words, it is the result of the capturing of excess photons, disturbing the redox state promoting the production of reactive oxygen species which could lead in particular to photosystem II damage (Barber & Andersson, 1992; Foyer & Noctor, 2000).

Apart from this photoinhibition, which is commonly observed under adverse conditions, specific effects of Cd on photosynthesis are mainly related to the suppression of the Calvin-Benson cycle reactions (Krupa *et al.*, 1993). Cd effects on Rubisco (ribulose-1,5-bisphosphate carboxylase oxygenase) may result from the substitution of Mg in the ternary enzyme-CO_2-metal complex or by reaction with SH-groups (Clijsters & Van Assche, 1985; Stiborova *et al.*, 1986). In addition, Cd inhibits enzymes of the CO_2 assimilation pathway (Stiborova *et al.*, 1986). Regarding photosystem II, Cd has been reported to affect the electron donor side (oxygen evolving complex) (Faller *et al.*, 2005; Garstka & Kaniuga, 1988; Kriedemann *et al.*, 1985; Mallick & Mohn, 2003; Sayed, 1998), to inhibit the reduction and oxidation rate of the primary electron acceptor Q_A (Strasser *et al.*, 1995) and to induce changes in the normal Q_A-Q_B equilibrium (Ciscato *et al.*, 1999). Photosystem I, however is either slightly or not at all inhibited by Cd (Clijsters & Van Assche, 1985; Atal *et al.*, 1991). Last but not least, Cd-induced structural damage such as the degradation of thylakoid acyl lipids (Krupa & Baszynski, 1985, 1989) and the antennae pigments (Kupper *et al.*, 1998) has also been reported to have detrimental effects on photosynthesis. This subject is further extensively discussed in chapter 5.

1.5 Oxidative stress

1.5.1 Reactive oxygen species production

In plant cells, reactive oxygen species (ROS) are produced as a by-product of aerobic cell metabolism in organelles with a highly oxidizing metabolic activity or with an intense rate of electron flow, such as chloroplasts, mitochondria and peroxisomes (for an extensive review see Arora *et al.*, 2002). In addition, ROS (Fig. 1.5) are produced by several oxidases present in the membrane and cytoplasm (*i.e.* NADPH oxidases and lipoxygenases). Among the numerous kinds of ROS species, superoxide ($O_2^{\cdot -}$), hydrogen peroxide (H_2O_2), hydroxyl radical ($^{\cdot}OH$) and singlet oxygen ($^1O_2$) are of particular concern because they have the potential to cause oxidative damage by reacting directly with biomolecules such as proteins, DNA, lipids and membranes (Valentine *et al.*, 1998). However, despite their toxicity, ROS are also functional as they mediate a variety of cellular responses, including hormone signaling, development, gravitropism, and programmed cell death (Kwak *et al.*, 2006; Foyer & Noctor, 2005; Mittler *et al.*, 2004; Van Breusegem & Dat, 2006).

For instance, the plasma membrane localized NADPH oxidase (NOX, EC 1.6.1.7) isoforms, also referred to as respiratory burst oxidase homologs (RBOH), mediate the apoplastic generation of superoxides and are involved in broad aspects of growth and physiological responses (Sagi & Fluhr, 2001; Simon-Plas *et al.*, 2002). RBOHs are involved in defence as they are induced in response to biotic stress such as pathogen attack (Torres *et al.*, 2002), and in response to abiotic stress such as anoxia/hypoxia and nitrogen stress (Branco-Price *et al.*, 2005). They are further involved in root hair growth and xylem development (Barceló, 2005; Foreman *et al.*, 2003) and in cellular signal transduction such as ABA signaling in case of water stress (Jiang & Zhang, 2002; Kwak *et al.*, 2003) and for the induction of defence genes in response to systemin and jasmonate during wound responses (Orozco-Cardenas *et al.*, 2001). Signaling was thereby suggested to occur most likely via a second messenger H_2O_2 (generated by extracellular superoxide dismutases).

Lipoxygenases (LOX, EC 1.11.71.12) are nonheme iron-containing dioxygenases that catalyze the addition of molecular oxygen to polyunsaturated

fatty acids with a (Z,Z)-1,4-pentadiene structural unit to give a unsaturated fatty acid hydroperoxide. This reaction initiates the synthesis of oxylipins, acyclic and cyclic compounds with several physiological functions. LOX are reported to be involved in different developmental stages and its expression levels are influenced by the source/sink status, ABA and during specific stress conditions such as wounding, pathogen attack and water stress (reviewed by Porta & Rocha-Sosa, 2002).

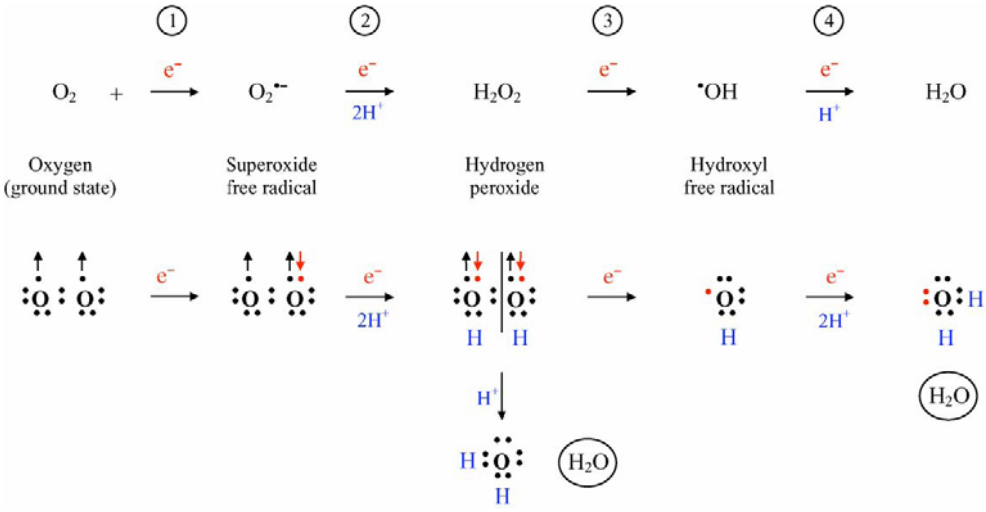

Fig. 1.5 *Consecutive four-step monoelectron reduction of dioxygen yielding reactive oxygen intermediates and $2H_2O$ (source: Edreva, 2005). Step 1 is superoxide generation by acceptance of one electron. This step is endothermic and hence rate-limiting. The next steps are exothermic and hence spontaneous. In step 2 the superoxide is reduced by acceptance of one electron and protonated by two H^+, this resulting in H_2O_2 formation. In step 3 H_2O_2 undergoes heterolytic fission in which one atom oxygen receives both electrons from the broken covalent bond. This moiety is protonated yielding one molecule H_2O. The other moiety receives one electron and is transformed in hydroxyl free radical ($^{\cdot}OH$). In step 4 $^{\cdot}OH$ receives one electron, and after protonation, yields one molecule H_2O.*

1.5.2 Quenching of reactive oxygen species

In order to avoid oxidative damage while keeping the ROS functionality, ROS are balanced against an extensive antioxidative defence system (Fig. 1.6) composed of enzymes as well as metabolites (Schützendübel & Polle, 2002). The enzymatic detoxification mechanisms comprise superoxide dismutases, catalases, peroxidases and peroxiredoxins, which are comprehensively reviewed by Arora *et al.* (2002) and Mittler *et al.* (2004). The metallo-enzyme superoxide dismutases (SOD, EC 1.15.1.1) are responsible for the dismutation of the reactive superoxide into less reactive H_2O_2 and O_2. The neutralization of superoxide also decreases the risk of formation of the extremely reactive hydroxyl radical from superoxide via the metal-catalysed Haber–Weiss-type reaction (Fig. 1.7). The three SOD isoenzymes are believed to operate in specific subcellular locations; FeSOD in chloroplasts, MnSOD predominantly in the peroxisomes and mitochondria and CuZnSODs in the cytosol, chloroplasts and peroxisomes. However, recently it has been reported that almost all of the isozymes of SOD have been detected in most of the cellular components. The tetrameric heme-containing enzyme, catalase (CAT, EC 1.11.1.6) converts H_2O_2 into H_2O and O_2 in the peroxisome (CAT1 and CAT2) and in the mitochondria (CAT3). Ascorbate peroxidase (APx, EC 1.11.1.11) is a heme-protein using ascorbic acid as an electron donor to scavenge H_2O_2 via the ascorbate-glutathione cycle (Asada, 1999). Ascorbate peroxidase quenches H_2O_2 (primarily produced by SOD), in the chloroplast (Asada, 2006) and cytosol, though Jimenez *et al.* (1997) have reported its occurrence in mitochondria as well. In the chloroplasts, SOD and APx exist in both soluble and thylakoid-bound forms. Superoxide generated at the membrane surface can thus be trapped and converted immediately to H_2O_2 to be scavenged by the membrane bound ascorbate peroxidase. Other H_2O_2 and peroxides quenching enzymes are guaiacol peroxidases (GPOD, EC 1.1.11.7), glutathione peroxidase (GPx, EC 1.1.11.9) and peroxiredoxins (Prx, EC 1.11.1.5) which use thioredoxin (Trx) as an electron donor (Lamkemeyer *et al.*, 2006) (Fig 1.6).

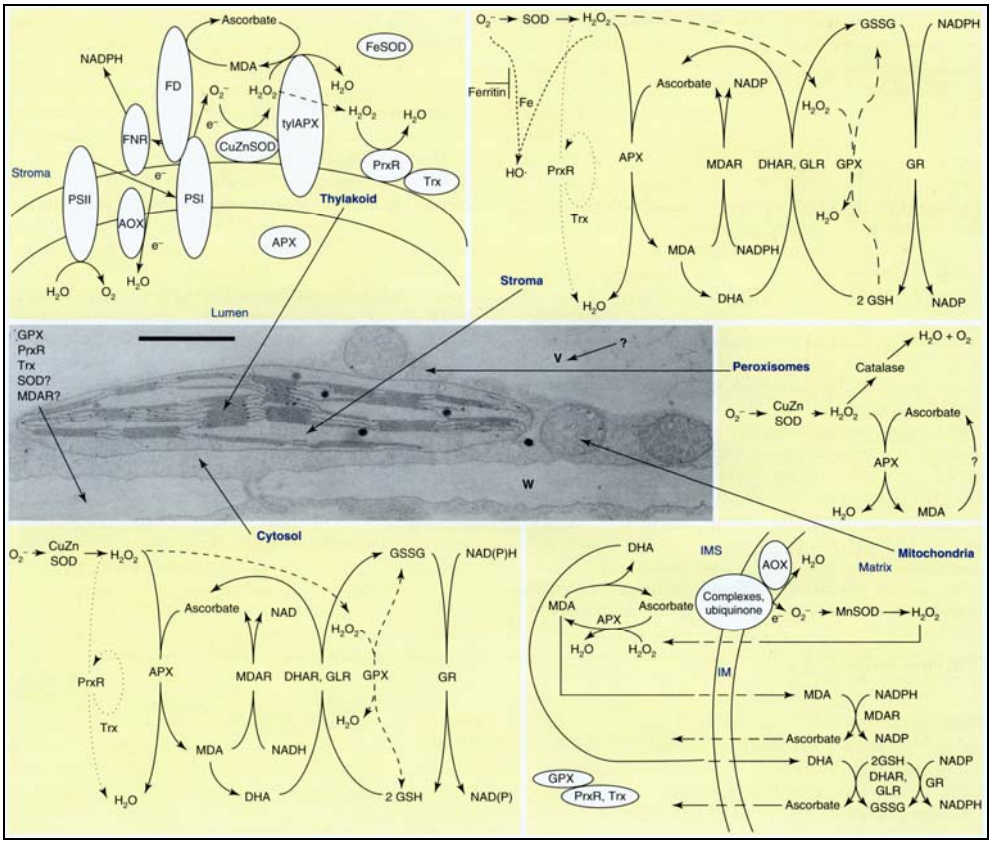

Fig 1.6 *Localization of reactive oxygen species (ROS) scavenging pathways in plant cells (source: Mittler et al., 2004). A transmission electron micrograph of a portion of a plant cell is used to demonstrate the relative volumes of the different cellular compartments and their physical separation (middle left). The enzymatic pathways responsible for ROS detoxification are shown. Membrane-bound enzymes are depicted in white, GPX pathways are indicated by dashed lines and PrxR pathways are indicated by dotted lines in the stroma and cytosol. Abbreviations: AOX, alternative oxidase; APX, ascorbate peroxidase; CAT, catalase; DHA, dehydroascrobate; DHAR, DHA reductase; FD, ferredoxin; FNR, ferredoxin NADPH reductase; GLR, glutaredoxin; glutathione peroxidase (GPX); GR, glutathione reductase; GSH, reduced glutathione; GSSG, oxidized glutathione; IM, inner membrane; IMS, IM space; MDA, monodehydroascorbate; MDAR, MDA reductase; PrxR, Peroxiredoxin; PSI, photosystem I; PSII, photosystem II; SOD, superoxide dismutase; Trx, thioredoxin; tyl, thylakoid; V, vacuole; W, cell wall.*

Fenton reaction	$M^{n+} + H_2O_2 \rightarrow M^{(n+1)+} + {}^{\cdot}OH + OH^-$
Reduction by superoxide	$O_2^{-\cdot} + M^{(n+1)+} \rightarrow M^{n+} + O_2$
Haber-Weiss reaction	$H_2O_2 + O_2^{-\cdot} \rightarrow {}^{\cdot}OH + OH^- + O_2$

Fig. 1.7 *The Haber-Weiss reaction summarizes the production of the hydroxyl radical by the Fenton reaction and the regeneration of M^{n+} by the oxidation of superoxide. M is a redox-active metal such as Fe or Cu.*

The antioxidant ascorbate is present in chloroplasts, cytosol, vacuoles and the leaf cell apoplast. Oxidation of ascorbate occurs in two sequential steps, first producing monodehydroascorbate, and if not rapidly re-reduced to ascorbate, the monodehydroascorbate disproportionates to ascorbate and dehydroascorbate (reviewed by Arora *et al.*, 2002). Glutathione, γ-glutamyl-cysteinyl-glycine (GSH) acts as a disulfide reductant to protect thiol groups of enzymes and it further reacts with singlet oxygen and hydroxyl radicals. It also participates in the regeneration of ascorbate from dehydroascorbate via the enzyme dehydroascorbate reductase (DHAR, EC 1.8.5.1). In such reactions GSH is oxidized to glutathione disulfide (GSSG). GSH is regenerated by glutathione reductase (GR, EC 1.6.4.2) (Arora *et al.*, 2002). The membrane-associated antioxidant, *α*-tocopherol, scavenges hydroxyl radicals, singlet oxygen, superoxide and lipid peroxides (see reviews of Munné-Bosch & Alegre, 2002 and Trebst, 2003). Carotenoids quench singlet oxygen and reduce singlet oxygen generation by absorbing excess excitation energy from chlorophyll (Frank & Cogdell, 1996).

1.5.3 Cd induced oxidative stress

In stress situations, the cellular redox equilibrium is disturbed and the increased ROS production (or reduced antioxidative defence) causes specific oxidative stress responses (Cuypers *et al.*, 2001). As Cd disturbs the cellular redox balance, oxidative stress has been reported to be an important component of the cellular Cd toxicity, irrespective of the exposure concentration or the organism (Semane *et al.*, 2007; Skórzyńska-Polit *et al.*, 2003; Smeets *et al.*, 2005; Stohs & Bagchi, 1995).

Possible underlying mechanisms, which can lead to oxidative stress, are the binding of Cd to sulfhydryl and or carboxyl groups or the replacement of essential cofactors (Zn, Mn, Fe, Ca…) by Cd. Since Cd itself is not redox-active, the increased ROS level should be induced via indirect mechanisms such as interaction with the antioxidative defence system, disruption of electron transport chains or induction of lipid peroxidation. The latter can be the result of a Cd-mediated increase in lipoxygenase (LOX) activity as the increase in LOX activity was found to be important in the oxidative stress induction after Cd application (Djebali *et al.*, 2005). Another potential mechanism for Cd giving rise

to oxidative stress is via the production of H_2O_2 through NADPH oxidase activity (Romero-Puertas *et al.*, 2004).

Chapter 2

Scope and objectives

2.1 Scope

As mentioned in chapter 1, contamination with cadmium is a worldwide problem. Also in Belgium there are several locations with Cd contamination. For example, in the Kempen (north east of Belgium), an area as large as 280 km^2 has become contaminated with Zn, Cd, and Pb because of the historic presence of several zinc smelters (Fig. 2.1). In the areas with the highest contamination (Lommel-Maatheide, (which has been excavated)), no plant life was possible (Fig. 2.2). But also in a large area surrounding the (former) smelters in the Kempen, cross-sectional population studies (CadmiBel and PheeCad) have demonstrated that the soil and various crops (leek, celery, beans and carrots) contain on average six times higher concentrations of cadmium than soil and crops in the control area (Staessen *et al.*, 1992, 1994). As a consequence, a 30% higher cadmium body burden was observed in the inhabitants of the polluted area than in inhabitants of the control area. This increased body burden was positively correlated with the amount of cadmium in the soil and vegetables (Staessen *et al.*, 1995) and was also correlated with several known symptoms as renal tubular dysfunction or damage (Buchet *et al.*, 1990), skeletal demineralisation (Staessen *et al.*, 1999) and increased risk of cancer (Nawrot *et al.*, 2006). Although Hogervorst *et al.* (2007) reported that the largest source of cadmium exposure in the polluted area appears to be house dust, it was confirmed that cadmium in vegetables represents a substantial contribution to the cadmium body burden in adults.

In addition, there is the potential danger to animals that depend upon the plants for survival and to the predators feeding on them. Cadmium can accumulate in their bodies, which can obviously influence biodiversity in a contaminated area. Also livestock consuming contaminated hay, accumulate Cd in their organs, which can enter the food chain. For example, cows may have large amounts of cadmium in their kidneys and liver (Sharma *et al.*, 1979).

Therefore, fundamental knowledge concerning sequestration and toxicity of Cd in plants is important to obtain a more complete picture of the impact of Cd on the environment.

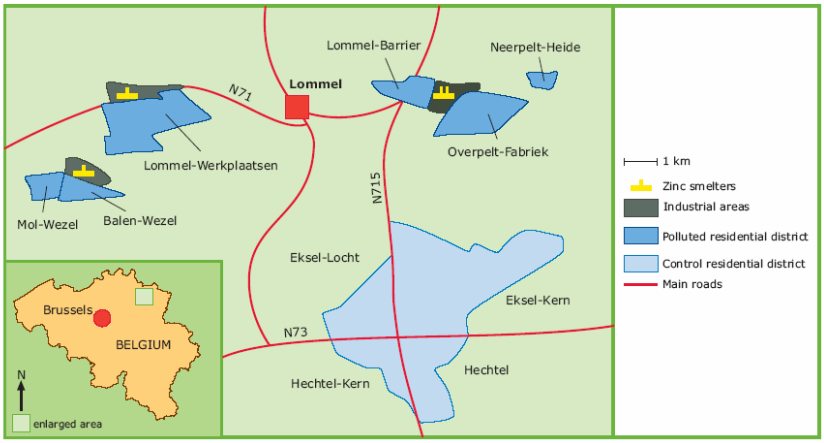

Fig. 2.1 *A drawing representing the localization of Cd contamination in the Kempen in the north east of Flanders, Belgium (source: Staessen et al., 1999).*

Fig. 2.2 *A picture of Lommel-Maatheide, before excavation, illustrating the absence of any plant life because of Zn, Cd and Pb pollution.*

2.2 Objectives

With this work, we tried to obtain additional knowledge concerning the sequestration and toxicity of Cd in the wild-type of *Arabidopsis thaliana* (ecotype Columbia). *Arabidopsis thaliana*, a small herbaceous annual plant belonging to the Brassicaceae, was the chosen study subject because it is a well-known and intensively used model plant in toxicological studies thanks to its widely available genetic information and easy cultivation. Unlike many toxicity studies, where high Cd exposure concentrations are used, this work focused on the investigation of Cd effects on plants exposed during a 21 day period to Cd concentration that were very low (0.1 µM Cd, however the effects were indiscernible from the control and therefore not discussed in the thesis), moderate low (1 µM Cd), moderate high (5 µM) and very high (50 µM). By using these concentrations, we tried to obtain environmentally relevant information on Cd toxicity (for more information about the choice of concentrations and exposure conditions, see chapter 3).

1) The most important part of this thesis was the subcellular localization study of Cd (using energy-dispersive X-ray microanalysis) in roots and leaves of the wild-type *Arabidopsis thaliana* (ecotype Columbia) exposed to environmentally relevant Cd concentrations and processed with an optimized high-pressure freezing/freeze-substitution procedure. The aims of this study were to localize Cd accumulation sites in the apoplast and symplast and to obtain additional information concerning possible transport routes for Cd in the leaves and roots of *Arabidopsis thaliana*. The results of this study are described in chapter 3.

2) Chapter 4 comprises the investigation of the Cd-induced effects on the leaf morphology, ultrastructure and photosynthetic parameters in relation to gene expression of ROS producers (lipoxygenases and NADPH oxidases) and ROS scavenging enzymes (catalase and three isoforms of superoxide dismutase). The aim of this study was to investigate the eventual role of Cd-induced oxidative stress in the cytological and physiological effects.

3) The results in chapter 4 pointed towards a Cd-induced decrease of photosynthesis activity, which was an indication of photoinhibition. Therefore, it was decided to profoundly examine the Cd effects on photosynthesis using chlorophyll *a* fluorescence transient analysis, complemented with quenching analysis and pigment analysis. The results are presented in chapter 5. The aim was to investigate the effects of Cd exposure on the photosystem II, a component known to be very sensitive to stress conditions and photoinhibition.

4) Chapter 6 was dedicated to the fluorimetric detection of Cd-induced singlet oxygen generation in a cell culture of *Arabidopsis thaliana*. Singlet oxygen is a reactive oxygen species of particular interest since it is regarded to be one of the crucial factors in the downregulation of photosystem II, a process which is clearly present in case of Cd exposure. The aims of this pilot study were to develop a fluorimetric analysis assay using the singlet oxygen sensitive fluorescent probe DanePy and to attend an initial series of experiments to elucidate possible pathways of Cd-induced singlet oxygen generation in cells.

Chapter 3

Subcellular localization of cadmium in roots and leaves of *Arabidopsis thaliana*

The results of this chapter have been published in:

Van Belleghem F, Cuypers A, Semane B, Smeets K, Vangronsveld J, d'Haen J, Valcke R. **2007.** Subcellular localization of cadmium in roots and leaves of *Arabidopsis thaliana*. *New Phytologist* **173:** 495-508.

3.1 Introduction

Cd accumulation in roots and leaves has been studied intensively for several plant species, revealing different accumulation strategies for tolerant and nontolerant plants (for a review see Seregin & Ivanov, 2001). However, the interpretation of Cd localization data remains difficult since, even in the same species, different studies using different techniques often deliver conflicting results (e.g. the Cd localization in *Zea mays* to be described). The main source of divergence found among energy-dispersive X-ray microanalysis (EDXMA) studies is most likely a combination of high exposure concentrations and a less adequate sample preparation.

High Cd concentrations are often applied to plants in order to compensate for the loss of elements during chemical fixation using exposure concentrations ranging from 100 µM to 2500 µM. Although these high exposure concentrations are sometimes necessary to enable detection of intracellular Cd, they have highly destructive effects on the cell structure, hindering the examination of Cd distribution within the cells (Vázquez *et al.*, 1992a; Wójcik *et al.*, 2005). In addition, high exposure concentrations are irrelevant, both from a physiological and an ecological point of view. Cd concentrations in the soil solution ranging from 0.32 µM to 1 µM are considered to represent a moderate pollution. Concentrations > 5 µM are considered to be highly polluted (Wagner, 1993).

The quality of the tissue preparation is the key factor in the accuracy of cellular element distribution analysis. Ideally, during fixation, all physiological activity is stopped instantly so that the cellular structure and subcellular distribution of elements are preserved as close to the living situation as possible. The most commonly used chemical fixation (glutaraldehyde) induces loss and redistribution of the elements, particularly during the fixation and dehydration steps (Davies *et al.*, 1991; Antosiewicz & Wierzbicka, 1999). Also the addition of Na_2S to precipitate the elements as a sulfide in the cells and organelles, in order to avoid washing out or delocalization during fixation, does not prevent element loss and, even worse, it causes redistribution and concentration of elements (Vázquez *et al.*, 1992b). High-pressure freezing is presently the only technique

assuring instant fixation of amorphous frozen tissues of *c.* 200 µm (Studer *et al.*, 1995; Shimoni & Müller, 1998). Combined with freeze-substitution, high-pressure freezing is proven sufficient to minimize risks of redistribution of elements in tissues for EDXMA (Orlovich & Ashford, 1995; Ribeiro *et al.*, 2001).

As described in the introduction, the wild-type of *Arabidopsis thaliana* (ecotype Columbia) was the chosen subject because it is a well-known and intensively used model plant in toxicological studies, but as yet little is known about the mechanisms of Cd sequestration in the roots and leaves, particularly at low exposure concentrations.

Recently a transmission electron microscopy (TEM)/EDXMA study was performed on the wild-type *Arabidopsis thaliana* by Wójcik & Tukiendorf (2004). Plants were exposed to a Cd concentration of 100 µM and fixation was performed using glutaraldehyde supplemented with Na_2S (1%, w/v). Cd was identified in dark deposits located in the middle lamella separating the endodermis from the pericycle. No Cd was detected in the cytoplasm, vacuoles and organelles or in cell walls of tissues other than the pericycle.

Further, nuclear microprobe analysis performed by Ager *et al.* (2003) demonstrated that in *Arabidopsis thaliana* (ecotype Columbia) exposed to high concentrations of 100, 250 and 500 µM $CdCl_2$, Cd was sequestered in the central region of the epidermal trichomes of leaves.

The objective of this study was to examine the localization of Cd using EDXMA in leaves and roots of wild-type *Arabidopsis thaliana* (ecotype Columbia) exposed to environmentally relevant Cd concentrations and processed with an optimized high-pressure freezing/freeze-substitution procedure.

3.2 Materials and methods

3.2.1 Plant culture and exposure to cadmium

Seeds of *Arabidopsis thaliana* (L.) Heynh (ecotype Columbia) were vernalized for 2 days at 4 °C and subsequently germinated for 4 days in 1 ml pipette tips (cut off at 1 cm) filled up with moist autoclaved rock wool and placed in a polystyrene board. After germination, the boards with the plants were placed floating in 3 l of $1/10^{th}$ Hoagland nutrient solution (pH 5.75) and grown for 21 days in a growth chamber using a 12 h photoperiod, with 150 µmol m^{-2} s^{-1} PAR at plant level, a 20/18 °C day/night temperature regime and a relative humidity of 65 %. The Hoagland nutrient solution was continuously aerated and refreshed every 3 days.
When 21 days old, the plants were exposed for another 21 days to 0, 0.1, 1, 5 and 50 µM Cd administered as $CdSO_4$ and refreshed every 3 days.

3.2.2 Preparation for electron microscopy and EDXMA

After the exposing period, samples from leaves and roots (immersed in hexadecane) were high-pressure frozen using a Leica EM PACT high-pressure freezer and freeze-substituted from 183 to 269 K in anhydrous acetone for a period of 96 h using a Leica EM AFS automatic freeze-substitution system. The tissues were impregnated and embedded in a Spurr's epoxy resin and 100 nm sections were obtained using a Leica Ultracut UCT ultramicrotome and mounted on coated aluminum grids (50 mesh).

EDXMA was performed in a Philips scanning transmission electron microscope (CM12) equipped with an EDAX PV9900 energy-dispersive X-ray (EDX) analyzer and a super ultrathin window. Micrographs were taken using a GATAN slow-scan CCD camera, the brightness and contrast of the images were optimized with DigitalMicrograph 3.4.3. The sections were analyzed using a single-tilt Be-holder, at an accelerating voltage of 120 kV and with a take-off angle of 45°. The EDX spectra with Cd Lα peaks (3.134 KeV) were recorded during an analysis period of 200 LSEC. The detection limit of the technique was 0.1-0.5 w%. The spectra were analyzed using the Superquant program (EDAX,

San Francisco, CA, USA) which separates the background from element specific peaks and deconvolutes the spectra for the correction of interference between elements. Since the analysis was standard-less, the element distribution was not expressed as weight percent but as a peak to background ratio (P/B) which is the ratio between the specific emission intensity of Cd above background and the nonspecific emission intensity of the background. All measuring parameters (section thickness, beam emission current, spot diameter, tilt angle) were kept constant throughout the analyses; therefore the P/B ratios can be used as a semiquantitative measurement of the element content in different cellular compartments which can be statistically compared (Sela *et al.*, 1990).

3.2.3 Experimental design and statistical analysis

Data presented for each cell compartment in the different tissues are means of 5 replicated measurements which were taken from 3 different plants per treatment. Since the data were not normally distributed, the statistical analysis on the Cd data was performed using the nonparametric *U*-test of Wilcoxon, Mann & Whitney.

3.3 Results and discussion

3.3.1 Effect of Cd on growth and appearance

The physiological and morphological effects of Cd on plants are well-known (see the review by Sanità di Toppi & Gabbrielli, 1999). In the current study, after 21 days of exposure, leaf chlorosis was observed from the concentration of 1 µM Cd, whereas anthocyanous-colored leaves appeared on the plants exposed to 5 µM and 50 µM (Fig. 3.1a). The leaf area was reduced starting at 5 µM Cd. Also inhibition of root growth was observed at the 5 and 50 µM concentrations (Fig. 3.1b). As a consequence, since the high-pressure frozen root diameter was constant (200 µm), the fixated root of plants exposed to 5 and 50 µM Cd was physiologically more developed than the root of plants exposed to the lower Cd concentrations. The sampling locations, indicated by arrows in Fig. 3.1b, demonstrate this fact that evidently had to be taken into account when evaluating the data.

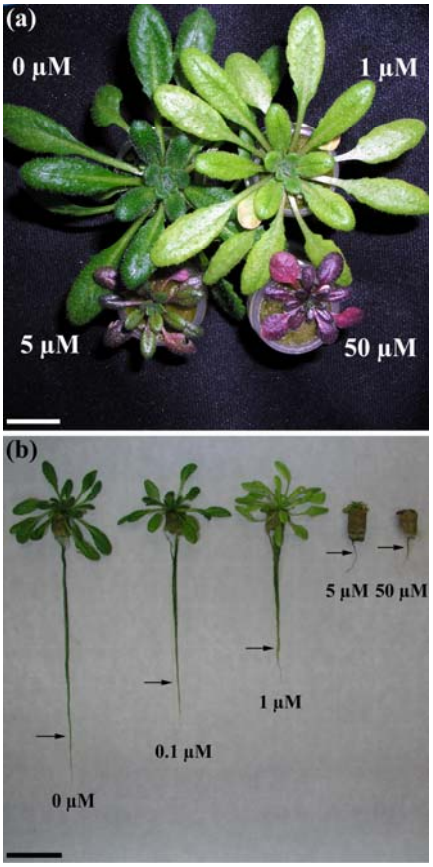

Fig. 3.1 *Effects of cadmium (Cd) toxicity on growth and appearance of Arabidopsis thaliana. (a) Effects of 0, 1, 5 and 50 µM Cd on the shoot. (bar, 1 cm). The bleached appearance of the leaves from the plant exposed to a concentration of 1 µM indicates chlorosis, whereas the growth inhibited leaves of 5 and 50 µM exposed plants are anthocyanous (dark purple) colored. (b) Effects of 0, 0.1, 1, 5 and 50 µM Cd on root growth (bar, 5 cm). The inhibition of root development caused by Cd toxicity explains the differences in age and development of the studied sections. The arrows mark approximately the sampling place for high-pressure freezing (200 µm root diameter).*

3.3.2 Subcellular localization of Cd

In Fig. 3.2, the intracellular Cd content in roots of plants exposed to 1, 5 and 50 µM Cd is presented together with the statistically significant differences in physiologically relevant compartments. When evaluating the Cd content, it is apparent that different exposure concentrations induce different amounts of accumulation. Obviously, plants exposed to the highest concentration (50 µM Cd) revealed the highest Cd accumulation, which at first seems to be more favorable for reliable EDX analysis. However, owing to the Cd toxicity, plasmolytic shrinkage was substantial at the 50 µM concentration, hindering precise subcellular localization of Cd. Moreover, because of plasmolytic shrinkage, the cytoplasmic Cd content was elevated not only by the increased Cd exposure but also as a result of the condensation of the cytoplasm. On the other hand, the 5 µM concentration induced lower (but detectable) Cd

accumulation without the detrimental plasmolytic shrinkage and was therefore much better suited for subcellular localization in *Arabidopsis thaliana*. Exposure to 1 µM Cd caused very low accumulation, whereas no Cd was detected at the 0.1 µM concentration (0.1 µM is therefore not mentioned in the discussion). The plasmolysis at 50 µM made comparison between 5 and 50 µM impossible; as a consequence, statistical comparison was limited to the relevant cell compartments within each exposure concentration. Although Cd was always present in vacuoles of the root exposed to 5 and 50 µM, obtaining reliable measurements of the vacuolar Cd content proved to be difficult. Only the analysis in the endodermal vacuole of plants exposed to 5 µM Cd gave consistent results usable for statistically comparison. Analysis in the leaves of plants exposed to 50 µM Cd designated the tracheids as the sole compartment with a detectable Cd content; this content is not presented in Fig. 3.2 but mentioned in the text.

In order to demonstrate the association of Cd with sulfur or phosphorus in the analyzed cell compartments, the S, P and Cd contents for the exposure concentration of 5 µM are shown in Fig. 3.3.

In this study, several granular deposits were observed in different cell compartments of the root. In Fig. 3.4, an EDX spectrum for each 'type' of granular deposit present in the symplast or apoplast at the 5 µM concentration is presented (Fig. 3.4 a-c, e- g). In addition, a spectrum of the granular deposits in the endodermal symplast (Fig. 3.4d) and Cd detected in the leaf tracheids (Fig. 3.4h) at the 50 µM concentration is included. Finally, a spectrum of the Spurr's epoxy resin is given to prove the absence of Cd, S and P in the resin itself (Fig. 3.4i).

(a)

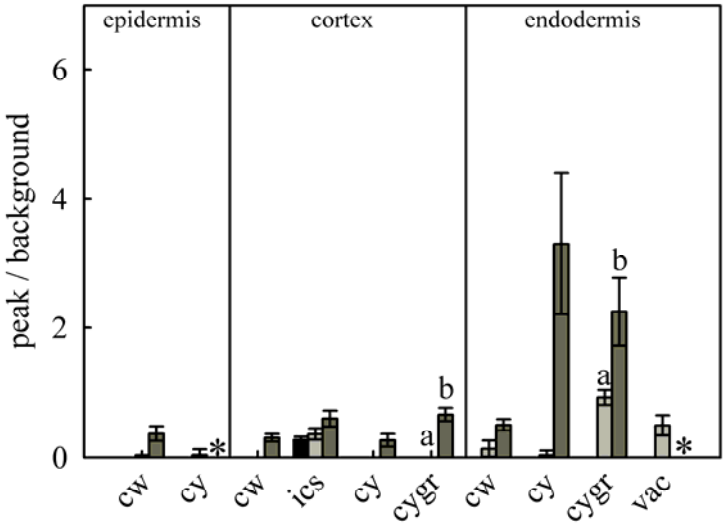
epidermis
cortex
endodermis
peak / background
0
2
4
6
a
b
a
b
*
*
cw
cy
cw
ics
cy
cygr
cw
cy
cygr
vac

(b)

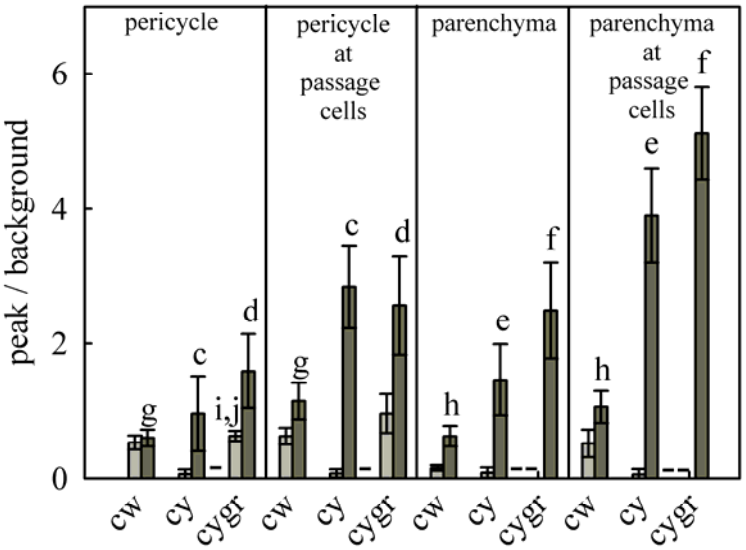
pericycle
pericycle at passage cells
parenchyma
parenchyma at passage cells
peak / background
0
2
4
6
g
c
i,j
d
g
c
d
h
e
f
h
e
f
cw
cy
cygr
cw
cy
cygr
cw
cy
cygr
cw
cy
cygr

(c)

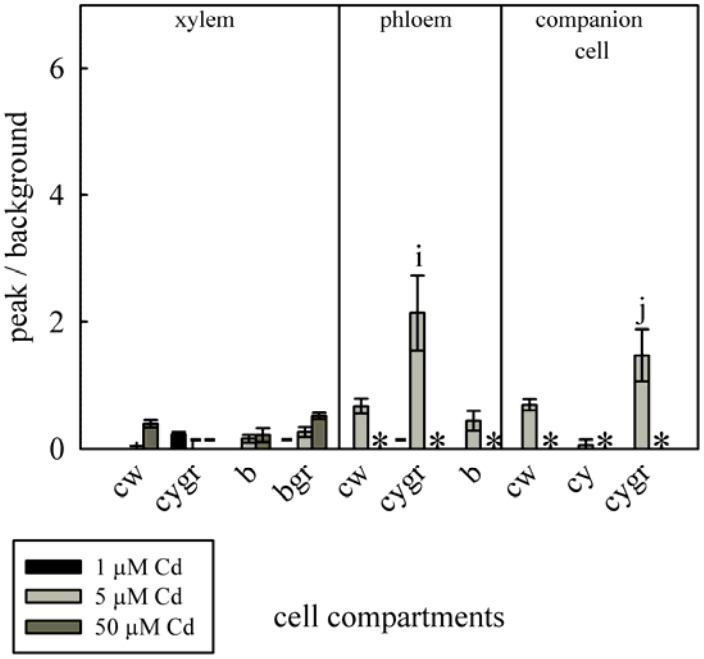

Fig. 3.2 *Contents of cadmium (Cd) in different cell compartments of Arabidopsis thaliana. The measured values are presented as means (± SE). Bars with the same letters (a–j) are significantly different. (a) Epidermis, cortex and endodermis; (b) pericycle, parenchyma of central cylinder; (c) xylem and phloem. cw, cell wall; cy, cytoplasm; ics, intercellular space; vac, vacuole; b, vascular bundle; cygr, granular deposit in cytoplasm; bgr, granular deposit in vascular bundle. *, absent data; –, granular deposit not present.*

(a)

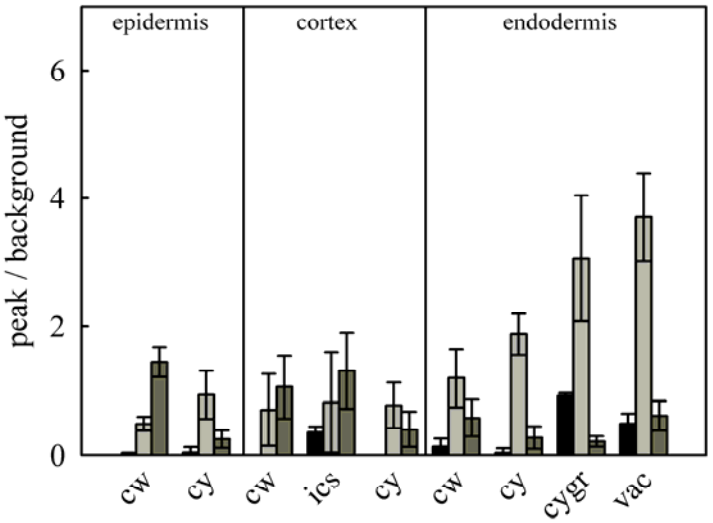
epidermis
cortex
endodermis
peak / background
0
2
4
6
cw
cy
cw
ics
cy
cw
cy
cygr
vac

(b)

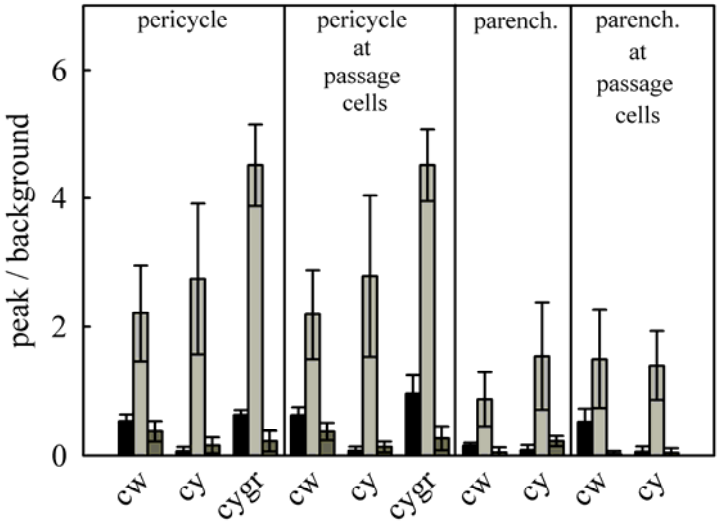
pericycle
pericycle at passage cells
parench.
parench. at passage cells
peak / background
0
2
4
6
cw
cy
cygr
cw
cy
cygr
cw
cy
cw
cy

(c)

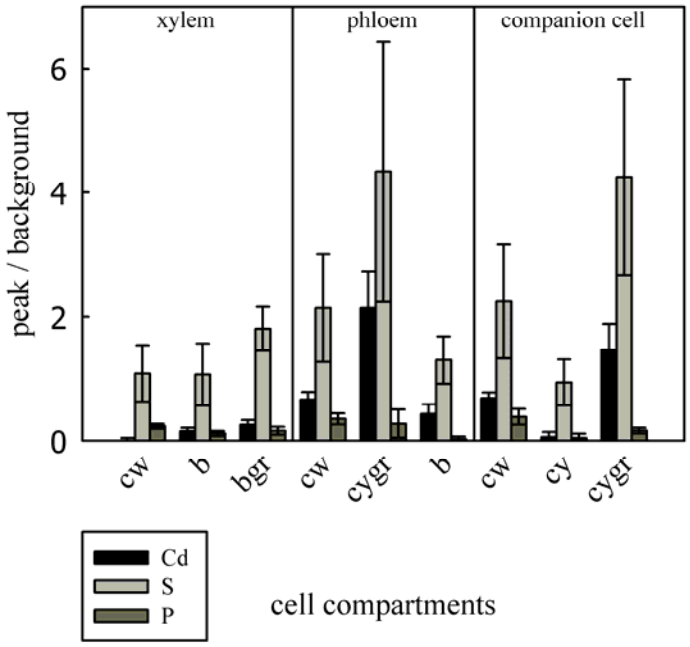

Fig. 3.3 *Association of phosphorus (P) and sulfur (S) with cadmium (Cd) in different cell compartments for Arabidopsis thaliana plants exposed to 5 µM Cd. The measured values are presented as means (± SE). (a) Epidermis, cortex and endodermis; (b) pericycle, parenchyma of central cylinder; (c) xylem and phloem. cw, cell wall; cy, cytoplasm; ics, intercellular space; vac, vacuole; b, vascular bundle; cygr, granular deposit in cytoplasm; bgr, granular deposit in vascular bundle.*

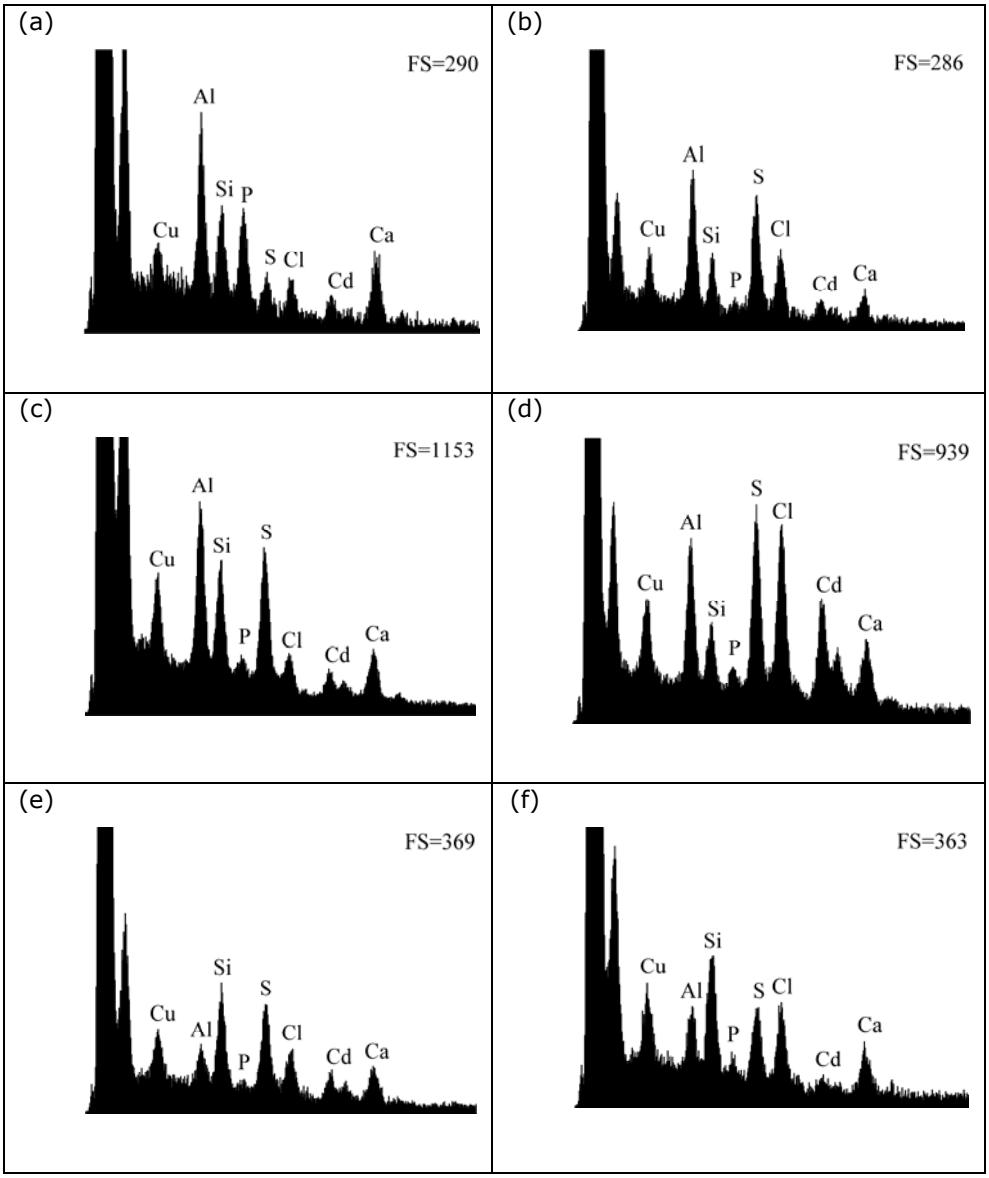
(a)
FS=290
Al
Si
P
Cu
S
Cl
Cd
Ca
(b)
FS=286
Al
S
Cu
Si
Cl
P
Cd
Ca
(c)
FS=1153
Al
Cu
Si
S
P
Cl
Cd
Ca
(d)
FS=939
S
Cl
Al
Cu
Cd
Si
Ca
P
(e)
FS=369
Si
S
Cu
Al
Cl
P
Cd
Ca
(f)
FS=363
Si
Cu
Al
S
Cl
P
Ca
Cd

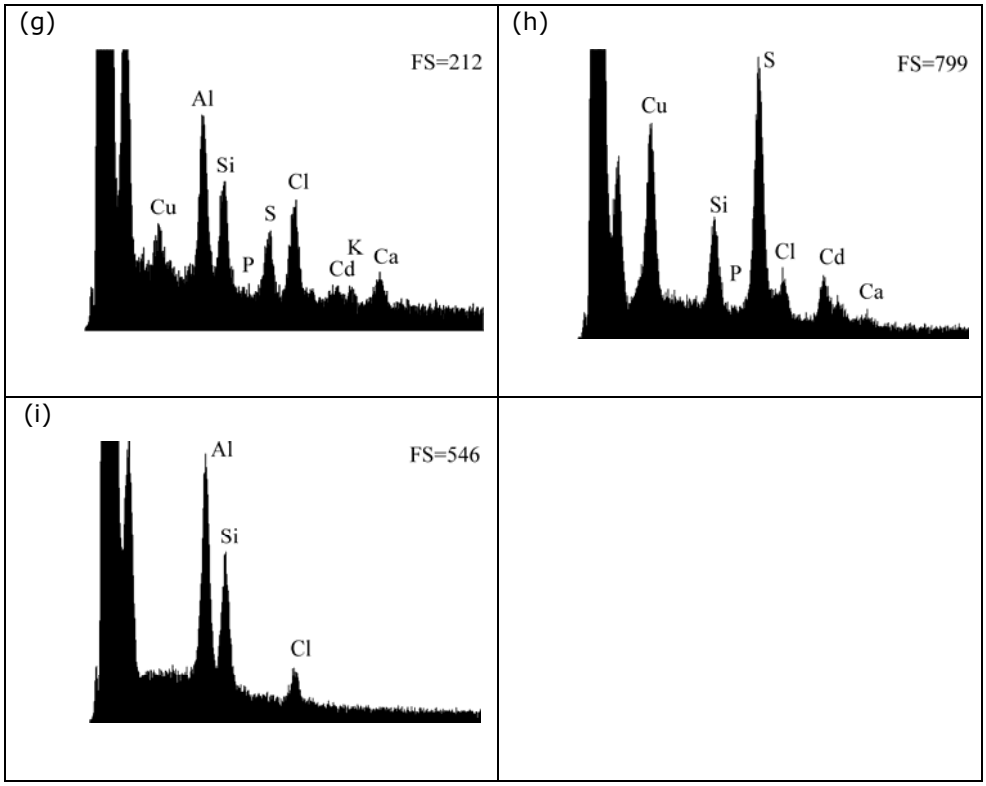

Fig. 3.4 *Energy-dispersive X-ray (EDX) spectra of the granular deposits present in the different cell compartments of Arabidopsis thaliana plants exposed to 5 µM Cd (or 50 µM when noted). The spectra contain the following elements: Cu Lα (0.923 KeV), Al Kα (1.487 KeV, from the aluminum grid), Si Kα (1.74 KeV), P Kα (2.014 KeV), S Kα (2.308 KeV), Cl Kα (2.622 KeV), Cd Lα (3.134 KeV), K Kα (3.314 KeV), Ca Kα (3.692 KeV). FS, impulse number. (a–h) EDX spectrum of the granular deposits bearing Cd in: (a) the cortical apoplast; (b) the endodermal vacuole; (c) the endodermal cytoplasm; (d) the endodermal cytoplasm (50 µM Cd); (e) the pericycle apoplast; (f) the central cylinder apoplast; (g) the bundle of the xylem; (h) the cytoplasm of the tracheids (50 µM Cd), with a large Cu peak originating from the Cu-grid. (i) EDX spectrum of a control measurement taken in the Spurr's epoxy resin (near the section of a tissue from a plant exposed to 50 µM Cd).*

3.3.3 Epidermis and cortex

Ions enter the root by means of a passive process driven by mass flow via the epidermal and cortical apoplast. The negatively charged carboxyl groups of the cell wall provide sites for cation exchange leading to the accumulation of positively charged ions, particularly divalent or polyvalent cations (Marshner, 1995).

Distinctive granular deposits were observed inside the cell wall and intercellular space in cortical tissue of plants exposed to 1, 5 (Fig. 3.5a and spectrum Fig. 3.4a) and 50 µM Cd. EDXMA of these granular deposits clearly demonstrated presence of Cd. Moreover, in plants exposed to low concentrations of Cd (1 µM), the intercellular space of the cortical cell walls was the only site (apart from the cytoplasm of the protoxylem) with detectable amounts of Cd (Fig. 3.2a). This observation supports the hypothesis of Wagner (1993) that at lower concentrations, Cd entering the root is retained in cell walls. Also, in hyperaccumulating plant species such as *Arabidopsis halleri* (in the rhizodermis; Küpper *et al.*, 2000) and *Thlaspi caerulescens* (Vázquez *et al.*, 1992b), the cortical apoplast is regarded as a primary site for Cd accumulation in the root. This result is not, however, in agreement with the EDXMA results of *Phaseolus vulgaris* (Vázquez *et al.*, 1992a) and *Zea mays* (Rauser & Ackerley, 1987; Wójcik & Tukiendorf, 2005), where Cd accumulation was found to be mainly symplastic. However, the latter results conflict with those of an older EDXMA study of Khan *et al.* (1984), revealing Cd accumulation merely in the cell wall between the endodermis and the pericycle of *Zea mays*. Moreover, a cell fractionation study (Lozano-Rodríguez *et al.*, 1997) and a histochemical localization study (Seregin & Ivanov, 1997) revealed the presence of Cd primarily in the apoplast of the *Zea mays* root. These conflicting results indicate the difficulty of the interpretation of Cd localization data as mentioned in the introduction. Nevertheless, based on the observations of the present study it can be concluded that the cortical apoplast of the nontolerant *Arabidopsis thaliana* should be considered as an early sequestration site of Cd in the root.

Distinct amounts of P in the granular deposits localized in the apoplast (Fig. 3.3a and spectrum Fig. 3.4a) suggest the association of Cd with phosphates ($Cd_3(PO_4)_2$). Previous research reported the deposition of Cd as

aggregates with phosphate in endodermal cell walls preventing the transport of Cd to the shoot in *Azolla filiculoides* (Sela *et al.*, 1990). Further, in the hyperaccumulator *Arabidopsis halleri* exposed to 100 µM Cd and 500 µM Zn, Cd phosphates have been observed in the apoplast of the rhizodermis (Küpper *et al.*, 2000). However, since the movement of P in the rhizosphere is limited by diffusion, resulting in depletion rather than accumulation (Marschner, 1995; Küpper *et al.*, 2000), it needs to be verified whether or not phosphate precipitation also occurs under natural environmental conditions.

Despite the high amount of damage to the cytoplasm as a result of the toxic effects of Cd at the highest exposure concentration (50 µM), electron-dense granular deposits containing Cd were observed inside the cortical cytoplasm (Fig. 3.5b). This implies that, at this high exposure concentration, Cd transport from the apoplast into the symplast was detectable by EDXMA. Unfortunately, because of the cellular damage it was not possible to pinpoint precisely the subcellular localization of the granular deposits in the cortex cells. In plants exposed to 1 and 5 µM Cd, similar but much smaller granular deposits were observed in the cytoplasm near the cell wall, but Cd content remained below the detection limit.

Cd may leak into the plant cells most likely via Ca, Fe and Zn uptake systems (Connolly *et al.*, 2002; Perfus-Barbeoch *et al.*, 2002). In addition, energy-dependent transmembrane transport of $CdCl_2$ from the apoplast into the symplast has been described in leaves of *Lepidium sativum* and *Solanum tuberosum* as a means to prevent solute accumulation in the apoplast (Heber *et al.*, 2002). Likewise, the symplastic sequestration presented here is possibly a way of retaining Cd in the cortical symplast, thereby reducing apoplastic transport towards the central cylinder.

The observed intracellular granular deposits were associated with S (50 µM data, not shown) rather than with P, indicating symplastic complexation of Cd with S-containing molecules, most likely Cd-phytochelatins, Cd-phytochelatins-sulfide and/or Cd-sulfide (Vögeli-Lange & Wagner, 1996). Phytochelatins are a family of metal-complexing peptides with a general structure $(\gamma\text{-Glu-Cys})_n\text{-Gly}$, wherein *n* varies from 2 to 11 (Grill *et al.*, 1985), and are synthesized (from glutathione by phytochelatin synthase) in the presence of Cd ions (Grill *et al.*, 1987; Maitani *et al.*, 1996; Schat *et al.*, 2002;

Wójcik & Tukiendorf, 2004, 2005; Semane *et al.*, 2007). Phytochelatins are essential for Cd tolerance in *Arabidopsis thaliana* as shown by Howden *et al.* (1995) in a study comparing a wild-type of *Arabidopsis thaliana* with cadmium-sensitive phytochelatin-deficient *cad1* mutants. The fundamental role in detoxification was further demonstrated through the isolation and expression of the phytochelatin synthase encoding genes from *Arabidopsis thaliana* (CAD1(*AtPCS1*)) and *Schizosaccharomyces pombe (SpPCS)* in *Escherichia coli* (Ha *et al.*, 1999) and the purification of *SpPCS* (Clemens *et al.*, 1999) and *AtPCS1* (Vatamaniuk *et al.*, 1999). These genes were found to be necessary and sufficient for *in vitro* GSH-dependent metal ion activated phytochelatin biosynthesis. It has to be noted, however, that phytochelatin mediated detoxification was found not to be responsible for adaptive Cd-tolerance in *Thlaspi caerulescens* (Ebbs *et al.*, 2002; Schat *et al.*, 2002) and Cd-tolerant *Silene vulgaris* (De Knecht *et al.*, 1992, 1994). Detoxification of Cd by phytochelatins occurs through sequestration, leading to the formation of aggregates of particles containing a Cd-sulfide crystallite core coated with phytochelatins (Reese *et al.*, 1992). Cd associated with phytochelatins has been detected particularly in the vacuole (Krotz *et al.*, 1989; Vögeli-Lange & Wagner, 1990; Nassiri *et al.*, 1997) indicating vacuolar sequestration, an important Cd detoxification process (see reviews by Sanità di Toppi & Gabbrielli, 1999 and Cobbett & Goldsbrough, 2002). Metallothioneins are other well-known cysteine-rich heavy metal-binding protein molecules; but their role in Cd detoxification seems to be of secondary importance, since in higher plants there is no indication of the existence of metallothioneins induced by Cd (Sanità di Toppi & Gabbrielli, 1999; Cobbett & Goldsbrough, 2002). Hence, considering the fact that, in *Arabidopsis thaliana* phytochelatins are strongly induced by Cd, the granular deposits observed in the current study are most likely Cd-sulfide particles coated with phytochelatin complexes as described by Reese *et al.* (1992). Nevertheless, further research (using other techniques, such as µ-EXAFS) is necessary to reveal the true chemical identity of these granular deposits.

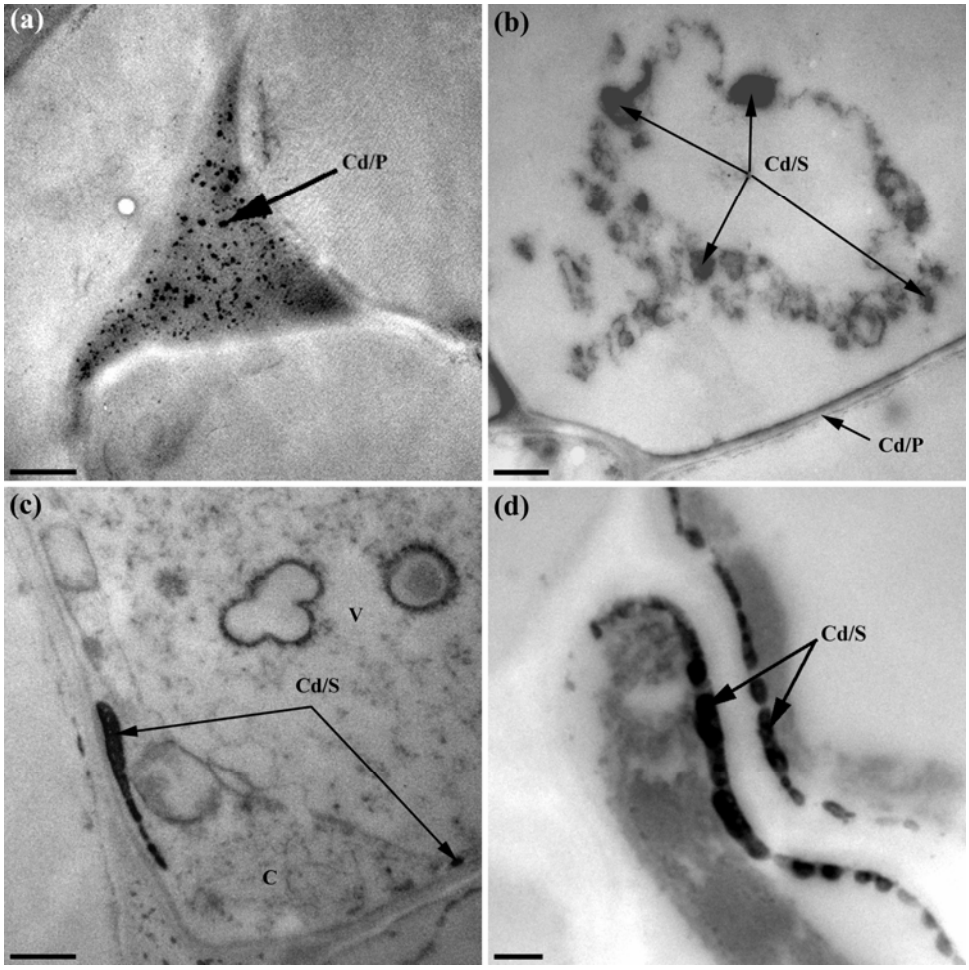

Fig. 3.5 *Electron micrographs illustrating the localization of cadmium (Cd) in the cortex and the endodermis of Arabidopsis thaliana plants. (a) Granular deposits in the intercellular space of the cortex from a plant exposed to 5 µM Cd (bar, 500 nm). (b) Granular deposits in the symplast of the cortex from a plant exposed to 50 µM Cd (bar, 1000 nm). (c) Granular deposits in the endodermis from a plant exposed to 5 µM Cd (bar, 500 nm). V, vacuole; C, cytoplasm. (d) Granular deposits in the endodermis from a plant exposed to 50 µM Cd (bar, 250 nm). Cd/S, granular deposits of Cd associated with sulfur; Cd/P, granular deposits of Cd associated with phosphorus.*

3.3.4 Endodermis

Owing to the presence of Casparian bands on the anticlinal (transverse and radial longitudinal) cell walls, the endodermis forms an effective barrier against apoplastic movement of ions which are routed towards the symplast (see the review by Ma & Peterson, 2003). Our measurements confirm the increased transport towards the endodermal symplast, as plants exposed to 5 and 50 µM Cd revealed a significantly ($P<0.01$) higher Cd accumulation in the cell compartments of the endodermal symplast than in the cortical symplast (Fig. 3.2a bars a, b). As mentioned before, because of less structural damage in the 5 µM exposed plants, the localization of the sequestration inside the endodermis was more precise than in plants exposed to 50 µM Cd. In the former plants, Cd was sequestered as very fine and uniformly distributed granular deposits in the vacuole (Fig. 3.5c and spectrum Fig. 3.4b). However, beside that, a large amount of Cd present in the endodermis was precipitated in the cytoplasm as large granular deposits located near the cell walls (Fig. 3.5c and spectrum Fig. 3.4c). This observation is in agreement with a study of Rauser and Ackerley (1987), reporting the presence of Cd in cytoplasm and vacuoles of mature cortical and stelar cells of the monocotyledons *Agrostis gigantea* and *Zea mays* exposed to 3 µM $CdSO_4$ for 4 days; however it should be mentioned that, in that study, glutaraldehyde fixation was used and no Cd-bearing granular deposits were observed in the cell walls. Using scanning electron microscopy and EDXMA, van Steveninck *et al.* (1990) observed sheet-like deposits of Cd associated with S in the symplast of daughter fronds of *Lemna minor* (exposed to 30 µM Cd), but it was not clear from their results whether the deposits were localized inside the cytoplasm or in the vacuole. Liu and Kottke (2003) observed electron-dense granular deposits in the cytoplasm of parenchyma cells of the monocotyledon *Allium sativum* treated with 100 µM to 1 mM Cd, but the granular deposits were precipitated inside small vesicles. They stated that these electron-dense granular deposits containing Cd (originating from the cell wall) enclosed by vesicles accumulated to form bigger precipitates in correlation with increasing external Cd and prolongation of treatment time. However, according to our observations, the Cd-bearing granular deposits were not associated with any cell organelle or vesicle. Although vesicles (a common effect of Cd toxicity)

were present in the cytoplasm of plants exposed to 5 and 50 µM Cd, no detectable amounts of Cd were found inside these vesicles.

In the endodermis of the 50 µM exposed plants, the number and size of the granular deposits was increased (Fig. 3.5d and spectrum Fig. 3.4d) and a higher content of Cd was measured in the cytoplasmic granular deposits and the cytoplasm compared to the 5 µM exposed plants (Fig. 3.2a). But, as mentioned earlier, the measured concentration in the cytoplasm at this exposure concentration was probably not only elevated by the increased Cd uptake but also by plasmolytic shrinkage.

In addition, as in the vacuoles, Cd accumulated in these granular deposits was associated with S (Fig. 3.3a), suggesting the same phytochelatin-associated sequestration as observed in the (central) cortical symplast. Therefore, two Cd/S sequestration sites seem to be present in the endodermal symplast, namely, vacuolar sequestration and cytoplasmic precipitation. As mentioned before, vacuolar sequestration is well studied and considered to be an important process preventing circulation of free Cd ions within the cytosol leading to Cd detoxification (Sanità di Toppi & Gabbrielli, 1999; Cobbett & Goldsbrough, 2002). The vacuolar transport of low-molecular-weight Cd-phytochelatin complexes (synthesized in the cytoplasm upon elicitation with Cd) and the formation of high-molecular-weight Cd-phytochelatin complexes within the vacuole is regulated in fission yeast *Schizosaccharomyces pombe* by the tonoplast localized *hmt-1* gene (hmt, heavy metal tolerance factor) encoding for the ATP-binding cassette (ABC) transporter HMT-1 (Ortiz *et al.*, 1992, 1995). Also in plants (oat roots) an ATP-dependent, proton gradient-independent activity, similar to that of HMT1, has been identified by Salt & Rauser (1995), whereas in *Caenorhabditis elegans* this process is present as Ce-HMT-1 (Vatamaniuk *et al.*, 2005). The transport of free Cd^{2+} across the tonoplast is also possible via a Cd^{2+}/H^{+} antiport (Salt & Wagner, 1993; Ortiz *et al.*, 1995).

In contrast with the well studied vacuolar sequestration, little is known about the role of cytoplasmic precipitation in regard to the control of cytoplasmic Cd toxicity. Although, as mentioned before, further research is necessary to reveal the true identity of the granular deposits, the observed formation of granular deposits of Cd/S in the cytoplasm is in agreement with the dynamic behavior of phytochelatin complexes, readily accreting small clusters into larger

particles as described by Reese *et al.* (1992). Whether or not this cytoplasmic precipitation acts independently from the vacuolar sequestration remains to be clarified, but since phytochelatin sequestration seems to be the underlying mechanism of both processes, some kind of interaction seems likely.

3.3.5 Central cylinder parenchyma cells

In the apoplast of plants exposed to 5 µM, large Cd-bearing granular deposits were observed in the middle lamella of the cell wall between the endodermis and the pericycle and between the pericycle cells (Fig. 3.6a and spectrum Fig. 3.4e). Similar observations were made in other studies (Khan *et al.*, 1984; Wójcik & Tukiendorf, 2004). However, according to our observations, the granular accumulation was not confined to the pericycle, but present in the cell walls all over the central cylinder. Interestingly, in contrast to the granular deposits in the cell wall between the endodermis and pericycle, these granular deposits were located near the plasmalemma and not in the middle lamella (Fig. 3.6b and spectrum Fig. 3.4f). The shift from the former type of deposits into the latter was observed in the cell walls between the pericycle cells and seems to have occurred in the vicinity of symplastic Cd accumulation (Fig. 3.6c, d). It should be mentioned that, based on a histochemical study, Seregin and Ivanov (2001) hypothesized that the pericycle cell walls have a specific structure and composition that practically force Cd ions out from the apoplastic transport in the stelar cells. Nevertheless, whether or not the observed shift in this study was the result of an active relocation (possibly linked to symplastic sequestration) remains to be determined. EDXMA further revealed that the granular deposits were associated with S (Fig. 3.3b), which clearly differentiates them from the fine granular Cd/P deposits located in the cortical apoplast (Fig. 3.3a). The observed association with S is in agreement with results from Wójcik and Tukiendorf (2004), but since phytochelatins are not believed to be present in the cell wall, the co-occurrence was, according to the authors, supposed to be caused by the formation of cadmium sulfide as a result of the addition of Na_2S during fixation. However, as no Na_2S was added in the current study, comparison with the low S content in the cell wall of unexposed plants (data not shown) clearly revealed that the granular deposits were indeed associated with

S. Further research is necessary to elucidate the chemical identity of these granular deposits.

Symplastic Cd accumulation was limited to the pericycle, marking its importance in reducing Cd transport through the apoplast as described by Seregin and Ivanov (2001). As observed in the endodermis, the symplastic accumulation was localized in the cytoplasm near the cell wall (Fig. 3.6c, d) and was associated with S (Fig. 3.3b). Nevertheless, notwithstanding this symplastic accumulation, the apoplastic sequestration seems to be predominant at this exposure concentration indicating the importance of apoplastic transport towards the xylem.

In plants exposed to 50 µM Cd, the cytoplasm of both the pericycle and the central cylinder parenchyma cells contained substantial amounts of granular Cd accumulation (Fig. 3.7a). Interestingly, a distinct accumulation pattern was observed across the central cylinder (Fig. 3.7b). A significantly ($P<0.01$) higher amount of granular precipitated Cd was found in the cytoplasm of parenchyma cells located between the endodermis and xylem poles compared to the adjacent parenchyma cells (Fig 2b, bars c, d, e, f). The same accumulation pattern (significant, $P<0.05$) was also present in the apoplast (Fig 2b, bars g, h). In fact, this pattern was also present in the apoplast at the 5 µM exposure concentration but not significantly and is therefore not discussed.

The observed pattern seems to be inherent to the presence of passage cells (endodermis cells remaining in state I) located opposite to the xylem poles and present in the roots of numerous plants, including *Arabidopsis thaliana* (Peterson & Enstone, 1996). The role of passage cells in the transport of Cd to the central cylinder has not been investigated as yet, but recently Cholewa & Peterson (2004) provided evidence that although Ca delivered to the xylem may move predominantly or entirely apoplastically, most or all of the Ca transport through the intact endodermis of *Allium sp.* roots is symplastic because of the impermeability of the endodermal Casparian bands to ions. This observation led them to propose that the movement of Ca is possible only through the cytoplasm of the passage cells of the endodermis, making them essential for the transport of Ca to the transpiration stream. Since Ca channels have been reported as Cd permeant (Perfus-Barbeoch *et al*., 2002), these results support

the hypothesis that passage cells are also crucial for the uptake of Cd in the central cylinder. Furthermore, for *Arabidopsis thaliana*, these results also indicate that Cd transport towards the central cylinder occurs, not only at lethal Cd concentrations as reported for *Zea mays* by Segerin and Ivanov (1997), but also at sublethal concentrations.

In summary, the results obtained on plants exposed to 5 µM demonstrate that the Cd sequestration, and most likely also the transport route within the central cylinder, was mainly apoplastic with some symplastic accumulation in the pericycle. When exposed to 50 µM Cd, however, the symplastic Cd sequestration was considerable, with a higher accumulation between the passage cells and the xylem. As in the cortex, symplastic accumulation can most likely be seen as a retention mechanism for high Cd concentrations in the roots, thereby reducing the apoplastic transport to the xylem and eventually the shoot.

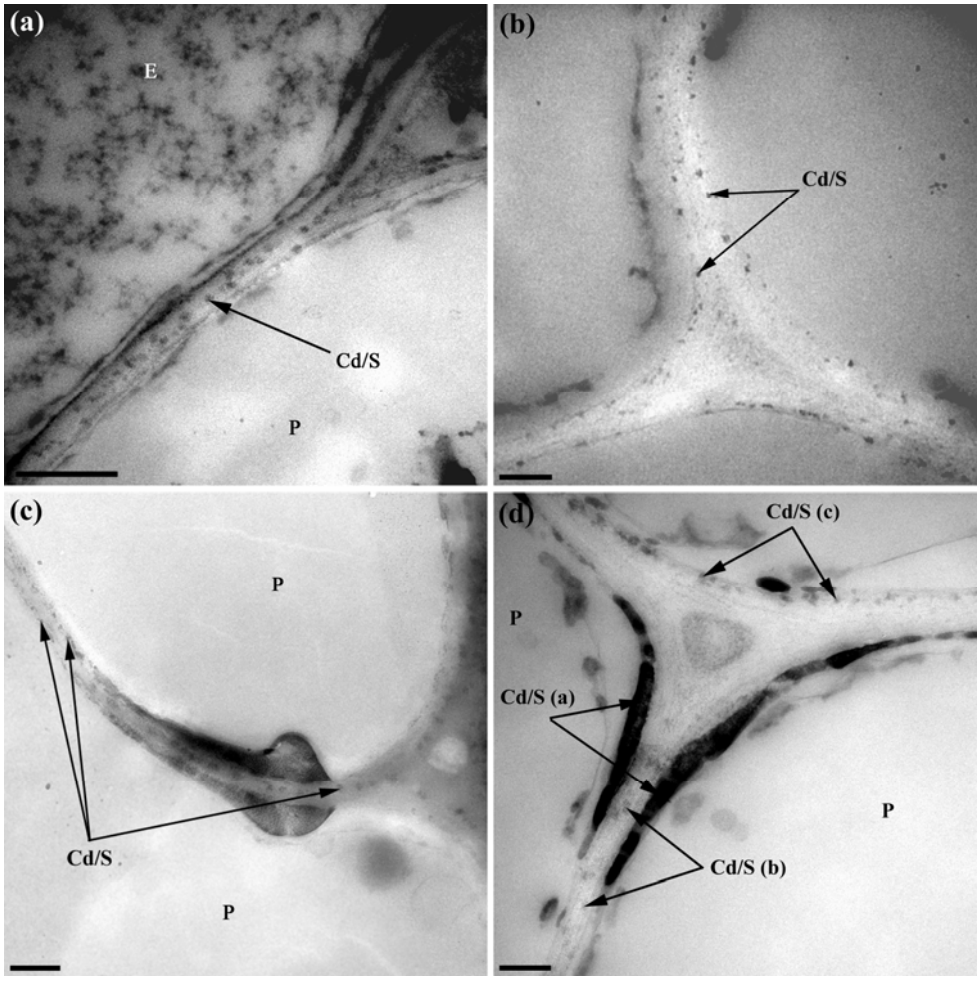

Fig. 3.6 *Electron micrographs (EMs) illustrating the localization of cadmium (Cd) in the apoplast of the central cylinder of Arabidopsis thaliana plants. (a) Granular deposits in the middle lamella of the cell wall between the endodermis and the pericycle from a plant exposed to 5 µM Cd (bar, 250 nm). (b) Granular deposits in the plasmalemma of the parenchyma cells from a plant exposed to 5 µM Cd (bar, 250 nm). (c) EM illustrating the shift of the granular deposits from the middle lamella towards the plasmalemma of the pericycle from a plant exposed to 5 µM Cd (bar, 500 nm). (d) EM illustrating the shift of the granular deposits from the middle lamella towards the plasmalemma of the pericycle from a plant exposed to 5 µM Cd (bar, 250 nm). Cd/S (a) labels the symplastic sequestration, Cd/S (b) labels the granular deposits in middle lamella, Cd/S (c) labels the granular deposits located in the plasmalemma. Cd/S, granular deposits of Cd associated with sulfur; E, endodermis; P, pericycle.*

3.3.6 Xylem and protoxylem

Low Cd content was detected in granular deposits located in the xylem of plants exposed to 1, 5 and 50 µM (Fig. 3.2c). Also measurements in the xylem bundle besides the granular deposits delivered low Cd signals for plants exposed to 5 and 50 µM. However, a pronounced difference was observed between the granular deposits in the xylem of plants exposed to 1 µM (Fig. 3.7c) and those observed in plants subjected to the higher Cd concentrations (5 and 50 µM) as depicted in Fig. 3.7(d). In the former plants, Cd was accumulated in dense granular deposits located in the cytoplasm near the cell wall as observed in the endodermis and central cylinder parenchyma cells. In addition, granular deposits were also present in the intercellular space. As mentioned in section 'Effect of Cd on growth and appearance', in plants exposed to 5 and 50 µM Cd, root growth inhibition resulted in high-pressure frozen roots tissue with xylem that had developed more and where the cytoplasm was no longer present. According to K. Ďurčeková (unpublished), Cd-induced root growth inhibition is at least partially the consequence of Cd-stimulated premature root development involving xylogenesis and root hair formation, which is correlated with shortening of root elongation zone and therefore with root growth reduction. The granular deposits in the xylem bundle were less dense and consisted of a coagulation of very small granular deposits (Fig. 3.7d (inset)). The observed coagulation was probably caused by a freeze-substitution artifact. Since the xylem bundle is an open space filled with amorphous frozen water and ions, it is likely that during the replacement of the amorphous ice by acetone, Cd (bound to organic molecules) has coagulated into larger granular deposits. This observation should be verified by EDXMA on frozen hydrated tissues.

In the xylem, Cd detected in the granular deposits was associated with S (Fig. 3.3c and spectrum Fig. 3.4g). In agreement with this, a recent study of M. Isaure *et al.* (unpublished) using micro X-ray fluorescence (µXRF) and microfocused X-ray absorption near edge structure (µXANES) demonstrated Cd bound to S in vascular bundles of freeze-dried roots of *Arabidopsis thaliana*. In this study, comparison with model compounds indicated the association of Cd with a cysteine-enriched organic molecule such as phytochelatin. Kevrešan *et al.* (2003) described the presence of phytochelatins in the xylem of *Glycine max*

(soybean) as a protection mechanism against Cd toxicity once all binding sites of the xylem cell wall were covered. However, in xylem sap of *Brassica juncea* exposed for 7 days to 0,6 mg l^{-1} Cd (= 5,3 µM Cd), Cd was observed in association with oxygen en nitrogen ligands (not with S as in the remainder of the root), indicating a phytochelatin-independent transport of Cd to the shoot (Salt *et al.*, 1995). The reason why phytochelatins were present in the xylem of *Arabidopsis thaliana* while absent in *Brassica juncea* was presumably because *Brassica juncea* is a Cd accumulator (Kumar *et al.*, 1995) with a high metal transport capacity from the root to the shoot. As a consequence, even under high Cd stress, the transport mechanism of Cd to the shoot was probably unaffected in *Brassica juncea*, whereas the 5 and 50 µM Cd exposure concentrations used in the current study inflicted significant stress in the nontolerant *Arabidopsis thaliana.* Accordingly, the observed association with phytochelatins in the xylem of *Arabidopsis thaliana* should be regarded as a response towards Cd stress. In addition to the role as detoxification mechanism, phytochelatins also seem to contribute to Cd transport. Beside the transport as free Cd ion (Leita *et al.*, 1996), organic acids (citrate), amino acids (e.g. histidine) and nicotianamine are considered to be the main metal chelators facilitating metal transport through the xylem (Cataldo *et al.*, 1988; Krämer *et al.*, 1996; Pich & Scholz, 1996). However, by performing transgenic expression of *TaPCS1* in a phytochelatin-deficient *Arabidopsis thaliana* mutant (*cad1-3*), Gong *et al.* (2003) demonstrated that phytochelatins can be transported through the xylem, consequently enhancing long-distance root-to-shoot Cd transport.

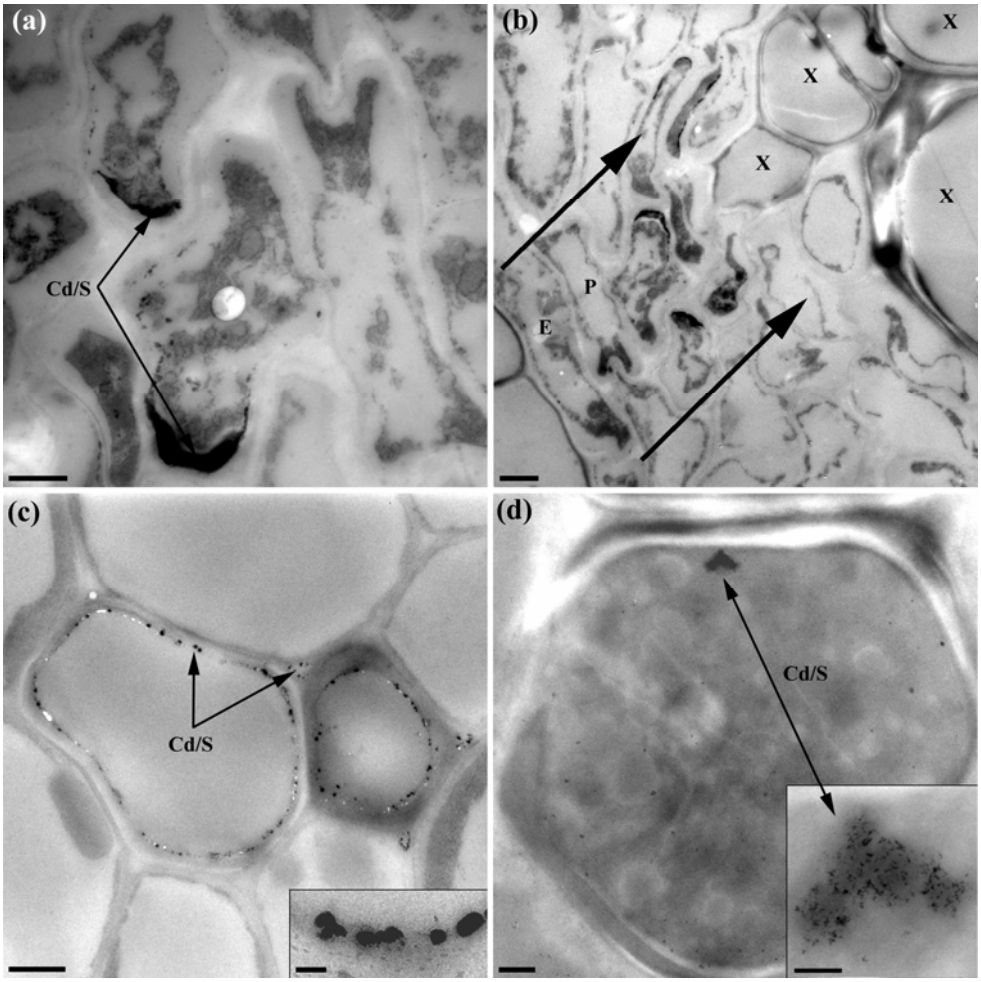

Fig. 3.7 *Electron micrographs illustrating the localization of cadmium (Cd) in the symplast of the central cylinder parenchyma cells and the xylem of Arabidopsis thaliana plants. (a) Large granular deposits in the central cylinder parenchyma cells from a plant exposed to 50 µM Cd (bar, 1000 nm). (b) The central cylinder parenchyma cells from a plant exposed to 50 µM Cd (bar, 2000 nm). The two arrows border the area of high accumulation between the passage cell and the xylem. E, endodermis; P, pericycle; X, xylem. (c) Granular deposits in the cytoplasm of the immature xylem from a plant exposed to 1 µM Cd (bar, 1000 nm). Inset, detail of the granular deposits in cytoplasm (bar, 100 nm). (d) Coagulated granular deposits in the vascular bundle of the mature xylem from a plant exposed to 5 µM Cd (bar 500 nm). Inset, detail of the coagulation (bar, 200 nm). Cd/S, granular deposits of Cd associated with sulfur.*

3.3.7 Phloem cells

As illustrated in Fig. 3.8a, in plants exposed to 5 µM Cd, a very strong accumulation of Cd was detected in the cytoplasm of the phloem and companion cells (Fig. 3.2c). Since no other parenchyma cells in the central cylinder showed such an elevated amount of accumulation, this significantly higher ($P<0.01$) cytoplasmic accumulation (Fig. 3.2b,c, bars i,j) could not be the result of Cd transport across the root but was most likely a result of retranslocation from the shoot. By applying ^{109}Cd to leaves of potato plants (*Solanum tuberosum*), Reid *et al.* (2003) showed that Cd can be rapidly distributed via the phloem to all tissues. Specific retranslocation of Cd in roots has been described by Cakmak *et al.* (2000) with ^{109}Cd applied to the leaves in diploid, tetraploid and hexaploid wheat (*Triticum* sp.). Therefore, this observed retranslocation in the root may be seen as a strategy protecting the shoot by accumulating preferentially in the root as observed in metal excluder plants. There were no granular deposits detected in the phloem bundle so it was not possible to examine the association of Cd with S or other ligands. In literature, the translocation of macromolecules in nonselective and/or selective modes over long distances is well described (Chen & Kim, 2006), but the transport mechanism of metals is still poorly documented (Briat & Lebrun, 1999). Nicotianamine is the sole molecule that has been identified in the phloem sap as a potential phloem metal transporter in association with Fe, Cu, Zn, and Mn (Stephan & Scholz, 1993). However, other unknown metal chelators have been described in the phloem, but the chemical identity and the role of these complexes in the phloem metal-transport needs to be clarified (Briat & Lebrun, 1999). Concerning cytoplasmic sequestration, Cd was associated with S in the phloem and companion cells (Fig. 3.3c), indicating similar symplastic precipitation as observed in the rest of the root.

The other exposure concentrations delivered far less useful information than did the 5 µM concentration. At 1 µM, the Cd content in the phloem was below the detection limit; whereas the extensive accumulation observed in the 50 µM exposed plants completely masked the accumulation pattern in the phloem.

3.3.8 Leaves

A systematical screening of the leaves revealed Cd content below (although sometimes at) the detection limit in mesophyll cells of both the palisade and spongy parenchyma of the high-pressure frozen leaf tissue. The sole site with detectable Cd/S content was located in the cytoplasm of the tracheids of plants exposed to 50 µM Cd (Fig. 3.8b and spectrum Fig. 3.4h), demonstrating the transport of Cd to the shoot. Correspondingly, measurements carried out by Wójcik and Tukiendorf (2004) on chemically fixated leaf tissue of *Arabidopsis thaliana* did not reveal any Cd signal in parenchyma cells (except for some dry edges of the leaf). In fact, the only real accumulation was observed in the central region of the epidermal trichomes by Ager *et al.* (2003) using nuclear microprobe analysis on *Arabidopsis thaliana* exposed to 100, 250 and 500 µM $CdCl_2$.

Although *Arabidopsis thaliana* is considered to be Cd nontolerant, it possesses basic metal tolerance allowing the regulation of metal homeostasis (Clemens, 2001) and in *Arabidopsis thaliana* (as in most plants) this is achieved by retaining Cd in the root (Bovet *et al.*, 2003). This excluder strategy of *Arabidopsis thaliana* has also been detected under exposure to excess Zn (Becher *et al.*, 2004; Weber *et al.*, 2004). Evidently, the shoot excluder strategy offers an explanation as to why, in the current localization study, Cd content in the mesophyll tissue was so low. Our results further indicated that the shoot excluder strategy is actually a combination of, on the one hand, Cd retention in the root (acting as a barrier) and, on the other, Cd retranslocation through the phloem from the leaves back towards the roots.

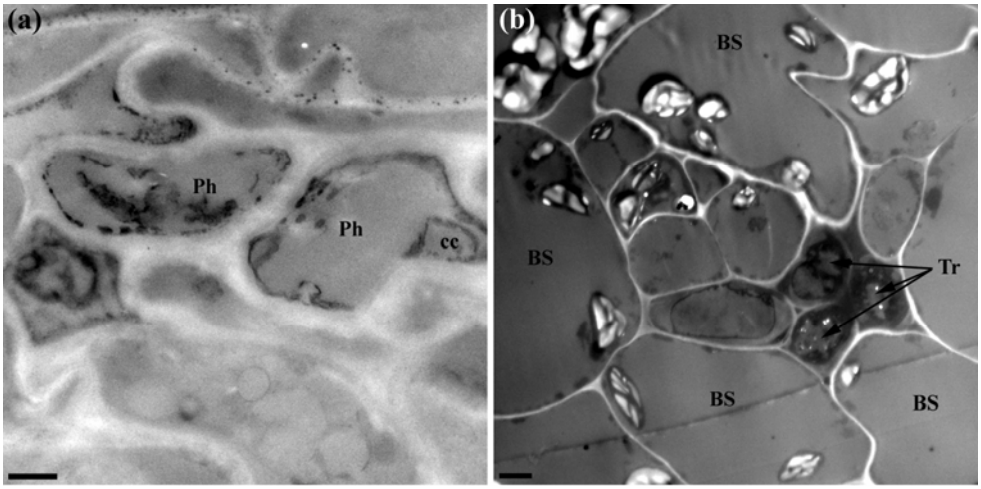

Fig. 3.8 *Electron micrographs (EMs) illustrating the localization of cadmium (Cd) in the root phloem and the leaf tracheids of Arabidopsis thaliana plants. (a) Granular deposits in the cytoplasm of the phloem and the companion cells from a plant exposed to 5 µM Cd (bar, 1000 nm), Ph, phloem cell; cc, companion cell. (b) Cd accumulation (recognizable as dark areas) in the cytoplasm of the leaf tracheids from a plant exposed to 50 µM Cd (bar, 1000 nm). Tr, tracheids; BS, bundle sheath.*

3.4 Conclusion

Exposing plants to lower Cd concentrations in combination with the use of high-pressure freezing and freeze-substitution is clearly an improvement over the generally applied high-concentration exposure and chemical fixation and dehydration. In this way, cytoplasmic precipitation of Cd, associated most likely with phytochelatins, was demonstrated beside the vacuolar sequestration. In addition, the presence of two types of granular deposits in the apoplast of the central cylinder was revealed. Moreover, it enabled us to draw a more precise image of the transport routes and sequestration sites of Cd in the root of *Arabidopsis thaliana*.

Since the transport route of Cd through the cortex is mainly apoplastic, the Cd/P accumulation may be regarded as an early sequestration site, whereas the cytoplasmic accumulation should be seen as a mechanism to retain Cd in order to reduce the apoplastic transport towards the central cylinder. The transport through the endodermis is forced through the symplast because of the

presence of Casparian bands, leading to vacuolar sequestration and cytoplasmic precipitation.

In the central cylinder, the sequestration (and consequently also the transport) of Cd appears to be mainly apoplastic, again with cytoplasmic accumulation decreasing Cd transport to the xylem. Furthermore, a distinct accumulation pattern suggests the passage cells being important in the migration of Cd to the central cylinder.

According to our findings, the sequestration in the root is further enhanced by the retranslocation of Cd from the leaves back towards the roots, confirming the excluder strategy of *Arabidopsis thaliana*.

3.5 Perspectives

Further analysis (μ-EXAFS) should be performed to reveal the true chemical identity of the granular deposits. In this way, it should be possible to discern cytoplasmic, vacuolar and apoplastic sulfur-associated granular deposits.

It would also be interesting to study Cd complexation in a GSH deficient *Arabidopsis* mutants for example *cad2-1* (±30 % GSH; Cobbett *et al.*, 1998) and/or *rml1* (3 % GSH; Vernoux *et al.*, 2000), to study the inhibitiory effects on the phytochelatin sequestration.

As the plants in this study were grown and exposed in a Hoagland nutrient solution, it would be interesting to compare these results with analysis results of plant grown and exposed in soil. This might for instance influence apoplastic accumulation in the cortex.

Chapter 4

The effects of Cd on the morphology and ultrastructure of *Arabidopsis thaliana* leaves in relation to oxidative stress.

4.1 Introduction

4.1.1 General background

Apart from the effects of Cd on the morphology and physiology (reviewed by Benavides *et al.*, 2005; Deckert, 2005; Sanità di Toppi & Gabbrielli, 1999), also the effects on the ultrastructure of particularly the chloroplast are well documented (Ouzounidou *et al.*, 1997; Rascio *et al.*, 1993; Skórzyńska-Polit *et al*., 1995). It was thereby reported that the destruction of the membranes are one of the major ultrastructural effects leading to, for instance, the disorganisation of the thylakoid system. Membrane damage has been reported to be the result of the peroxidation of unsaturated lipids in biological membranes, which is one of the most prominent symptoms of oxidative stress (Djebali *et al.*, 2005). As described in the general introduction (chapter 1.5.3), since Cd disturbs the cellular redox balance by interfering with the antioxidative system, oxidative stress has been reported to be an important component in the cellular Cd toxicity (Semane *et al.*, 2007; Skórzyńska-Polit *et al*., 2003; Smeets *et al.*, 2005; Stohs & Bagchi, 1995). In addition, also Cd-mediated increases in lipoxygenase (LOX) activity (Djebali *et al.*, 2005) and NADPH oxidase activity (Romero-Puertas *et al.*, 2004) have been related to increased oxidative stress.

In this study, some morphological, ultrastructural and physiological effects of Cd were related with induction of the oxidative defence system.

4.1.2 Objective

The aim of the present work was to investigate the effects of exposure to toxic Cd concentrations on physiological parameters, leaf morphology and ultrastructure of *Arabidopsis thaliana* in relation to gene expression of ROS producers (LOX1/2 and RBOHD/F/C) and ROS scavenging enzymes (CAT, CuZn-SOD, Fe-SOD and MnSOD).

4.2 Materials and methods

4.2.1 Plant Culture

Seeds of *Arabidopsis thaliana* (L.) Heynh (ecotype Columbia) were vernalized for 2 days at 4 °C and subsequently germinated for 4 days in 5 ml pipette tips (cut off at 1 cm) filled up with moist autoclaved rock wool and placed in a polystyrene board. After germination, the boards with the plants were placed floating in 3 l of $1/10^{th}$ Hoagland nutrient solution (pH 5.75) and grown for 21 days in a growth chamber using a 12 h photoperiod, with 150 µmol m^{-2} s^{-1} PAR (photosynthetic active radiation) at plant level, a 20/18 °C day/night temperature regime and a relative humidity of 65 %. The Hoagland nutrient solution was continuously aerated and refreshed every 3 days.
When 21 days old, the plants were exposed for another 21 days to 0, 1, 5 and 50 µM Cd administered as $CdSO_4$ and refreshed every 3 days.

4.2.2 H_2O_2 measurement

The Amplex Red Hydrogen Peroxide/Peroxidase Assay Kit (Molecular Probes, Inc) was used to measure the hydrogen peroxide (H_2O_2) levels in the leaves. This is a one-step fluorimetric method that uses 10-acetyl-3,7-dihydroxyphenoxazine to detect H_2O_2. A triplicate of 50 mg leaf samples was processed for each exposure concentration and measured together with a H_2O_2 standard curve. The fluorescence emission (590 nm) was measured at an excitation wavelength of 530 nm using a PTI (Photon Technology International) QuantaMaster Model QM-6/2005 spectrofluorometer equipped with FeliX32 Software & BryteBox Interface.

4.2.3 Water content and gas exchange measurements

The water content of the shoot was calculated relative to the dry weight. The stomatal conductance to water vapour (g_s, mol H_2O m^{-2} s^{-1}) and photosynthesis rate (A, µmol m^{-2} s^{-1}) were measured using a LCA4 (ADC Bioscientific Ltd., Hoddesdon, UK) infrared gas analyzer for 4 plants simultaneously, positioned under a glass cuvette (at 150 µmol photons m^{-2} s^{-1} PAR and 20 °C). A triplicate of 4 plants was used for each Cd exposure concentration.

4.2.4 Light microscopy

Samples from leaves of equal age were fixed for 4 hours at 4 °C in 2 % glutaraldehyde and malachite green 0.01 %, buffered in 0.05 M sodium-PIPES (pH 7.5). After dehydration in a graded ethanol series, the tissues were impregnated and embedded in paraffin. Sections (8 µm) were obtained using a Leica MS 2000R rotary microtome equipped with steel knives. The sections were stained with safranine and aniline and mounted on DePex (BDH). The tissues were examined using a Polyvar Reichert-Jung interference microscope and the images were digitized with an Olympus camedia C-5050 zoom digital camera.

4.2.5 Electron microscopy

Samples (max 1 mm^2) from leaves of equal age were fixed using vacuum infiltration for 4 hours at 4 °C in 2 % glutaraldehyde and 0.01 % malachite green, buffered in 0.05 M sodium-PIPES (pH 7.5). The fixed tissues were rinsed 3 times 30 minutes in 0.05 M sodium-PIPES (pH 7.5) and post-fixed in 2 % osmium tetroxide, buffered in 0.2 M sodium cacodylate at 4 °C. Subsequently, the tissues were rinsed once in 0.2 M sodium cacodylate and twice in aq. dest. before staining in 2 % uranyl acetate (in aq. dest.) overnight. After dehydration in a graded acetone series, the tissues were impregnated and embedded in Spurr's epoxy resin. Ultrathin sections (65 nm) were obtained using a Leica Ultracut UCT ultramicrotome and mounted on coated copper grids (50 mesh). The sections were examined using a Philips EM 208S transmission electron microscope operating at 80 kV and digitized with a Morada 3.0 TEM

camera controlled by iTEM FEI (version 5.0) software from Olympus Soft Imaging Solutions GmbH. The spongy parenchyma cell size, the palisade parenchyma cell height to width aspect ratio, and the cuticle thickness were measured on digitized sections (magnification = 11000 x) using iTEM FEI (version 5.0) software. Three plants were examined per exposure concentration, with a total of 25 measurements per plant.

4.2.6 Analysis of gene expression

Frozen leaf tissue (approximately 100 mg) was ground thoroughly in liquid nitrogen using a mortar and pestle. RNA was extracted using the RNeasy Plant Mini Kit (Qiagen). The concentration of the RNA was determined spectrophotometrically at 260 nm (Nanodrop, Isogen Life Science). The RNA purity was also checked spectrophotometrically by means of the 260/280-ratio. First strand cDNA synthesis was primed with an oligo$(dT)_{16}$-primer according to the manufacturer's instructions using Taqman Reverse Transcription Reagents (Applied Biosystems), and equal amounts of start material (RNA) were used (1 µg). Quantitative PCR was performed with the ABI Prism 7000 (Applied Biosystems), Taqman chemistry. Assay mixes (primers and probes) were designed and optimized by Assays-by-design (Applied Biosystems) and following genes were determined: *RBOHC* (At5g51060), *RBOHD* (At5g47910), *RBOHF* (At1g64060), *LOX1* (At1g55020), *LOX2* (At3g45140), *FSD1* (At4g25100), *CSD2* (At2g28190), *CAT1* (At1g20650) and *MSD1* (At3g10920). As a reference gene *ACT2* (At3g18780) was used. PCR amplifications were performed in a total volume of 25 µl, containing 5 µl cDNA sample, 12.5 µl Taqman Universal Master Mix (Applied Biosystems), 1.25 µl assay mix and 6.25 µl RNase-free H_2O. All samples were tested in duplicate for the housekeeping gene as well as for the genes of interest.

The efficiencies of the target genes related to the reference gene were examined and approved. Gene expression data were calculated relatively to the reference gene following the $2^{-\Delta\Delta Ct}$ method (Livak & Schmittgen, 2001).

4.2.7 Statistics

Since our data, after testing with the Shapiro–Wilk-test and Levene-test, revealed nonnormality and nonconstancy of error terms (Neter *et al.*, 1996), the statistical analyses were based on a nonparametric Kruskal–Wallis and a post hoc multiple comparison test (Lehmann, 1975). All data are presented relative to the control (1: marked as a dashed line in the graphs) ± S.E. and significance ($P<0.05$) is marked with and asterisk.

4.3 Results

4.3.1 Effects on growth and physiological parameters

In the current study, after 21 days of exposure, leaf chlorosis was observed in plants exposed to 1 µM Cd, whereas anthocyanous-coloured (purplish-red) leaves appeared in the 5 µM Cd and 50 µM Cd exposed plants (Fig. 4.1). The inhibition of growth (depicted in Fig. 4.2a as fresh weight relative to the control), already significant at 1 µM Cd, was more pronounced at the higher Cd concentrations. Compared to the control, the water content decreased slightly at 5 µM Cd whereas a strong decrease was observed at 50 µM Cd (Fig. 4.2b). Stomatal conductance (Fig. 4.2c) and photosynthesis rate (Fig. 4.2d) were significantly decreased at all Cd exposure concentrations.

Fig. 4.1. *Photographs illustrating the morphological effects on growth and appearance of Arabidopsis thaliana seedlings exposed during 3 weeks to 0, 1, 5 and 50 µM Cd (bar, 10 mm).*

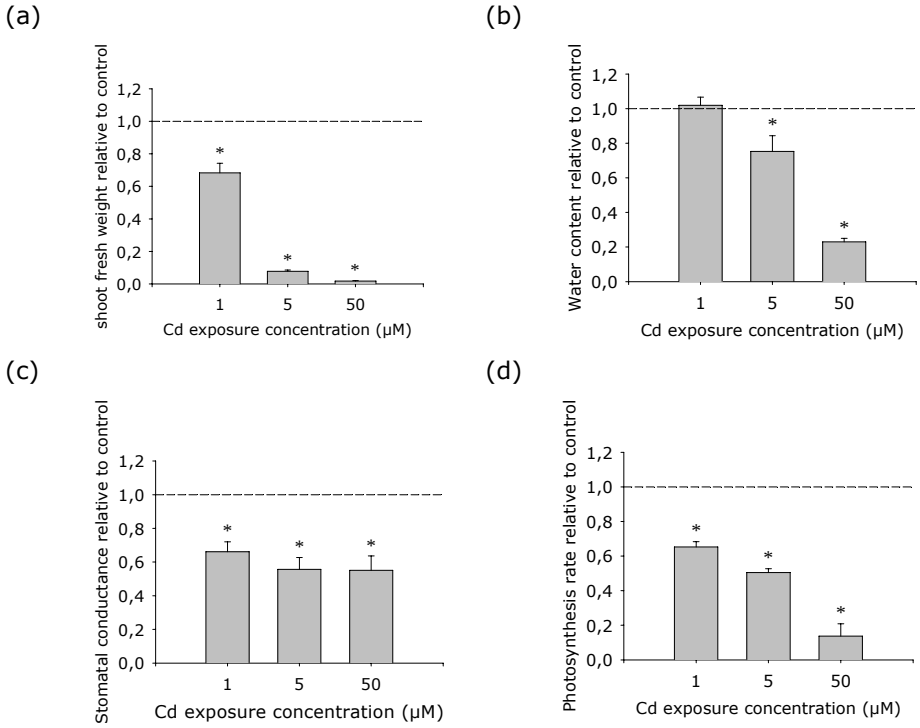

Fig. 4.2. *Cd-induced physiological effects on Arabidopsis thaliana seedlings exposed during 3 weeks to 0, 1, 5 and 50 µM Cd. (a) fresh weight of the shoot, (b) water content of the shoot, (c) stomatal conductance, (d) photosynthesis rate. All values are presented relative to the control (1: marked as a dashed line) ± SE. Bars marked with an asterisk are significantly different from the control (P<0.05).*

4.3.2 Effects on palisade cell shape, mesophyll cell size and cuticle thickness

Compared to the light micrograph of the control plants (Fig. 4.3a), morphological changes at the cell level were observed at all Cd exposure concentrations (Fig. 4.3b, c, d). More specifically, exposure to all Cd concentrations caused a reduction in spongy parenchyma cell size (Fig. 4.4a) and the height to width aspect ratio of the palisade cells decreased significantly at 1 µM Cd to become approximately 1 (spherical) at 5 and 50 µM Cd (Fig. 4.4b). The cuticle thickness was significantly increased at 5 and 50 µM Cd (Fig. 4.4c).

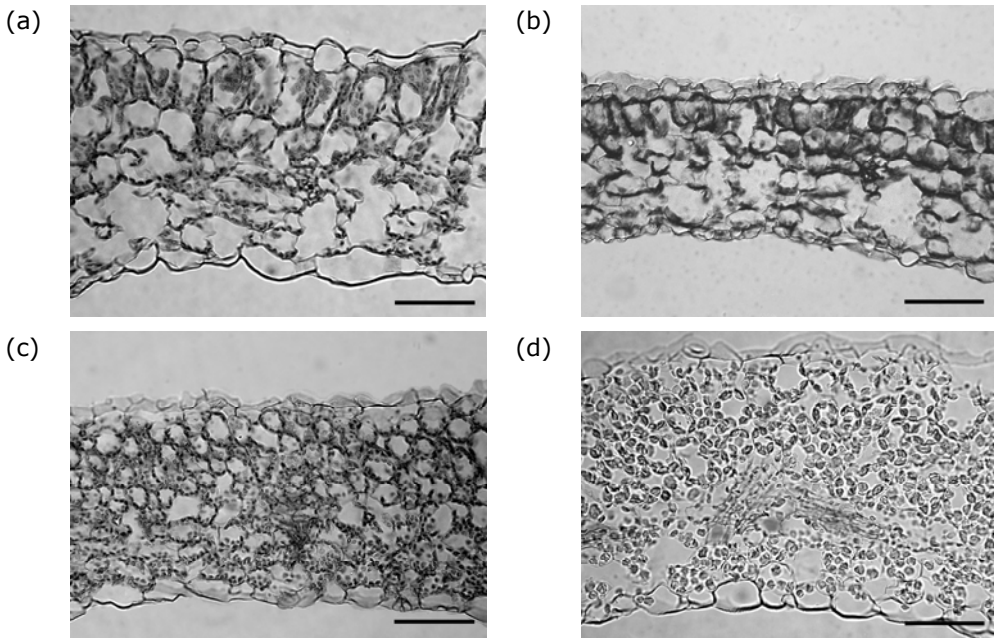

Fig. 4.3. *Light micrographs illustrating the effects on the leaf structure of Arabidopsis thaliana seedlings exposed during 3 weeks to 0, 1, 5 and 50 µM Cd (bars, 25 µm). Cross-section of a leaf of Arabidopsis thaliana exposed to (a) 0 µM Cd, (b) 1 µM Cd, (c) 5 µM Cd and (d) 50 µM Cd.*

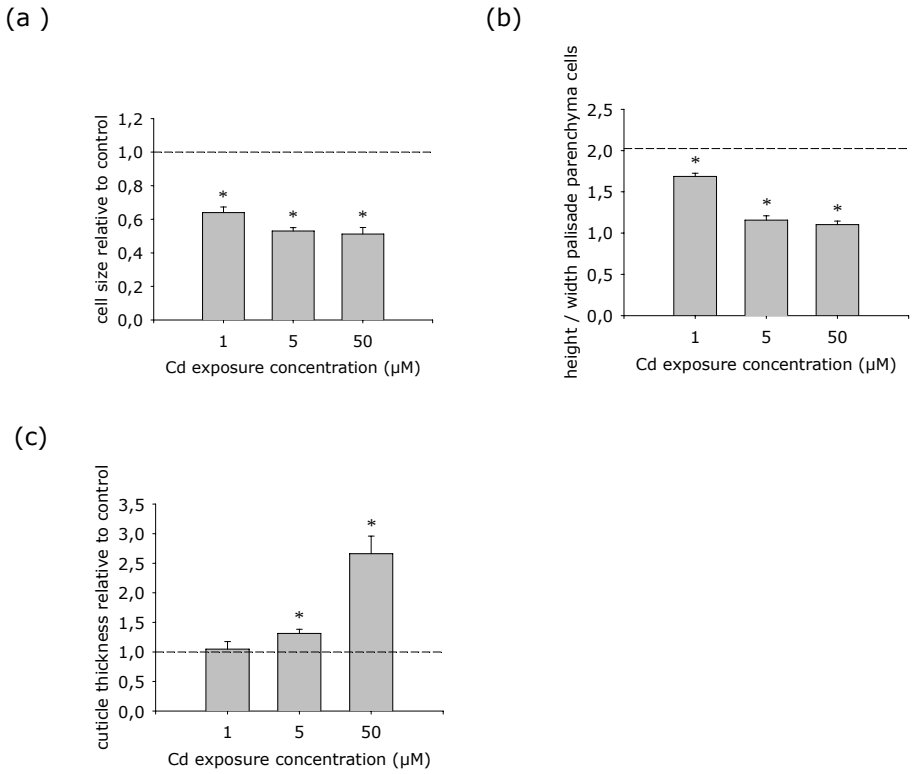

Fig. 4.4. *Cd-induced effects on cell size, cell shape and cuticle thickness of Arabidopsis thaliana seedlings exposed during 3 weeks to 0, 1, 5 and 50 µM Cd. (a) spongy parenchyma cell size, (b) palisade parenchyma cell height to width aspect ratio, (c) thickness of the cuticle. The values of (a) and (c) are presented relative to the control (1: marked as a dashed line) ± SE, whereas (b) represents the original data ± SE (the control is marked as a dashed line). Bars marked with an asterisk are significantly different from the control (P<0.05).*

4.3.3 Effects on chloroplasts and mitochondria

The chloroplasts of the control plants were typical mesophyll chloroplasts (Fig. 4.5a) with a clearly visible envelope, a well developed inner membrane structure composed of regularly arranged grana stacks and stromal membranes (Fig. 4.5b). Additionally, starch granules as well as less and more electron-dense plastoglobuli (lipid droplets) were present in the stroma. In chloroplasts of plants exposed to 1 µM Cd, there was no indication of membrane damage but the grana stacking was reduced considerably (Fig. 4.5c,d). At 5 µM Cd, the distension of the chloroplast envelope and a large fraction of the thylakoids, together with the increased amount of plastoglobuli suggested the deterioration of the membrane integrity. In addition, the starch accumulation decreased considerably, changing the typically discoidal shape of the chloroplast into a more deflated appearance (Fig. 4.5e,f). At 50 µM Cd, the bloated chloroplasts were almost entirely filled up with enormous starch granules (Fig. 4.5g). The stroma between the starch granules contained heavily distended thylakoid membranes with an undulating appearance and large electron-dense plastoglobuli (Fig. 4.5h). Ultrastructural effects of Cd on mitochondria were observed at the highest exposure concentration only; *i.e.* a slightly distended outer membrane and a decreased density of the mitochondrial matrix (data not shown). Nevertheless, since no visible effects on the structural organisation of the mitochondria could be observed, their functional activity probably remained unaffected. No effects on the nucleus, endoplasmic reticulum and Golgi complex were observed.

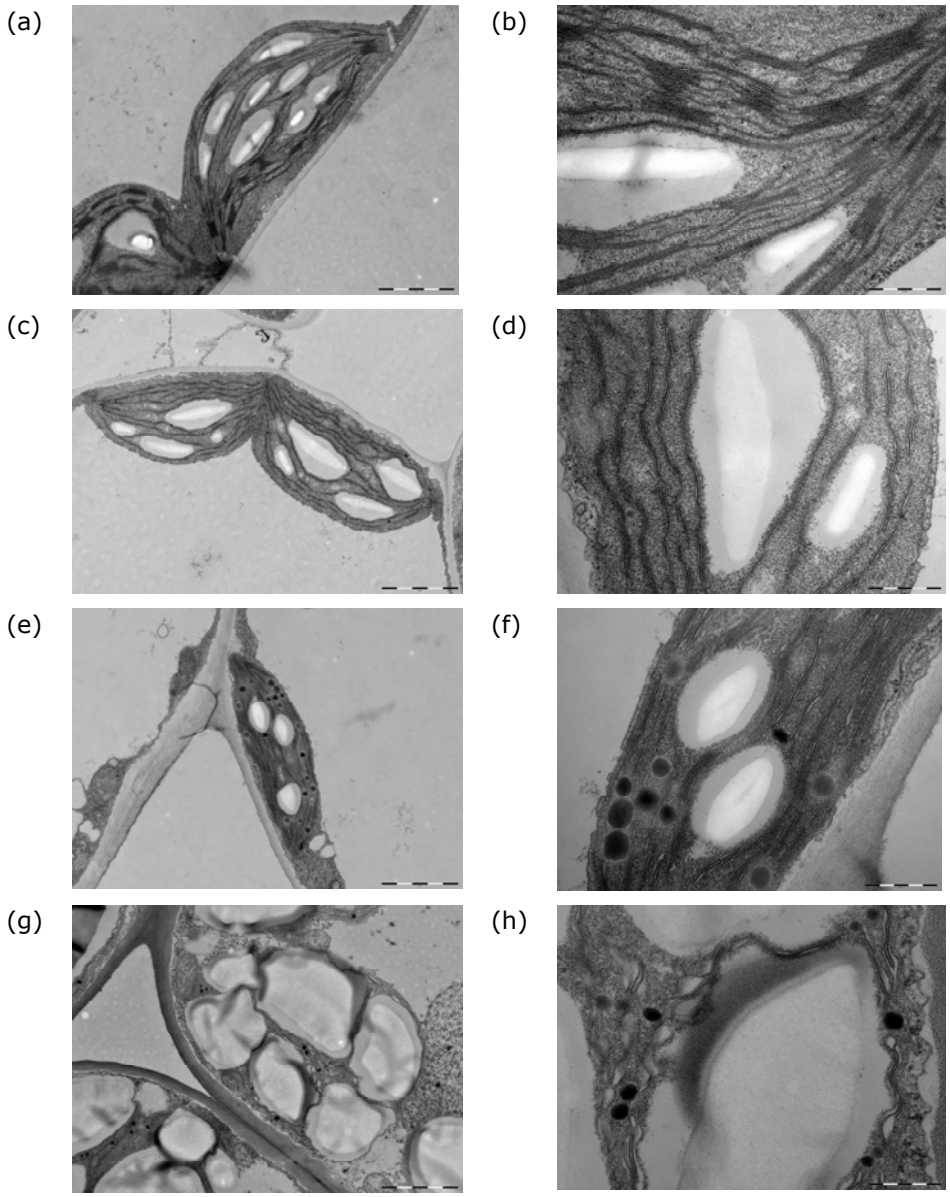

Fig. 4.5. *Electron micrographs illustrating the effects on the ultrastructure of the chloroplast of A. thaliana seedlings exposed during 3 weeks to 0, 1, 5 and 50 µM Cd. Chloroplast exposed to (a) 0 µM Cd, (c) 1 µM Cd, (e) 5 µM Cd, (g) 50 µM Cd (bars, 2000 nm). Details of the thylakoid system within the chloroplast exposed to (b) 0 µM Cd, (d) 1 µM Cd, (f) 5 µM Cd, (h) 50 µM Cd (bars, 500 nm).*

4.3.4 Gene expression

4.3.4.1 ROS-production

Compared to the control, the H_2O_2 levels were increased in all three Cd exposure concentrations albeit only significantly at 5 and 50 µM Cd (Fig. 4.6a). All three NADPH oxidase gene isoforms *RBOHC/D/F* showed a similar response pattern (Fig. 4.6b, c, d), a slight induction at 1 µM Cd, tremendous increases at 5 µM Cd and at 50 µM Cd, levels comparable again with the *RBOHC/D/F* mRNA levels observed in the leaves of the 1 µM Cd exposed plants. The induction of *RBOHC* was *c.* 10 times higher as compared to the *RBOHD/F* mRNA induction. The cytoplasmic lipoxygenase *LOX1* gene remained at control level at 1 µM Cd but was strongly enhanced - 20 times as compared to the control - in leaves of plants exposed to 5 µM Cd and higher (Fig. 4.6e). Also the plastidial lipoxygenase *LOX2* gene displayed a strong enhancement at 5 µM Cd with a ten fold increase as compared to the control, but was again comparable to the control level at 50 µM Cd (Fig. 4.6f).

4.3.4.2 ROS quenching

The plastidial Fe-SOD gene *FSD1* was strongly induced (25 times) after exposure to 5 µM Cd but at 50 µM Cd, the induction was limited to a level of *c.* 5 times the control value (Fig. 4.7a). The plastidial CuZn-SOD gene *CSD2* was reduced under all Cd treatments (Fig. 4.7b). The level of the mitochondrial Mn-SOD gene *MSD1* mRNA was induced from exposure to 5 µM Cd (Fig. 4.7c). The peroxisomal catalase gene *CAT1* mRNA level remained at control level at 1 µM Cd but was *c.* 10 fold enhanced at the higher Cd concentrations (Fig. 4.7d).

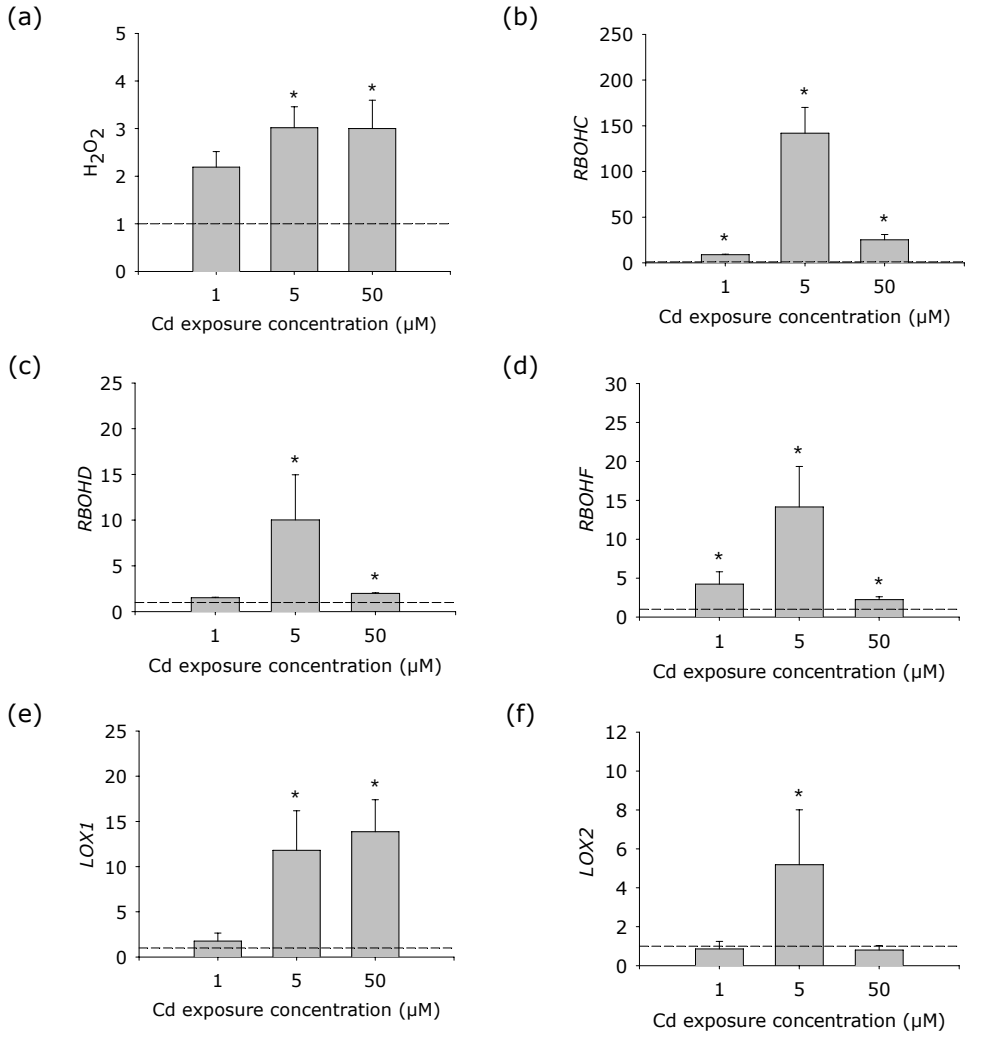

Fig. 4.6. *The effects of Cd on (a) the relative H_2O_2 production and (b-f) gene expression of ROS producing enzymes, i.e. (b) the NADPH oxidase RBOHC gene; (c) the NADPH oxidase RBOHD gene; (d) the NADPH oxidase RBOHF gene; (e) the cytoplasmic lipoxygenase LOX1 gene; (f) the plastidial lipoxygenase LOX2 gene. All values are presented relative to the control (1: marked as a dashed line) ± SE. Bars marked with an asterisk are significantly different from the control (P<0.05).*

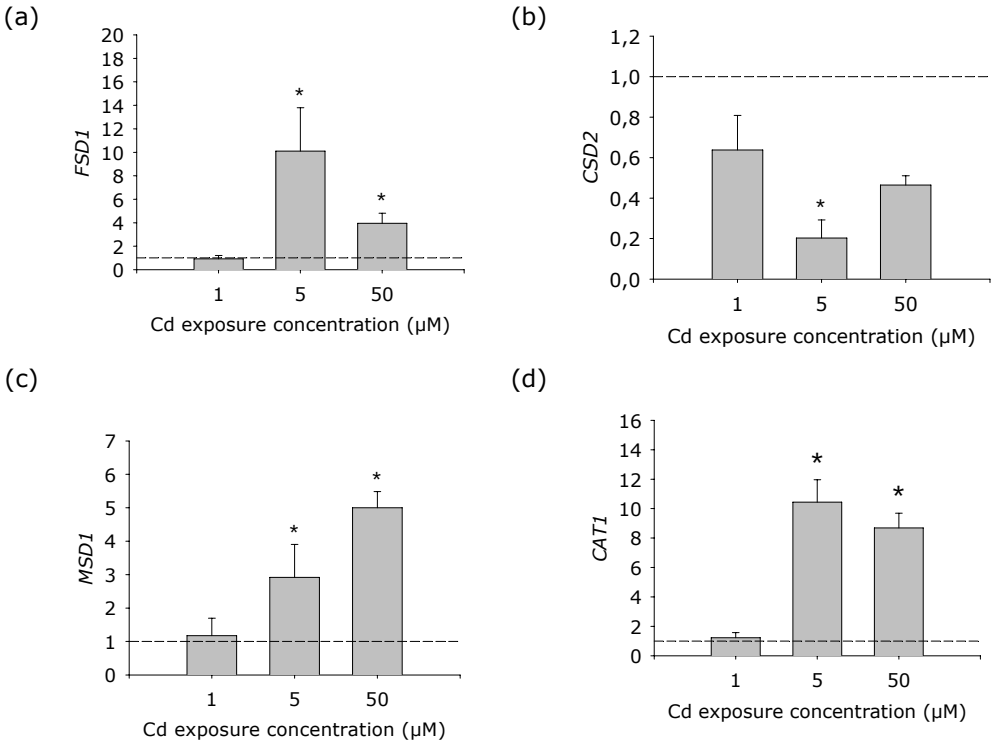

Fig. 4.7. *The effects of Cd on gene expression of ROS scavenging enzymes, i.e. (a) the plastidial Fe-superoxide dismutase FSD1 gene; (b) the plastidial CuZn-superoxide dismutase CSD2 gene; (c) the mitochondrial Mn-superoxide dismutase MSD1 gene and (d) the peroxisomal catalase CAT1 gene. All values are presented relative to the control (1: marked as a dashed line) ± SE. Bars marked with an asterisk are significantly different from the control (P<0.05).*

4.4 Discussion

4.4.1 Morphological effects of Cd on appearance and ultrastructure

4.4.1.1 Changes in appearance and leaf anatomy

The physiological and morphological effects of Cd on plants have been described extensively (see the review by Sanità di Toppi & Gabbrielli, 1999). As illustrated in chapter 3, leaf chlorosis was already observed after an exposure to 1 µM Cd whereas anthocyanous-colored leaves appeared in plants exposed to 5 µM and 50 µM Cd (Fig. 4.1). Chlorosis, which has been linked to a decrease in the number of chloroplasts (and hence in the amount of chlorophyll) per unit of leaf area has been related with Cd toxicity (Baryla *et al.*, 2001) and is also one of the most apparent symptoms of water stress. Anthocyanins are suggested to act as an antioxidant, inhibiting lipid peroxidation resulting in lower malonydialdehyde levels as observed in Cd exposed *Phaseolus coccineus* (Skórzyńska-Polit & Krupa, 2006). However, in *Arabidopsis thaliana*, subject of the current study, anthocyanins were not observed in the palisade and spongy parenchyma but they were located solely in the vacuoles of the epidermal cell layer. These observations are in agreement with the current theory that anthocyanins accumulate merely in peripheral tissues exposed to high irradiance and have a photoprotective function through light attenuation. In this way anthocyanins are known to reduce photoinhibition under adverse environmental conditions such as water stress (for a review see Steyn *et al.*, 2002) and Cd exposure.

Although the decreased leaf growth can be caused by several unfavourable conditions including Cd toxicity, it is also a nonspecific response to water stress and contributes to a decline in water losses (Veselov *et al.*, 2003). The smaller size of the leaf cells under Cd stress (leading to lower shoot weight (Fig. 4.2a)) is reported to be caused by the formation of stronger cross-binding between the pectin molecules in the middle lamella leading to a decreased cell expansion growth (see the review by Prasad, 1995). However, growth inhibition under (water) stress is considered to be a result of the reduction of both cell division and elongation (Heckenberger *et al.*, 1998). Interestingly, recently

growth inhibition (and chlorosis) in *Arabidopsis thaliana* has also been related to genetic programs that are activated after the release of singlet oxygen has been perceived by the plant (Wagner *et al.*, 2004), which could suggest an indirect effect of photoinhibition to plant growth.

The strongly decreased water content in the 5 and 50 µM Cd exposed plants (Fig. 4.2b) are indicative for a disturbed water balance which is considered to be one of the main effects of Cd toxicity (Barceló & Pochenrieder, 1990; Vitória *et al.*, 2003) resulting in Cd-induced water stress. In order to reduce water loss, increased stomatal closure leads to decreased stomatal conductance (Fig. 4.2c) (Barceló & Pochenrieder, 1990; Jones, 1998).

The strongly increased cuticle thickness in the plants exposed to 50 µM Cd (Fig. 4.4c) is in accordance with the results of a Cd exposure study on the cuticle wax accumulation in barley by Hollenbach *et al.* (1997). In that study the relation was demonstrated between Cd-induced wax accumulation and an ABA mediated increased gene expression of lipid transfer proteins (LTP) functioning as a transfer for cutin and/or wax monomers to the cuticle. Interestingly, upregulation of LTP genes has also been observed under water stress, resulting in increased wax layer thickness forming an additional barrier against water loss as indicated by the negative correlation between wax thickness and epidermal conductance in tobacco (Cameron *et al.*, 2006). Altogether, the observed physiological effects, caused by Cd stress, are most likely related to the reduction of water loss.

4.4.1.2 Ultrastructural effects of Cd in relation to gene expression of ROS producers and quenchers

While mitochondria and peroxisomes were not visibly affected under increasing Cd exposure concentrations, the chloroplast appeared to be very sensitive, even at the moderate exposure level of 1 µM Cd (Fig. 4.5). According to Djebali *et al.* (2005), one of the causes of the decreased grana stacking under Cd stress (observed at 1 µM Cd exposure, Fig. 4.5d) is similar to senescence, *i.e.* a decline in polar lipid content of the chloroplast membrane. Correspondingly, decreased grana stacking as a symptom of leaf senescence has also been observed in plants under water stress and is related with increased oxidative stress (Munné-Bosch *et al.*, 2001). Water stress, in general or in this

case as a result of Cd-stress, is known to inhibit photosynthetic activity, most likely in addition to the Cd specific photosynthesis inhibition. In our study, a significant decrease of the photosynthetic rate at 1 µM Cd was observed (Fig. 4.2d). Inhibition of photosynthesis by adverse conditions is reported to cause an increased sensitivity to photoinhibition because of an imbalance between light capture, CO_2 assimilation and carbohydrate utilization (Foyer & Noctor, 2000; Long *et al.*, 1994). This might lead to increased oxidative stress resulting in the observed decrease of grana stacking (see the review by Mullet & Whitsitt, 1996). In addition, it is also possible that at 1 µM Cd exposure, Cd-induced sensitivity to photoinhibition leads to a dynamic adjustment of grana stacking as a strategy to reduce photoinhibition in a similar way as in case of response to high light (e.g. shade-sun transition) as discussed by Anderson and Osmond (1987). In general, grana stacking is known to be dependent on binding interactions between light-harvesting complexes and inversely correlated with growth and light intensity (see the review by Allen & Forsberg, 2001).

These observed ultrastructural effects at 1 µM Cd exposure were concomitant with an upregulation of NADPH-oxidase genes (significant for *RBOHF and RBOHC*), an increased H_2O_2 content (although not significant) and the decrease of the stomatal conductance leading to inhibition of the photosynthesis rate. *RBOHF* and *RBOHD* are guard cell-expressed NADPH-oxidase catalytic subunit genes, which are reported to mediate stomatal closure by ABA signaling, with involvement of H_2O_2 and NO production (Kwak *et al.*, 2003; Bright *et al.*, 2006). It is therefore suggested that ROS derived from RBOHD and RBOHF are involved in the ABA-signaling mechanism that controls plant growth responses in drought conditions (Gapper & Dolan, 2006). The fact that the transcription of drought- and ABA-responsive genes has been reported to be also Cd-responsive in *Brassica juncea* L. (Fusco *et al.*, 2005), further strengthens the hypothesis that Cd imposes water stress and that abscisic acid may be involved in the Cd plant response, most likely also leading to an increased *RBOHD* and *RBOHF* expression.

In addition, RBOHD and RBOHF are also involved in methyl jasmonate induced stomatal closure (Suhita *et al.*, 2004). RBOHC has a function in ROS signaling in root hair growth (Foreman *et al.*, 2003; Carol *et al.*, 2005),

however, the upregulation in the leaves at 1 µM Cd suggests also an involvement in a ROS-mediated Cd response.

In conclusion, the upregulation of NADPH-oxidases, concomitant with decreased stomatal conductance and photosynthetic rate, should be considered as a signaling response to Cd toxicity and related with the Cd-induced disturbance of the water balance, most likely in order to counteract water loss leading to the observed ultrastructural effects. The relative importance of NADPH-oxidases expression at this exposure concentration is further emphasized by the absence of significant effects on the gene expression of the measured antioxidative enzymes.

At the 5 µM Cd exposure level, the disorganization of thylakoid membranes and the increase of the number of plastoglobuli (Fig. 4.5e-f) can be considered as indications of membrane damage, possibly resulting from increased levels of oxidative stress (Fig. 4.6a). The decreased chloroplastic starch accumulation suggests an increase of starch hydrolysis leading to an increase of soluble carbohydrate levels, which is thought to be a response to low levels of Cd for plant detoxification mechanisms (Kim *et al.*, 2003). However, a decrease in starch content is not specifically associated with Cd stress as it seems to be also a response to many abiotic stress conditions including water stress (Keller & Ludlow, 1993; Pelleschi *et al.*, 1997; Zellnig *et al.*, 2004).
The strong induction of the *RBOHD/F/C* genes at 5 µM Cd further emphasizes the earlier described importance of NADPH oxidases in ROS mediated Cd response and may contribute to a significant increase of H_2O_2 content in the shoot (Fig. 4.6a). In fact, Romero-Puertas *et al.* (2004) reported that in Cd-exposed plants, NADPH oxidases could be the main source of H_2O_2, primarily accumulated in the plasma membrane of transfer (associated with phloem sieve elements), mesophyll and epidermal cells and in the tonoplast of bundle sheath cells, with only a limited accumulation occurring in mitochondria and peroxisomes.

The highly enhanced mRNA levels of *LOX1* and *LOX2* at 5 µM Cd are in agreement with the increased lipoxygenase enzyme activity observed in *Arabidopsis thaliana* exposed to 5 and 50 µM Cd for 7 days (Skórzyńska-Polit *et al.*, 2006), in *Phaseolus coccineus* exposed to 25 µM Cd (Skórzyńska-Polit & Krupa, 2006) and in *Lycopersicon esculentum* exposed to 100 µM Cd for 10 days

(Djebali *et al.*, 2005). As lipoxygenases are considered to be an important source of chloroplast lipid peroxidation under Cd exposure (Djebali *et al.*, 2005), the enhanced gene expression at 5 µM Cd is indicative for the role of cytoplasmic LOX1 and the plastidial lipoxygenase LOX2 in membrane damage observed in the chloroplast. The levels of mRNAs lipoxygenases are known to be modulated during development processes as well as under stress responses such as wounding and water stress (Bell *et al.*, 1995, Porta *et al.*, 1999) with involvement of phytohormones such as jasmonic acid (JA), its methyl ester (MeJA) or abscisic acid (ABA) (Melan *et al.*, 1993). Xiang and Oliver (1998) suggested that specifically jasmonates might be involved in the response of *Arabidopsis* to elements as Cd and Cu (leading to upregulation of GSH metabolic genes), which was later confirmed by the results of Montillet *et al.* (2004). Although the involvement of the oxylipin jasmonic acid (JA) in metallic element-induced gene expression is not clear (Xiang and Oliver, 1998), it is known to be involved in the response of plants to water stress (Gao *et al.*, 2004). Therefore, it can be hypothesised that the Cd-induced oxidative stress resulting in the observed ultrastructural membrane damage should at least partially be attributed to the increased *LOX1/2* expression, most likely related to the Cd-induced disturbance of the water balance.

Both *FSD1 and CSD2* are independently regulated and are considered to be involved in the protection of *Arabidopsis* plastids against different oxidative stresses (Kliebenstein *et al.*, 1998). The strong induction of the nuclear gene *FSD1* encoding for Fe-SOD (localized in the stroma of the chloroplast) is an indication of increased detoxification activity at the transcript level in response to the increased oxidative stress. However, the reduced expression of the nuclear *CSD2* encoding for CuZn-SOD (localized on the thylakoids of chloroplast) does seem to indicate that the transcription of this gene is negatively affected at this exposure level. Concerning the other ROS producing organelles, the enhanced mRNA levels of the gene *MSD1* encoding for mitochondrial Mn-SOD and the gene *CAT1* encoding for peroxisomal catalase indicate that at 5 µM Cd, the antioxidative defence system is strongly responsive to Cd toxicity in these organelles.

50 µM Cd was highly toxic for the most sensitive organelle, *i.e.* the chloroplast, leading to extensive thylakoid distension caused by severe membrane damage (Fig. 4.5g,h). As suggested by Pietrini *et al.* (2003), Cd induced starch accumulation at the highest exposure concentration is most likely caused by a decreased phosphate recycling between cytosol and chloroplasts because of the binding of Cd to the cytosolic thiol-dependent enzyme fructose-1,6-bisphosphatase and reduced sucrose synthesis. Although, accumulation of starch within leaves has not been related to water stress, it is neither a Cd specific process as it has been linked to an increased reactive oxygen species formation caused by a variety of adverse conditions, like for instance high light stress (Layne & Flore, 1993).

The expression of *RBOHD/F/C* genes was considerably decreased compared to the expression at 5 µM Cd, suggesting a Cd-induced impairment of the NADPH-oxidase signaling system. Likewise, the inhibition of the gene expression of *LOX2* is indicative for the impairment of the plastidial lipoxygenase signaling, however cytoplasmic lipoxygenase appeared to be less vulnerable as the gene expression of *LOX1* remained at a high level.

The decreased expression of *FSD1,* (encoding for plastidial Fe-SOD) indicates that, at the highest exposure concentration, Cd toxicity was affecting the plastidial antioxidative defence system at the transcript level.

Mitochondria and peroxisomes seemed less vulnerable, displaying less significant ultrastructural damage which was probably directly related with the ability of these organelles to maintain an elevated antioxidative response. This was manifested in the mRNA expression levels of the catalase gene *CAT1* and the Mn-SOD gene *MSD1* being, respectively, similar and slightly increased as compared to the leaves of 5 µM Cd exposed plants.

The reason as to why the relative H_2O_2 content at 50 µM Cd was not further increased in comparison with 5 µM Cd was most likely the result of the inhibited expression of the NADPH-oxidase genes in combination with the decreased SOD expression in the chloroplast. As the H_2O_2-content was not correlated with the increased membrane damage, ROS-species other than H_2O_2, such as superoxide, hydroxyl radical and singlet oxygen might be involved in oxidative stress which is in agreement with the current literature (see the review by Asada, 2006).

4.4.2 The different levels in Cd toxicity: signaling versus stress

As H_2O_2 content increased under all investigated Cd exposure conditions, the question rises whether Cd responses are mediated by or as a consequence of ROS, *i.e.* ROS signaling versus oxidative damage.

The rise in the H_2O_2 content of the leaves of 1 µM Cd exposed plants might be attributable to the induction of NADPH-oxidases and could be designated as a signaling response to Cd toxicity. Although no ultrastructural membrane damage was observed, this signaling was congruent with the grana unstacking process, a nonspecific response to decreased photosynthetic activity induced by several abiotic stress conditions including water stress. These observations are in fact consistent with the hypothesis of Kacperska (2005), suggesting that in plants responding to mild stress, a disturbance of water balance is the primary stress-induced event inducing a mild stress-sensing system, enabling the adjustment of plant growth and metabolism to stressful conditions.

In 5 µM Cd exposed plants, the increased expression of NADPH-oxidase and lipoxygenase genes were congruent with an increasing disturbance of the water balance leading to nonspecific symptoms as growth inhibition and increased cuticular wax accumulation. At this exposure concentration, the combined signaling action of both NADPH-oxidases and lipoxygenases might represent a direct response to Cd-induced water stress and should be considered as an important additional source of oxidative stress on top of the oxidative stress caused by processes like, for instance, the inhibition of antioxidative enzymes. The highly increased lipoxygenase signaling, concomitant with membrane damage should therefore be considered as a signaling reaction under severe stress, most likely in combination with phospholipid signaling, since activation of membrane bound phospholipases deliver free polyunsaturated fatty acids, which are a substrate for LOX (Kacperska, 2005; Spiteller, 2003). However, the strongly increased gene expression of antioxidative enzymes was an indication of the remaining ability of the plant to adapt to the stress condition inflicted by Cd at this exposure concentration.

The highly toxic 50 µM Cd concentration, inducing severe water stress and plastidial ultrastructural damage, imposed an impairment of the signaling functions of the NADPH-oxidases and the chloroplastic LOX2 together with a strong inhibition of chloroplastic Fe-SOD mRNA. Therefore, the increased plastidial ultrastructural damage was most likely caused by ROS, at least partly as a result of the inhibition of antioxidative gene expression, indicating the decreased ability of the plant to respond to the high oxidative stress levels in that organelle.

4.5 Conclusion

The results of this study have demonstrated that, at the 1 µM and 5 µM Cd exposure concentrations, much of the morphological and ultrastructural effects caused by Cd toxicity are related to the disturbance of the water balance leading to nonspecific symptoms of Cd-induced water stress. The strongly induced NADPH-oxidase and lipoxygenase signaling was thereby considered as an important contributor of oxidative stress, leading to lipid peroxidation and membrane damage. However, at 50 µM Cd, the inhibition of the antioxidative defence system seemed to be more important.

4.6 Perspectives

For this study, only the wild-type *Arabidopsis thaliana* was used. Since the expression of NADPH-oxidases seem to have a distinct role in the response to Cd, the use of NADPH-oxidase mutants, more specific knockouts for the genes *rbohc*, *d*, *f*, and *d*/*f* could give us more information on the specific effect of the various NADPH oxidase enzymes on the morphology, ultrastructure, photosynthesis rate, H_2O_2 production and the expression of genes of pro-oxidant and antioxidative enzymes.

Similarly, it would also be interesting to study the effects of Cd in glutathione (GSH) and/or ascorbate (AsA) *Arabidopsis* mutant plants.

Chapter 5

Examination of Cd-effects on the photosynthetic efficiency of *Arabidopsis thaliana* using chlorophyll *a* fluorescence and pigment analysis

5.1 Introduction

5.1.1 Cd and photosynthesis in perspective with current results

In previous chapter, a Cd-induced decrease of photosynthesis activity, indicating photoinhibition, was observed for all exposure concentrations (1, 5 and 50µM Cd). As described in the general introduction, inhibition of photosynthesis is a common symptom from adverse conditions (for instance biotic or abiotic stress), which is the result of an increased sensitivity to photoinhibition which could lead in particular to photosystem II damage (Barber & Andersson, 1992; Foyer & Noctor, 2000; Long *et al.*, 1994). In the case of Cd toxicity, this photoinhibition can be at least partly attributed to the disturbance of the water balance (for instance because of stomatal closure), most likely augmented by the more specific effects of Cd on photosynthesis (inhibition of Calvin-Benson cycle, inhibition of the oxygen evolving complex, etc… (see chapter 1, general introduction). For instance, the Cd-induced inhibition of photosynthesis was observed along with severe ultrastructural damage to thylakoid membranes (in particular at 5 and 50 µM Cd, see chapter 4). In order to further investigate the impact of the used Cd concentrations on photosynthesis of *Arabidopsis thaliana*, the component known to be sensitive to stress conditions, photosystem II, was examined using chlorophyll *a* fluorescence transient analysis, complemented with a quenching analysis and pigment analysis.

Chlorophyll *a* fluorescence transient analysis allows non-invasive, near instantaneous measurements of key parameters of light capture and electron transport of photosystem II and is therefore a good way to study the vitality of plants under stress conditions (Strasser & Strasser, 1995; Strasser & Tsimilli-Michael, 2001; Strasser *et al.*, 1999, 2000, 2004). In this way, chlorophyll *a* fluorescence transient analysis should deliver interesting information regarding detrimental effects of Cd at the level of the reaction centres of photosystem II.

5.1.2 Fast chlorophyll *a* fluorescence

Most of the light absorbed by the antenna pigment molecules within the photosynthetic membrane is utilized to drive photosynthesis (photochemistry) or will be dissipated as heat, but a small proportion, a few percent of the absorbed light at most, is reemitted as chlorophyll *a* fluorescence. These three processes occur in competition, such that any increase in the efficiency of one will result in a decrease in the yield of the other two. Therefore, by measuring the yield of chlorophyll fluorescence, information about changes in the efficiency of photochemistry and heat dissipation can be achieved.

The fast fluorescence transient analysis is based on the characteristic induction of emission, which occurs when a dark-adapted sample is illuminated. Upon illumination, the fluorescence yield rapidly rises over a time period of around 1 s to a maximum (F_M) and then slowly decreases (Fig. 5.1). This fluorescence transient has been termed the Kautsky phenomenon (Kautsky & Hirsch, 1931) and has been explained as a consequence of reduction of electron acceptors in the photosynthetic electron transport pathway, downstream of PSII, notably plastoquinone and in particular, Q_A (see reviews by Dau 1994; Govindjee, 1995).

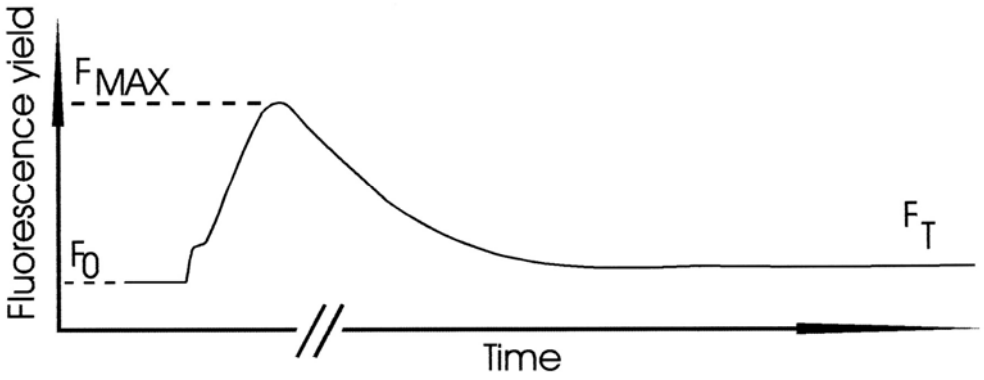

Fig. 5.1 *Schematic overview of the Kautsky curve (adapted from Tyystjärvi et al. (1999)). The yield of chlorophyll a fluorescence is low when the quinone electron acceptor Q_A of PSII is oxidized (F_0), and high when it is reduced (F_M). A sudden increase in light intensity after dark adaptation results in a transient accumulation of Q_A^-, which is reflected as a transient increase in the fluorescence yield. After a few seconds, the fluorescence starts decreasing towards F_T because of an increase in the rate at which electrons are transported away from PSII by either photochemical quenching (increased activity photosynthesis) and nonphotochemical quenching (NPQ = the increase in the efficiency with which energy is converted to heat).*

Fig. 5.2a depicts the schematic structure of photosystem II including the components involved in the electron transport pathway whereas Fig. 5.2b depicts the Z scheme which illustrates the energy values and reaction times of the electron transport components of photosystem II.

a

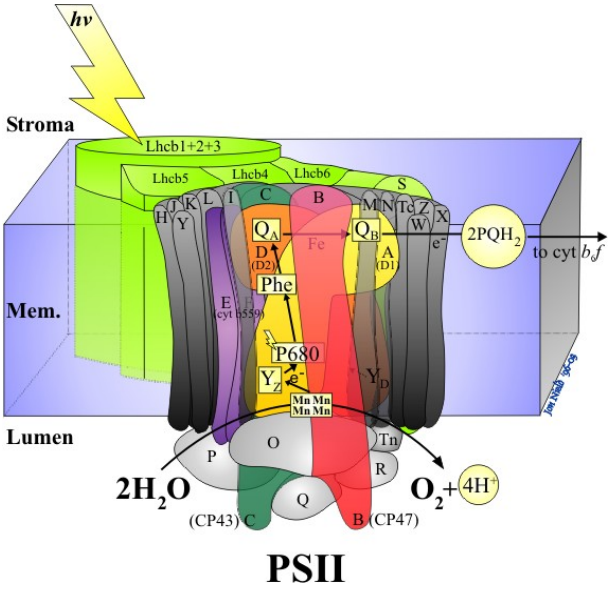

b

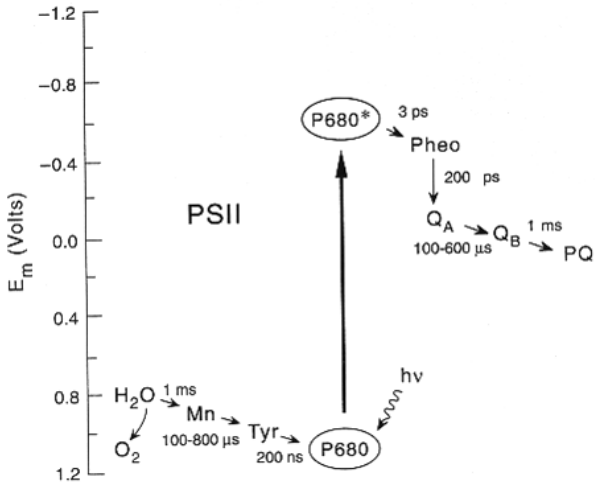

Fig. 5.2 *A schematic display of electron transport in photosystem II with; (a) an illustration of the protein structure of photosystem II involved in electron transport (http://www.bio.ic.ac.uk/research/barber/psIIimages/PSII.html) and (b) a depiction of the Z scheme which illustrates the energy values and reaction times of the electron transport components of photosystem II (http://www.life.uiuc.edu/govindjee/paper/fig8.gif).*

Basically, light trapped by light-harvesting pigment antenna complexes is funneled through to the reaction centre of photosystem II. An electron coming from the excited chlorophyll $P680^*$ in the reaction centre is transferred to pheophytin and from there further to a tightly bound plastoquinone (Q_A), and then to the loosely bound plastoquinone (Q_B or PQ). Q_B accepts two electrons one after the other and is therefore reduced to Q_B^{2-}. Subsequently, the reduced Q_B^{2-} takes two protons from the stroma side of the medium, yielding a fully reduced plastohydroquinone (PQH_2). PQH_2 has lower affinity for the Q_B binding site and is therefore released from the photosynthesis complex while it is rapidly exchanged by oxidized PQ. Plastohydroquinone is the final product of photosystem II and it will transfer the electrons to Cyt b_6f, the next protein complex in the electron transport chain. The loading of electrons onto PQ is coupled to the binding of protons in the stromal side of the membrane and the unloading of the electrons to Cyt b_6f is associated with the discharge of protons into the thylakoid lumen. This helps producing the electrochemical potential needed for ATP synthesis. By non-cyclic electron transport an electron deficit is created in the reaction centre. This is compensated by electrons derived from the oxidation of water releasing oxygen and protons in the lumen. Four manganese cations and a tyrosine residue (Yz) are involved in the transport of electrons from water to chlorophyll.

Before an electron is transferred to Q_A (*i.e.* in oxidized state), the reaction centre is open and the fluorescence at F_0 is the emission from the excited chlorophylls in photosystem II antennae in competition with excitation energy transfer to RCII, which takes place before the excitons reach the reaction centre (Krause & Weis, 1991). In other words, oxidized Q_A acts as a quencher (Duysens & Sweers, 1963) of the chlorophyll fluorescence of the antenna. However, when Q_A in a reaction centre is reduced (Q_A^-), the reaction centre is closed and the chlorophyll fluorescence of the antenna increases (Strasser *et al.*, 2004) as quenching by energy transfer to the reaction centres decreases.

The rise to F_M has a number of phases, visible on a $\log_{10}$ time scale (Fig. 5.3): first a rise from the origin (F_0) to an intermediate step (F_J) and then a second slower rise involving a second intermediate (F_I) to a peak (at F_M) (Govindjee, 1995).

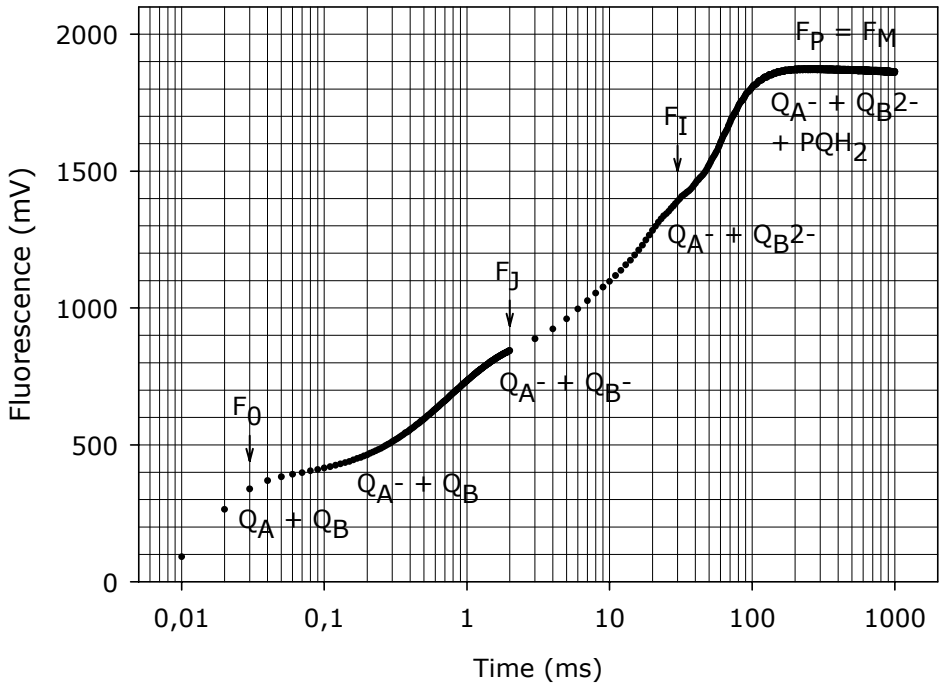

Fig. 5.3 *A detailed illustration of the part of the Kautsky curve used for fluorescence analysis.*

The minimum fluorescence F_0 is measured when Q_A is oxidized (open reaction centres) which means that, as mentioned above, the fraction of excitation energy lost to chlorophyll *a* fluorescence is low.

The F_0 to F_J transient reflects the primary photochemical reaction, which is the transfer of an electron from P680 to Q_A. Once Q_A has been reduced, it is not able to accept another electron until it is reoxidized by passing the electron onto a subsequent electron carrier (Q_B). During this period, the reaction centre is closed and the fluorescence rises. In addition, the fluorescence rise can also be affected by the donor side of photosystem II (Schreiber and Neubauer, 1987) and is related to different fluorescence quenching in different redox states of the oxygen evolving complex (S-states) (Hsu, 1993). The effect of the donor side was also reported by Lazár (2003) using theoretical simulations.

The plateau at F_J has been attributed to the reoxidation of Q_A^- by Q_B. In addition, the activation of P700 induces an oxidation pressure (causing a depletion of electron transport intermediates between P700 and Q_B), also the activation of ATP synthase and conversion of S_2 + S_3 to S_0 + S_1 states seem to have an effect (reviewed by Hill *et al.*, 2004).

The F_J to F_I transient is attributed to the further reduction of Q_A, whereas the plateau of F_I is attributed to the reduction of Q_B^- to Q_B^{2-} (leading to reoxidation of Q_A^-). Schreiber and Neubauer (1987) suggested that this section of the curve can also be influenced by inhibition of the donor side and more specifically, by the kinetics of water splitting enzymes. In agreement, Pospíšil and Dau (2000) reported that the J-P transient rate constant (in photosystem II membranes thus lacking the I step) is directly proportional to the steady state rate of oxygen evolution.

The F_I to F_M transient is attributed to the filling of the plastoquinone pool. During the first few seconds of illumination the electron flow out of PQ/PQH_2 is minimal resulting in a significant reduction of the PQ pool and a further reduction of the electron flow from Q_A/Q_B. This causes Q_A to become fully reduced leading to the maximum fluorescence yield F_M. The F_I to F_M transient can be affected by inhibition of the oxygen evolving complex, as it leads to a lack of electrons to reduce the oxidized PQ pool which acts as a fluorescence quencher (Neubauer & Schreiber, 1987). It has been suggested that the F_I to F_M transient is also influenced by a transient limitation at the acceptor side of photosystem I (most likely by inactive ferredoxin-$NADP^+$ oxidoreductase) (Schansker *et al.*, 2005).

A few seconds after F_M is reached, the fluorescence level typically starts to fall again, over a time-scale of a few minutes. This phenomenon, termed fluorescence quenching, is explained in two ways. Firstly, there is an increase in the rate at which electrons are transported away from PSII; this is due mainly to the light-induced activation of enzymes involved in carbon metabolism and the opening of stomata. Such quenching is referred to as 'photochemical quenching'. At the same time, there is an increase in the efficiency with which energy is converted to heat. This latter process is termed 'nonphotochemical quenching' (NPQ). In a typical plant, changes in these two processes will be complete within *c.* 15–20 min and an approximate steady-state is attained, although the time

taken to reach this state can vary significantly between plant species (see the review by Maxwell & Johnson (2000)).

During the actual fast chlorophyll *a* fluorescence analysis, there are more points measured of the polyphasic rise of the fluorescence transient than the ones mentioned above ($F_{0\ (30\mu s),}$ $F_{1\ (50\mu s)}$, $F_{2\ (100\mu s)}$, $F_{3\ (300\mu s)}$, $F_4 = F_{J\ (2\ ms)}$, $F_5 = F_{I\ (30\ ms),}$ F_P ($=F_M$)). This allows the calculation of a selection of physiological relevant chlorophyll fluorescence parameters and the calculation of energy fluxes and quantum yields on the level of the reaction centres by using the energy flux theory of Strasser, which was further developed as the JIP test (Strasser & Strasser, 1995; Strasser *et al.*, 2000, 2004). The energy fluxes theory is described in the 'materials and methods' whereas the physiological implication of the calculated parameters is discussed in detail in the 'results and discussion'.

5.1.3 Objectives

To study the Cd induced changes of the energy fluxes of photosystem II with chlorophyll *a* fluorescence transient analysis performed on *Arabidopsis thaliana* exposed to 0 µM, 1 µM, 5 µM and 50 µM Cd.

To relate the changes of the energy fluxes with changes of dissipation of heat by analysis of the nonphotochemical quenching (NPQ) using a fluorescence imaging system.

To relate the above effects on changes in pigment content by HPLC pigment analysis.

5.2 Materials and methods

5.2.1 Plant Culture

Seeds of *Arabidopsis thaliana* (L.) Heynh (ecotype Columbia) were vernalized for 2 days at 4 °C and subsequently germinated for 4 days in 5 ml pipette tips (cut off at 1 cm) filled up with moist autoclaved rock wool and placed in a polystyrene board. After germination, the boards with the plants were placed floating in 3 l of $1/10^{th}$ Hoagland nutrient solution (pH 5.75) and grown for 21 days in a growth chamber using a 12 h photoperiod, with 150 µmol m^{-2} s^{-1} photoactive radiation at plant level, a 20/18 °C day/night temperature regime and a relative humidity of 65 %. The Hoagland nutrient solution was continuously aerated and refreshed every 3 days. When 21 days old, the plants were exposed for another 21 days to 0, 1, 5 and 50 µM Cd administered as $CdSO_4$ and refreshed every 3 days.

5.2.2 Plant Efficiency Analysis

After an exposure period of 21 days, the photosynthetic efficiency was analyzed on 5 leaves of similar age per plant. After 30 min dark adaptation, chlorophyll *a* fluorescence transients were recorded and digitized using a Plant Efficiency Analyzer (PEA, Hansatech Instruments, Ltd. King's Lynn Norfolk, UK). Because of the small leaf area, the excitation light from the array of six red light emitting diodes (peak wavelength at 650 nm, 3000 µmol m^{-2} s^{-1} PAR) had to be focused on the leaf surface using an optical fiber, which resulted in an actual PAR of *c*. 1800 µmol m^{-2} s^{-1}. Chlorophyll fluorescence was detected using a PIN-photodiode after passing through a long pass filter. The fluorescent signal was recorded every 10 µs for the first 2 ms and every 1 ms thereafter up to 1s.

5.2.3 Analysis of fluorescence transient

The measured points of the polyphasic rise of the fluorescence transient ($F_{0\ (30\mu s)}$, $F_{1\ (50\mu s)}$, $F_{2\ (100\mu s)}$, $F_{3\ (300\mu s)}$, $F_4 = F_{J\ (2\ ms)}$, $F_5 = F_{I\ (30\ ms)}$, F_P ($=F_M$)) were analyzed using the Biolyzer software (Biolyzer© R.M. Rodriguez, The Bioenergetics Laboratory, University of Geneva, Geneva, Switzerland). This method is based on the energy flux theory of Strasser, further developed as the JIP-test (Strasser & Strasser, 1995; Strasser *et al.*, 2000, 2004), which allowed the derivation of a selection of chlorophyll fluorescence parameters (tF_M, F_V/F_0, M_0, V_J, V_I, Area, S_M and N). Also energy fluxes and quantum yields on the level of the reaction centres were derived using this theory. Fig. 5.4 is a depiction of the simplified scheme of the energy fluxes cascade in photosystem II, hereby photons absorbed by the antennae pigments are referred to as the absorption flux (ABS). Although a fraction of this excitation energy is dissipated (DI) (as heat, fluorescence, and energy transfer to other systems), most of it is transferred as the trapping flux (TR) to the reaction centres. In the reaction centres, the excitation energy is converted to redox energy (reduction of Q_A to Q_A^-) leading to an electron transport flux (ET), which is necessary to drive the photosynthetic apparatus. According to the JIP test, the specific energy fluxes for ABS, TR, and ET per PSII reaction centre are ABS/RC, TR_0/RC, ET_0/RC and DI_0/RC. The flux ratios are: the maximum quantum yield of PSII photochemistry $(\varphi P0)$, the efficiency with which a trapped exciton can move an electron into the electron transport chain further than Q_A^- (ψ_0), and the quantum yield of electron transport beyond Q_A $(\varphi E0)$. The concentration of active photosystem II reaction centres is RC/CS. Finally, the performance index (PI_{ABS}), combines the three main functional steps (light energy absorption, excitation energy trapping, and conversion of excitation energy to electron transport) of photosynthetic activity by a PSII reaction centre complex into a single multiparametric expression. This expression is indicative for the photosynthetic efficiency. All parameters are described in detail in 'Results and discussion'.

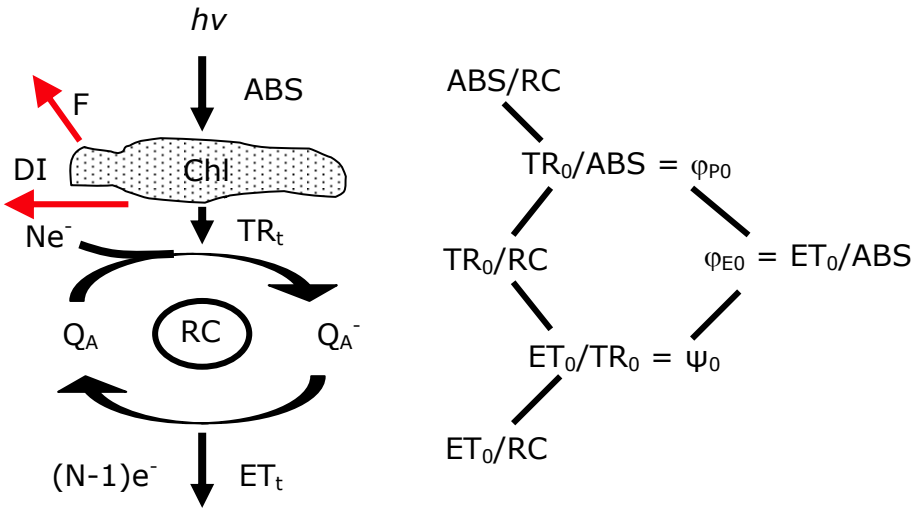

Fig. 5.4 *Schematic energy flux model from Strasser & Strasser (1995) for the energy cascade from light absorption to electron transport. ABS = absorbed photon flux, DI = dissipated and de-excitation fluxes, F = fluorescence emission, RC = reaction centre, TR = trapping flux by RC (= reduction of Q_A), ET = electron transport beyond Q_A^-. For an explanation of the flux ratios, see text.*

5.2.4 Measurement of NPQ with the Fluorescence Imaging System

In order to study fluorescence quenching, a chlorophyll fluorescence imaging system (FIS) was developed in our lab (Dr. M. Ciscato, PhD thesis (2000)). This instrument is capable of capturing digitized fluorescence images of plants subjected to two different light intensities: a lower intensity (*Actinic*) at 100 µmol $m^{-2}s^{-1}$ (λ < 650 nm) and a higher intensity at 1100 µmol $m^{-2}s^{-1}$ (λ < 650 nm). One control (0 µM Cd) and three treated plants (1, 5 and 50 µM Cd) were taken out of the hydroponics and put into large test tubes filled with their corresponding hydroponics solution and dark adapted for at least 30 min inside the instrument's cabinet (Fig. 5.5). After dark adaptation, fluorescence imaging was carried out for the 4 plants simultaneously, using the protocol 'quenching pulses', in which a saturating pulse of 1 s was applied at time intervals of 0, 2, 5, 10, 20, 30, 60, 90, 120, 180, 240 and 300 s after the onset of continuous actinic illumination. During this protocol an M-image (maximum intensity) was grabbed at each high intensity pulse and an S-image (steady state image) was

grabbed in the continuous actinic light just before the next high intensity pulse, using the developed program Grabix running under a Linux operating system (X-Window environment). Prior to each experiment, two reference images (a dark and a background image) were recorded in order to calibrate the system. The correction was carried out in three steps: first the dark image was subtracted from the sample image; then the result was divided by the background image (from which the dark signal has also been subtracted); finally the result was multiplied by a constant given by the mean intensity value of the background image for normalization purposes. In this way, possible fluctuations of light intensity because of aging of the lamps and non-homogeneity of the illumination were accounted for. For the actual statistical image analysis, the images obtained by the processing technique were subsequently statistically analyzed using a R-script (Dr. M. Ciscato, PhD thesis (2000)) for the 'R' statistical package. For each series of corrected images to follow the time course of the fluorescence quenching, coordinates of 5 regions of interest (ROI's), which were in fact a selected area on 5 leaves per plant, were entered into the program. The fluorescence value of each ROI was calculated as the integral of the pixel values in the ROI. The nonphotochemical energy dissipation was calculated for each excitation pulse (at 0, 2, 5, 10, 20, 30, 60, 90, 120, 180, 240 and 300 s) as $(F_M - F_M')/F_M'$ where F_M was the maximal fluorescence (at t = 1 sec) and F_M' is the fluorescence measured during the specific saturating pulse. In this way, a dataset was obtained with NPQ values for each excitation point for the four Cd exposure levels.

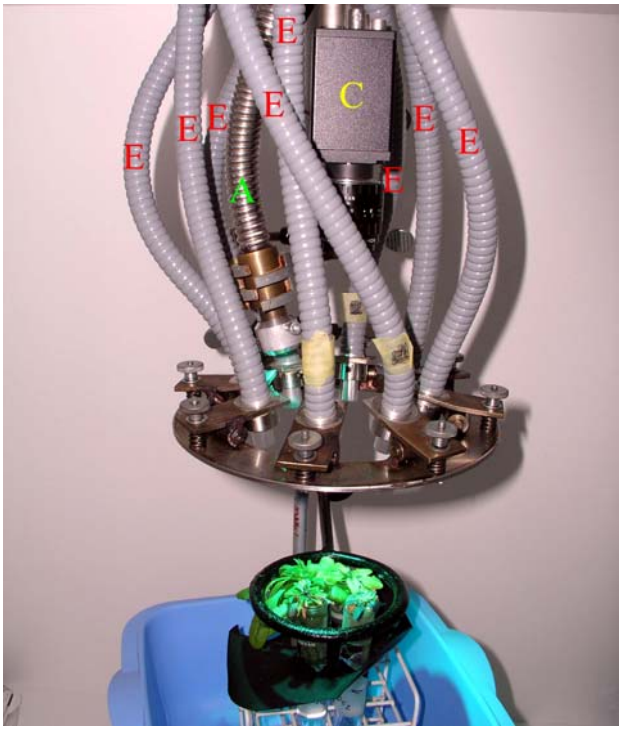

Fig. 5.5 *A view inside the cabinet where 4 Arabidopsis plants, exposed to 0, 1, 5, 50 µM Cd, respectively, are positioned for FIS analysis. The 8 light guides (E) of the 4 cold light sources are used for the 1100 µmol m^{-2} s^{-1} excitation light, the light guide (A) is used for the 100 µmol m^{-2} s^{-1} actinic light. The camera in the middle (C) is fitted with a B+W red filter 30.5E/0.92 and connected to the digitizing software Grabix.*

5.2.5 Pigment analysis

Leaf samples, taken from plants exposed to 0, 1, 5 and 50 µM Cd, were weighed and kept at -70°C until pigment extraction. The photosynthetic pigments were extracted in 80 % acetone (Lichtenthaler & Wellburn, 1983). The actual pigment analysis was performed in collaboration with Prof. Dr. F. Franck (Département des sciences de la vie/Biochimie végétale, Université de Liège) using a method described by Cardol *et al.* (2003). 25 µl of pigment extract were subjected to reverse phase HPLC analysis using a set-up comprising a 616 pump, a 717 plus autosampler and a 996 online photodiode array detector (Waters, Milford, MA, USA). A Nova Pak C18, 60A column (length 150 mm, pore size 4 µm) was used

for separation. Acquisition and data treatment were performed using the Millenium software (Waters). Pigments were eluted during 2 min with a gradient from 100 % solvent A (80% methanol, 20% 0.5 M amonium acetate pH 7) to 100 % solvent B (90% acetonitrile in water), then during 20 min with a gradient from 100 % solvent B to 31 % solvent B and 69 % solvent C (ethyl acetate) and during 3 min with a gradient from the latter solvent mixture to 100 % solvent A. The solvent flow rate was 1 ml min^{-1}. Concentrations of individual pigments were determined using authentic references prepared by chromatography on silica gel thin-layer plates (chlorophyll *a* and *b*) or pigments purchased from DHI-Water and Environment (Horstholm, Denmark).

5.2.6 Experimental design and statistical analysis

For each exposure concentration, PEA and NPQ analysis was performed on 5 leaves of 3 independently exposed plants in a replicate of 2 experiments. Statistical analysis was conducted for all measurements using the General Linear Model (GLM) procedure (Statistical Analysis Systems Institute version 9.1). After testing and removal of outliers (Cook's Distance) the Shapiro–Wilk and Levene tests were used to test for normality and homogeneity of variance (Neter *et al.*, 1996). Where necessary, parameters were transformed in order to meet the assumptions of ANOVA. In cases of significant treatment effects, these analyses were followed by tests of treatment differences using Tukey test. All values presented here are nontransformed.

5.3 Results and discussion

5.3.1 Cd induced effects on the vitality of the photosynthesis measured with the plant efficiency analyser (PEA)

5.3.1.1 Presentation of the fast chlorophyll fluorescence data

Fig. 5.6 illustrates the effects of Cd exposure on the unprocessed transient fluorescence curve. Fig. 5.7 depicts the same transient curve data that has been normalized at 50 µs (F_1) and F_P (= F_M) in order to visualize the variable fluorescence at point I and J and the effects on F_0.

All measured and calculated parameters, discussed in this chapter, are presented in Table 5.1, whereas the spider plot on Fig. 5.8 offers a graphical illustration of the relative impact of Cd on these parameters.

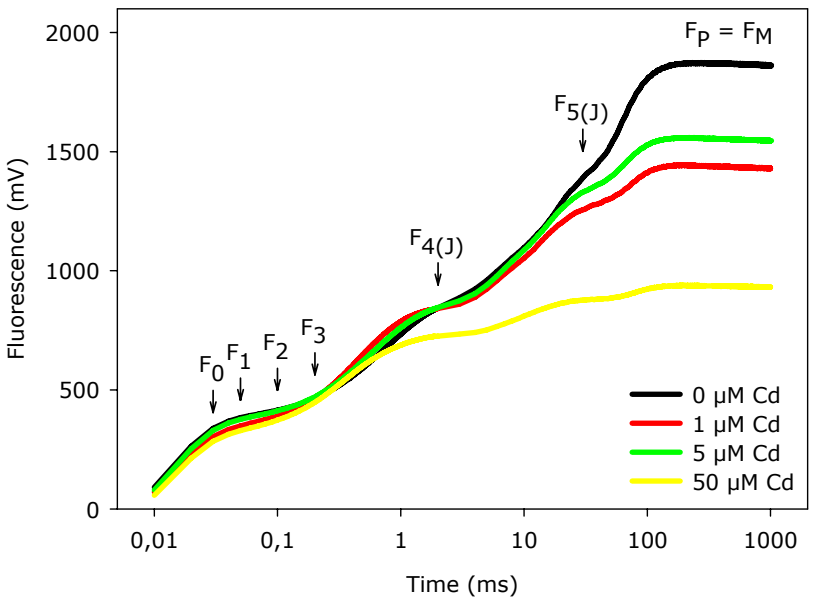

Fig. 5.6 *An illustration of the effect of Cd on the chlorophyll a polyphasic rise, measured by the plant efficiency analyzer in Arabidopsis thaliana. The transient is plotted on a logarithmic time scale from 10 µs to 1 s the raw fluorescence transient.*

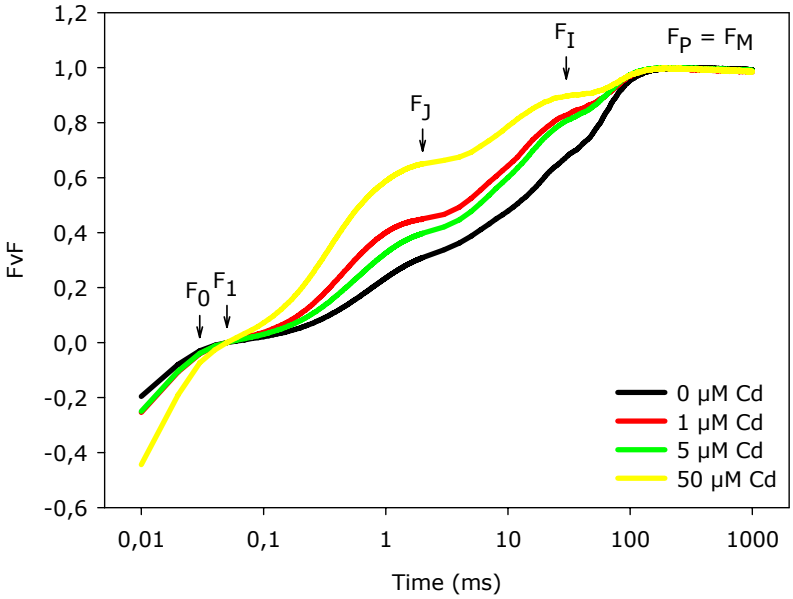

Fig. 5.7 *The transient FvF represents the normalization at F_1 and F_M and visualizes the Cd-induced effects on the kinetics of the Q_A visible at point I and J and the relative decrease of F_0.*

Treatment	0 µM			1 µM			5 µM			50 µM		
F_0	360	±	4,5	322	±	6,6 *	348	±	7,9	295	±	7,5 *
F_M	1824	±	29,2	1389	±	45,3 *	1533	±	42,2 *	1148	±	45,6 *
F_1	380	±	5,1	349	±	7,0 *	374	±	8,4	321	±	8,8 *
F_2	412	±	5,5	385	±	7,7	410	±	9,4	354	±	10,3 *
F_3	511	±	8,0	507	±	12,1	529	±	14,0	468	±	17,1
F_4	876	±	14,9	811	±	19,6 *	850	±	18,4	725	±	27,0 *
F_5	1453	±	25,0	1214	±	34,7 *	1301	±	31,1 *	1042	±	39,7 *
Fv/F_0	3,7936	±	0,0361	2,9662	±	0,0855 *	3,1263	±	0,1151 *	2,5676	±	0,0869 *
M_0	0,3609	±	0,0078	0,6363	±	0,0425 *	0,5685	±	0,0465 *	0,7513	±	0,0583 *
Vj	0,3437	±	0,0059	0,4528	±	0,0125 *	0,4190	±	0,0139 *	0,4999	±	0,0186 *
Vi	0,7441	±	0,0106	0,8366	±	0,0072 *	0,8034	±	0,0088 *	0,8744	±	0,0059 *
$PHI(P_0)$	0,7911	±	0,0016	0,7446	±	0,0056 *	0,7524	±	0,0074 *	0,7151	±	0,0073 *
PSI_0	0,6563	±	0,0059	0,5472	±	0,0125 *	0,5810	±	0,0139 *	0,5001	±	0,0186 *
$PHI(E_0)$	0,5193	±	0,0054	0,4090	±	0,0121 *	0,4391	±	0,0138 *	0,3605	±	0,0163 *
$PHI(D_0)$	0,2089	±	0,0016	0,2554	±	0,0056 *	0,2476	±	0,0074 *	0,2849	±	0,0073 *
Sm	24,717	±	0,5364	18,932	±	0,5967 *	21,474	±	0,7521 *	16,806	±	0,7270 *
N	26,077	±	0,8399	25,525	±	1,0730	27,966	±	1,7059	23,566	±	0,7446
Sum k	2,6397	±	0,0372	2,8951	±	0,0598 *	2,7070	±	0,0592	3,1840	±	0,0912 *
kn	0,5516	±	0,0096	0,7415	±	0,0250 *	0,6657	±	0,0191 *	0,9122	±	0,0412 *
kp	2,0881	±	0,0289	2,1536	±	0,0435	2,0414	±	0,0543	2,2718	±	0,0616
ABS/RC	1,3299	±	0,0242	1,8580	±	0,0949 *	1,7748	±	0,1132 *	2,0603	±	0,1143 *
TR_0/RC	1,0519	±	0,0189	1,3722	±	0,0615 *	1,3152	±	0,0699 *	1,4538	±	0,0665 *
ET_0/RC	0,6910	±	0,0153	0,7359	±	0,0238	0,7467	±	0,0304 *	0,7025	±	0,0194
DI_0/RC	0,2780	±	0,0058	0,4859	±	0,0344 *	0,4596	±	0,0441 *	0,6065	±	0,0487 *
RC/CS_0	288,01	±	6,001	201,38	±	10,835 *	229,12	±	12,554 *	167,48	±	9,652 *
PI(abs)	55,572	±	1,9960	23,979	±	2,7828 *	32,165	±	3,9858 *	16,890	±	2,3458 *

Table 5.1 *The measured and calculated fluorescence variables of 21 day old plants exposed for another 21 days to 0, 1, 5 and 50 µM Cd. All variables are presented with standard error, the presence of an asterisk marks an significant difference (P<0.05) with the control (0 µM Cd).*

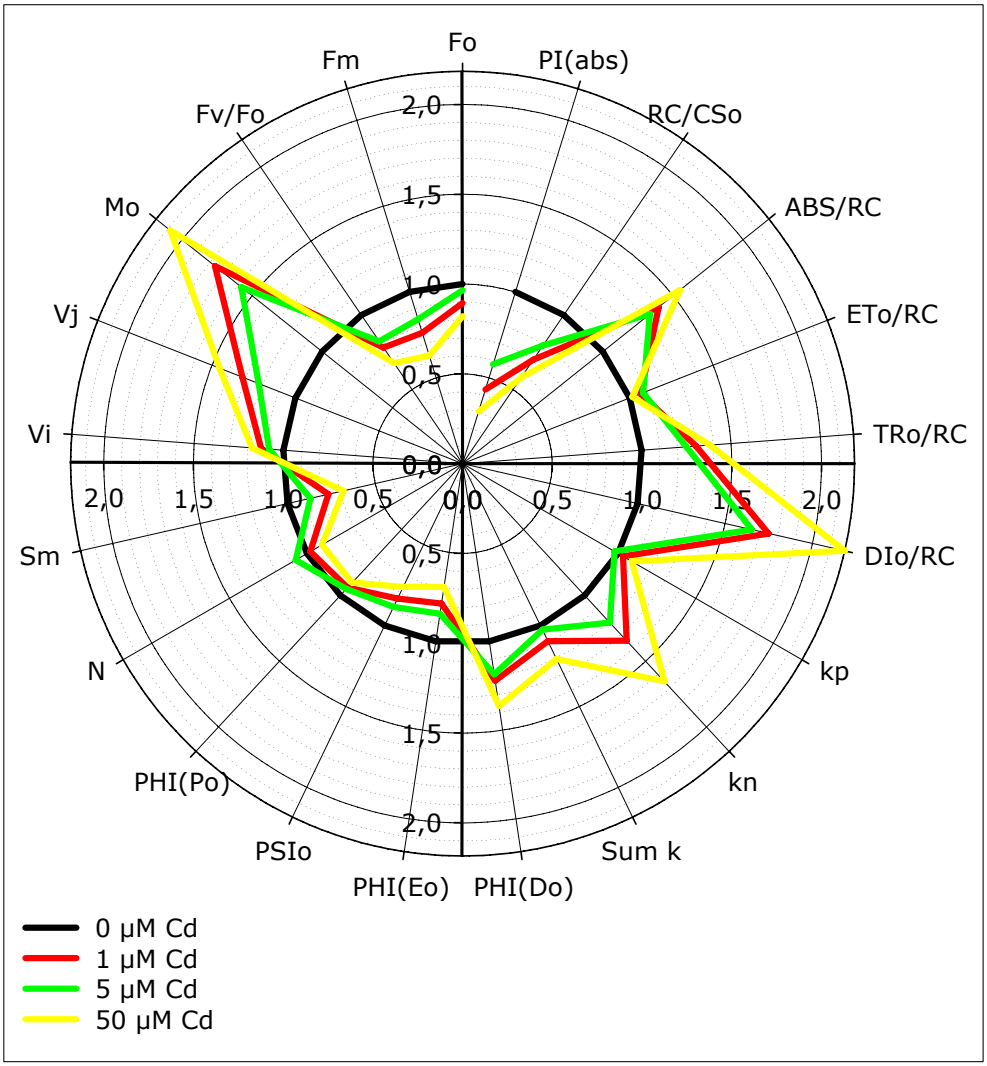

Fig. 5.8 *A spider plot illustrating the Cd-induced changes of the measured and calculated fluorescence variables relative to the control (0 µM Cd). For a detailed discussion of the parameters, see text.*

5.3.1.2 Technical fluorescence parameters

The minimal fluorescence (F_0), as already mentioned in the introduction, is the emission from the excited chlorophylls in photosystem II antennae in competition with excitation energy transfer to RCII, which takes place before the excitons reach the reaction centre (Krause & Weis, 1991). A significant decrease of F_0 was observed for 1 µM Cd and 50 µM Cd but - interestingly - not for 5 µM Cd. Different environmental stresses increase F_0, probably because of decreased efficiency of energy transfer from the antenna chlorophyll *a* to the reaction centres and/or inactivation of PSII reaction centres indicating irreversible membrane damage (Krause, 1988). However, since F_0 was decreased in this study, irreversible membrane damage does not seems to be the major Cd-induced effect on *Arabidopsis thaliana* at these exposure levels. A possibly explanation for the decreased F_0 could be that photochemically inactive photosystem II centres may act as dissipative sinks, thereby decreasing F_0 (Öquist *et al.*, 1992). The formation of photochemically inactive reactions centres has been suggested for wheat seedling exposed to Cd by Atal *et al.* (1991).

The conversion of photochemically active reaction centres into photochemically inactive or non-Q_B-reducing or 'silent' reaction centres involves the degradation of D1 protein (currently designated as PsbA). In fact, this is the case when the rate of inactivation exceeds the capacity for rapid and efficient repair of non-functional PSII reaction centres by *de novo* synthesis of D1 protein (*psbA* gene product in PSII reaction centre). The operation of the PSII repair cycle involves coordinated regulation of degradation and synthesis of D1 protein. When the supply of newly synthesized D1 protein is insufficient, such as under stress, the degradation process also slows down, resulting in the accumulation of non-functional PSII reaction centres (see the review by Trebst (2003)). The transfer to silent reaction centres also involves inhibition of the oxygen evolving complex. This mechanism leads to the oxidation of alternative electron donors like the carotenoids, Cyt b_{559} and chlorophyll *z* (Crofts & Horton, 1991; Krieger *et al.*, 1992; Schreiber & Neubauer, 1990). These silent reaction centres act as exciton traps thereby preventing over-reduction of the PSII plastoquinone electron acceptor. However, the rates and yields of the cyclic electron transport

pathways are very low and have limited ability to dissipate excess energy under stress conditions (Barber & De las Rivas, 1993; Poulson *et al.*, 1995). As a consequence, the nonphotochemical dissipation of excitation energy occurs merely via the antenna pigments involved with the xanthophyll cycle (see Fig. 5.11 and the discussion further below) (Demmig-Adams & Adams, 1996; Geiken *et al.*, 1998; Krupa *et al.*, 1993; Strasser, 2000).

Another explanation for the decreased F_0 could be a decreased fluorescence yield because of reduced chlorophyll content in photosystem II antenna (Ouzounidou *et al.*, 1997; Linger *et al.*, 2005), possibly because of substitution of Mg in chlorophyll by Cd in the biosynthesis (Kupper *et al.*, 1998). However, it has to be mentioned that Cd dependent chlorosis in *Brassica napus* was reported not to be caused by a direct intervention in chlorophyll biosynthesis but by a reduction in the chloroplast density per cell (Baryla *et al.*, 2001). Since the Cd-induced decrease in chlorophyll content was significant (Fig. 5.9), which was also demonstrated by the presence of chlorosis at 1 µM Cd (Fig. 3.1), the decrease of F_0 is therefore most likely a combined effect of decreased chlorophyll content (because of decreased light harvesting complex size and/or chloroplast density) with higher nonphotochemical dissipation. The different response at 5 µM Cd indicates most likely an increased protective adaptation in the 5 µM exposed plants compared to the 1 µM exposed plants. This could in fact, explain the divergent results concerning Cd-induced reduction of F_0 from other studies as for instance, a decreased F_0 was also observed by Pietrini *et al*. (2003) and Azevedo *et al*. (2005) but no change was reported by Di Cagno *et al*. (1999), Mallick and Mohn (2003) and Balakhnina *et al*. (2005).

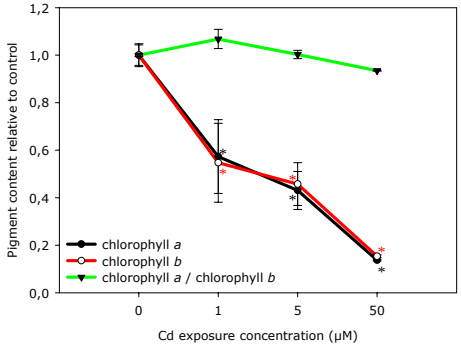

Fig. 5.9 *The effect of Cd exposure on the contents of chlorophyll a and b, and the ratio of both pigments. All data is presented relative to the control (0 µM). The data points marked with an asterisk are significantly different (P<0.05) from the control.*

The maximal fluorescence (F_M) expresses the state of photosystem II when all pheophytin, Q_A, Q_B and PQH_2 molecules are in a reduced state. It was significantly decreased at 1 µM, 5 µM and 50 µM Cd (with again 5 µM Cd performing better than 1 µM Cd). The relatively steep decline of F_M along with the fact that it decreased faster than F_0 (according to the significantly increasing F_0/F_M $(= \varphi_{D0})$) is again an indication of the importance of energy dissipation via nonphotochemical pathways. A similar observation has been made for the LHCII of corals exposed to bleaching conditions (Hill *et al.*, 2004).

The change in F_M is also related with F_V/F_0 $(= k_P/k_N)$ which reflects the efficiency of electron donation to the photosystem II reaction centres (Skórzyńska-Polit & Baszynski, 2000) and the rate of photosynthetic quantum conversion at photosystem II reaction centres (Babani & Lichtenthaler, 1996). The Cd-induced decrease in F_V/F_0 therefore reflects a decrease in the relative contribution of the trapping flux to the total de-excitation fluxes of excited chlorophyll (Havaux *et al.*, 1991; Strasser *et al.*, 2000). As a consequence, F_V/F_0 is shown to be related to increased q_N (Ouzounidou *et al*., 1993). Cd-induced decrease of F_V/F_0 has also been linked to the detrimental effect on the oxygen evolving complex, most probably by disintegration of the oxygen evolving system by free fatty acids (Garstka & Kaniuga, 1988) or by replacing manganese from the oxygen evolving complex (Kriedemann *et al.*, 1985; Sayed, 1998; Mallick & Mohn, 2003). Nonetheless, according to Kriedemann *et al*. (1985) Mn-deficiency is correlated with an increase of F_0 (indicating irreversible damage to thylakoids), which is not in agreement with our observations. Recently, Faller *et al.* (2005) delivered evidence that in *Chlamydomonas reinhardtii* and in isolated photosystem II, Cd in the low-µM range does not inhibit the oxygen evolving complex itself (*i.e.*, there was no competition observed between Cd and Mn) but that Cd binds competitively to the essential Ca-site in photosystem II during photoactivation (*i.e.*, assembly of the water splitting complex in the last step in the assembly of Photosystem II before it becomes functional). As Cd seems to inhibit photoactivation only and not the assembled photosystem II, the Ca-Cd competition is not likely to influence the parameter F_V/F_0.

Therefore, the decreased F_V/F_0 (even at the highest Cd exposure concentrations) suggests the presence of protection mechanisms such as nonphotochemical energy dissipation, rather than an actual disintegration of the system.

5.3.1.3 The transient curve kinetics

According to the curve kinetics M_0, V_J and V_I, some effects of decreased electron transport efficiency are discernable. M_0 is the net rate of photosystem II closure and is defined by $M_0 \left(= dV/dt_0 = 4\left(F_{300\mu s} - F_0\right)/\left(F_M - F_0\right)\right)$. M_0 represents electron trapping per reaction centre $\left(TR_0/RC\right)$ minus electron transport per reaction centre $\left(ET_0/RC\right)$. M_0 rate increases significantly under Cd exposure (Fig. 5.8), which is normally an indication of inhibited Q_A^- reoxidation (or inhibited electron transport beyond Q_A^-). However, since trapping TR_0 takes place in both active and silent reaction centres while the electron transport ET_0 is almost certainly limited to active reaction centres, the increase of M_0 (thus increased trapping minus steady electron transport) should actually be seen as a result of the increased formation of silent reaction centres.

The reduced efficiency of electron transport in the photochemically inactive reaction centres is reflected in the increased V_J. V_J is the variable fluorescence at 2 ms or step J $\left(V_J = \left(F_J - F_0\right)/\left(F_M - F_0\right)\right)$, representing the number of reaction centres closed at 2 ms as a proportion of the total number than can be closed (Strasser & Strasser, 1995). V_J was significantly increased under Cd exposure, indicating an increased proportion of closed reaction centres after 2 ms or reduced efficiency of the transport of an electron to move further than Q_A^- + Q_B into the electron transport chain (Strasser & Strasser, 1995; Strasser *et al.*, 2000). This is obviously a typical sign for the presence of non-Q_B-reducing reaction centres.

For the same reason, also at step I (30 ms), $V_I \left(= \left(F_I - F_0\right)/\left(F_M - F_0\right)\right)$ was increased significantly under Cd exposure. Since V_I represents the proportion of reaction centres which are closed after 30 ms illumination, an increase of V_I is the result of an accumulation of reduced plastoquinone, indicating a reduced efficiency of electron transport beyond Q_A + Q_B^{2-}/PQH_2 (Strasser & Strasser, 1995; Strasser *et al.*, 2000).

It is clear that the decreased electron transport efficiency at I and J are related to the inactivation of the central core protein D1 (PsbA) of PSII thereby blocking the energy transfer between Q_A and Q_B reduction. However, as described in the introduction, the transient kinetics (especially M_0 and at the J step) may also be influenced by changes dependent of the S-states of the oxygen evolving complex (Hill *et al.*, 2004; Hsu, 1993), as inhibition of S-states induces the inactivation of photosystem II (Atal *et al*., 1991). As mentioned before, this process has also been related to the formation of silent reaction centres.

S_M is defined as the normalized area above the transient $(S_M = \text{Area}/(F_M - F_0))$ and represents the working integral of the energy needed to close all reaction centres (Strasser *et al.*, 1999). The apparent decrease under Cd suggests that less energy is needed to close all reaction centres (Appenroth *et al.*, 2001), which is obviously a result of the decreased number of active reaction centres (or, the increased number of inactive reaction centres).

N, the turnover number of Q_A, defines how many times Q_A has been reduced to Q_A^- in the time span from t_0 to t_{FM} and is related to S_M as calculated according to $N = S_M M_0/V_J$ (Strasser *et al.*, 1999). Because of the fact that V_J increased less than M_0 (slower closure rate of the reaction centres), the decrease of S_M is compensated and consequently only minor (non-significant) effects on N were observed under Cd exposure.

5.3.1.4 Quantum yield or flux ratios

The maximum quantum yield of primary photochemistry φ_{P0} is measured in terms of TR_0/ABS or F_V/F_M $((F_M - F_0)/F_M = 1 - F_0/F_M)$. This parameter has been reported not to be very sensitive in case of Cd exposure because of the Cd-induced increase of q_N (Greger & Orgen, 1991; Krupa *et al.*, 1993; Skórzyńska-Polit & Baszynski, 1997). Although in this study, *Arabidopsis thaliana* displayed a significant decrease of φ_{P0} even at the lowest exposure concentration, the φ_{P0} values ranged from 0.79 to 0.71 only, which does not indicate the presence of severe stress (Fig. 5.8). This is obviously the result of the proportional decrease of both F_0 and F_M, which prevents a sharp change of this ratio. Irreversible damage to thylakoids membranes is accompanied by φ_{P0}

values smaller than 0.5 (Hetherington *et al.*, 1989, Greer *et al.*, 1991, Öquist *et al.*, 1993). This means that even at the 50 µM Cd exposure concentration, which induces oxidative stress causing severe damage to thylakoids (see chapter 4), the actual yield of photosystem II remains relatively intact.

ψ_0 expresses the probability that a trapped exciton can move an electron into the electron transport chain and is calculated by $(1 - V_J) = (ET_0/RC)/(TR_0/RC) = ET_0/TR_0$. However, a decreased ψ_0 does not specifically mean that Cd induced a lower yield of the transport of an electron to move further than Q_A^- + Q_B into the electron transport chain in an active reaction centre (as described later by the specific fluxes of active reaction centres). As a matter of fact, it indicates that a certain degree of reaction centres are silent, thus trapping excitons without resulting in reduction of Q_B and consequently leading to a decreased ψ_0.

φ_{E0} expresses the maximum quantum yield in terms of moving electrons further than Q_A^-, or that a photon will move an electron into the ET-chain. $\varphi_{E0} = (TR_0/ABS)(ET_0/TR_0) = \varphi_{P0}\psi_0 = ET_0/ABS$. The same consideration as for ψ_0 is also valid for this parameter since a decreased φ_{E0} indicates that a certain degree of reaction centres are silent, thus absorbing excitons without resulting in electron transport.

The significantly increased quantum yield of energy dissipation φ_{D0} $(= F_0/F_M)$ is, as mentioned before, an indication of increased energy dissipation via nonphotochemical quenching in the antennae (Hill *et al.*, 2004).

5.3.1.5 De-excitation constants

Whereas the photochemically de-excitation constant k_P remains the same, the nonphotochemical de-excitation constant k_N which is the summation of k_H (for heat dissipation) and k_F (for fluorescence emission) increases significantly indicating increased nonphotochemical de-excitation.

This leads to an increased Sum k $(= k_P + k_N)$, which indicates yet again the presence of increased dissipation of absorbed energy as a protection mechanism against Cd-induced photosynthesis inhibition rather than actual

damage (Bussotti *et al.*, 2005), which was in fact also suggested on the basis of the observed decrease of F_0.

5.3.1.6 Specific energy fluxes (per photochemically active reaction centres (RC))

ABS/RC is defined as the total absorption capacity per photochemically active reaction centre and is calculated as $(TR_0/RC)/(TR_0/ABS) = (TR_0/RC)/\varphi P_0 = (M_0/V_J)/[1-(F_0/F_M)]$. A significantly increased ABS/RC for all Cd exposure concentrations indicates an apparent increase of the (relative) antenna size by the formation of silent reactions centres. In other words, as photochemically active reaction centres have been transformed into silent reaction centres with modified conformation (acting as dissipative exciton traps), the relative (not absolute) size of the antenna per photochemically active reaction centre is increased (Strasser *et al.*, 2000, 2004). This parameter actually allows the calculation of the fraction of the reaction centres, which have remained active after Cd exposure by $((ABS/RC)_{control}/(ABS/RC)_{exposed})$ (Strasser *et al.*, 2004). In this way it was calculated that compared to the control, 71 % (1 µM Cd), 75 % (5 µM Cd) and 65 % (50 µM) of the reaction centres remained photochemically active after 21 days of Cd exposure.

TR_0/RC $(= M_0(1/V_J))$ is defined as the maximal trapping rate of photosystem II which represents the maximal rate by which an exciton is trapped per photochemically active reaction centres resulting in the reduction of Q_A. The Cd-induced significant increase of TR_0/RC in combination with the decreased TR_0/ABS $(= \varphi P_0)$ is once more an indication of the protective down-regulation of photosystem II by forming silent reaction centres (Strasser & Tsimilli-Michael, 2001; Strasser *et al.*, 2004).

Concomitantly, because of the increased number of silent dissipative reaction centres, the nonphotochemical dissipation increases. This results in a strongly increased DI_0/RC $(= (ABS/RC) - (TR_0/RC))$, which is the ratio of the total dissipation of untrapped excitation energy from all reaction centres with respect to the number of active reaction centres. Dissipation occurs as heat, fluorescence and energy transfer to other systems.

$ET_0/RC \left(= TR_0/RC - M_0 = M_0 1/V_J \psi_0\right)$ defines the probability of electron transport beyond Q_A^- in an active reaction centre, or in other words, the probability of reoxidation of reduced Q_A^- via electron transport in an active RC. ET_0/RC remained stable and tended to increase (only significantly for 5 µM Cd) which is an indication that in the active reaction centres, the electron transport (ET_0) is not compromised at all (!) under Cd exposure. However, this indication is only valid if the electron transport is completely inhibited in the silent reaction centres. Moreover, in combination with the decreased $ET_0/ABS \left(= \varphi_{E0}\right)$, it is again an indication of increased dissipation by silent reaction centres (Strasser & Tsimilli-Michael, 2001; Strasser *et al.*, 2004).

5.3.1.7 Density of photochemically active reaction centres

$RC/CS_0 \left(= F_0\, \varphi_{P0}\, V_J/M_0\right)$ is defined as the density of the photochemically active reaction centres per cross section. As many reaction centres had become silent, obviously, the density of the photochemically active reaction centres was significantly reduced under Cd exposure.

5.3.1.8 Performance index

The performance index (PI_{ABS}), combines the three main functional steps (light energy absorption, excitation energy trapping, and conversion of excitation energy to electron transport) of photosynthetic activity by a PSII reaction centre complex into a single multiparametric expression. More specifically, PI_{ABS} combines the density of photochemically active reaction centres $\left(RC/ABS\right)$ with the performance of the light reactions $\left(\varphi_{P0}/(1-\varphi_{P0})\right)$ and the performance of the dark reactions $\left(\psi_{P0}/(1-\psi_{P0})\right)$ (Srivastava *et al.*, 1999; Strasser *et al.*, 1999; Tsimilli-Michael *et al.*, 2000).

$$PI_{ABS} = \left(\frac{\gamma_{RC}}{1-\gamma_{RC}}\right)\left(\frac{\varphi_{P0}}{1-\varphi_{P0}}\right)\left(\frac{\psi_0}{1-\psi_0}\right)$$

$$= \left(\frac{RC}{ABS}\right)\left(\frac{\varphi_{P0}}{1-\varphi_{P0}}\right)\left(\frac{\psi_0}{1-\psi_0}\right)$$

$$= \left(\frac{1 - (F_0/F_M)}{M_0/V_J}\right)\left(\frac{F_M - F_0}{F_0}\right)\left(\frac{1 - V_J}{V_J}\right)$$

PI_{ABS} is much more sensitive than $\varphi P0$ (quantum yield of primary photochemistry calculated using F_0 and F_M only), because it takes, apart from F_0 and F_M, also V_J and M_0 (thus dependent on the shape of the fluorescence transient) into account. As both M_0 and V_J were increased under Cd exposure because of the transformation of a fraction of the photochemically active reaction centres into silent reaction centres, leading to an (absolute) reduced Q_A^- reoxidation and reduced efficiency electron transport further than Q_A^- + Q_B, respectively, the PI_{ABS} was significantly decreased under increased Cd-exposure.

5.3.2 Nonphotochemical quenching (NPQ) in relation to pigment ratios and the xanthophyll cycle

The results of the fast fluorescence analysis revealed that the electron transport taking place in the photochemically active reaction centres is protected by the formation of silent reaction centres (also known as photoinhibition) which function as exciton traps that dissipate their excitation energy as a protective mechanism against Cd-induced increased sensitivity to high light stress.

A sensitive and robust way to investigate the contribution of dissipation of excitation energy in the antenna system via pathways other than those involved in photochemistry and fluorescence is the measurement of the nonphotochemical quenching (NPQ) of chlorophyll fluorescence (Maxwell & Johnson, 2000; Schreiber, 2004). The most obvious alternate pathways of NPQ are direct heat losses and excitation transfer to other molecules, such as for example carotenoids, and intersystem crossing to chlorophyll *a* triplets. As mentioned in the materials and methods, NPQ was measured with the fluorescence imaging system (FIS) and was calculated as $(F_M - F_M')/F_M'$ also known as the Stern-Volmer relationship (Stern & Volmer, 1919; Papageorgiou, 1975). Fig. 5.10, depicting the mean NPQ measured by the FIS at the different analysis time points, displays a graph with a shape of a damped oscillation. This pattern, also observed in earlier experiments to study effects of a viral infection on *Nicotiana benthamiana* (Dr. Massimo Ciscato, pers. comm.), originates from the fact that the plants were dark adapted prior to the analysis. When the actinic light was applied, photosynthesis regained its activity following a damped oscillation pattern (as observed for most biochemical processes regaining their

homeostasis). As a result of this pattern, most information was derived from the NPQ values at the deflection point of the curve, thus at 60 s, 90 s and 120 s of actinic radiation. As expected, NPQ increased under Cd-exposure, which was significant for 5 µM and 50 µM Cd. This result is in agreement with the results of Di Cagno *et al.* (2001) who observed increased NPQ in sunflowers under Cd exposure. The increase of NPQ, which is also related to other unfavourable conditions including water stress, has been associated with the induction of the xanthophyll cycle (Verhoeven *et al.*, 2001). The xanthophyll cycle is mediated by three xanthophylls: violaxanthin, antheraxanthin and zeaxanthin. In normal conditions, violaxanthin (V) functions as an antenna pigment by transferring energy to chlorophyll *a*. However, in case of stress-induced increased light sensitivity (leading to photoinhibition), a regulated de-epoxidation/epoxidation transforms the diepoxide violaxanthin into the carotenoid zeaxanthin (Z), via the intermediate monoepoxide antheraxanthin (A). Antheraxanthin and zeaxanthin are two quenching xanthophylls, which facilitate the dissipation of excess excitation energy directly within the light-harvesting antennae. This cycle is triggered by low pH within the photosynthetic lumen, causing the activation of the membrane bound violaxanthin de-epoxidase and the protonation of the PsbS protein, causing a change in conformation that activates the binding of zeaxanthin. As follows, the protonated PsbS–zeaxanthin complex is thought to impose conformational changes on the neighbouring light-harvesting complexes that effectively switches these units into a quenched state in which nonphotochemical de-excitation of $Chl^{\bullet}$ is favoured (Fig. 5.11). In this way, high contents of xanthophylls thermally dissipate the excess excitation energy to protect the silent reaction centres (Demmig-Adams & Adams, 1996; Demmig-Adams *et al.*, 1990; Gilmore & Yamamoto, 1993; Golan *et al.*, 2006; Li *et al.*, 2000, 2004; Niyogi *et al.*, 1998, 2001; Ottander *et al.*, 1995). Moreover, zeaxanthin has been suggested to contribute to photoprotection in another way, *i.e.* by removing epoxy groups from the oxidized bonds of fatty acids of thylakoid glycerolipids or by directly reacting with ROS (Schindler & Lichtenthaler, 1994; Lichtenthaler, 1996).

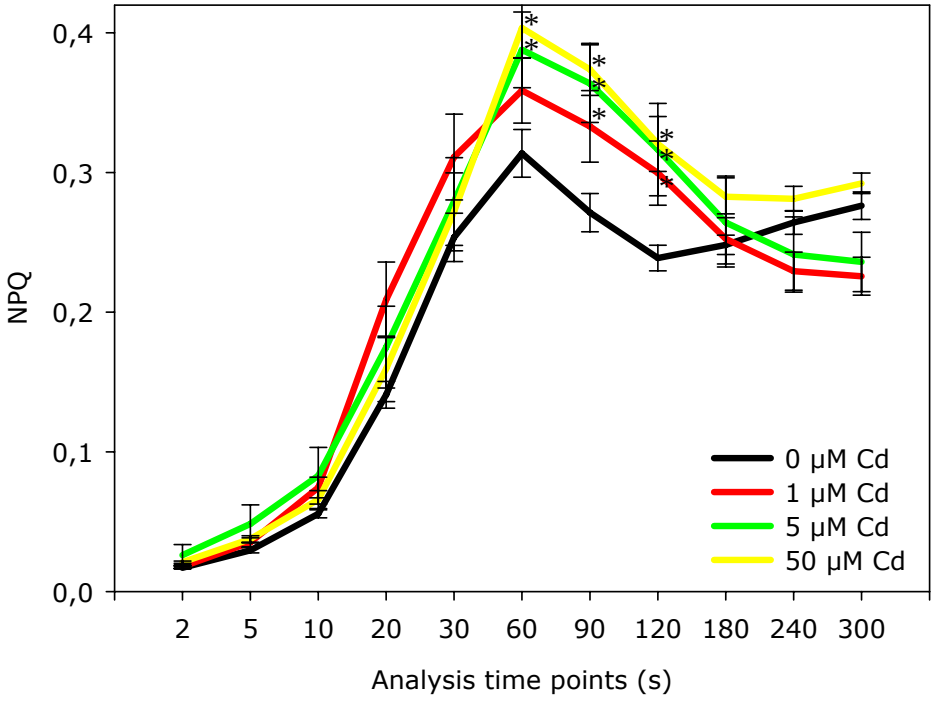

Fig. 5.10 *Illustration of the Cd-induced effects on the NPQ, measured by the fluorescence imaging system at different analysis time points. The data points marked with an asterisk are significantly different (P<0.05) from the control.*

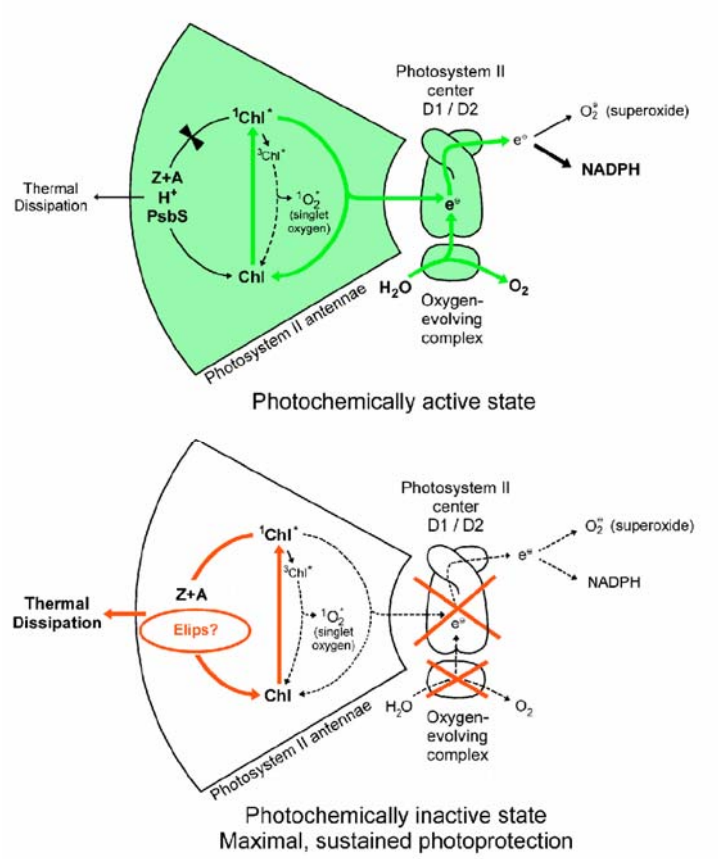

Fig. 5.11 *Schematic depiction of photon absorption in PSII antennae and photochemistry in PSII cores in photochemically active and inactive state (source figure: Adams / Demmig-Adams Group, Department of EPO Biology, University of Colorado). Thermal energy dissipation is facilitated by the xanthophyll cycle pigments zeaxanthin and antheraxanthin (Z+A) and PsbS protein upon thylakoid overacidification. In case of sustained high light stress, the photochemically active reaction centres are transformed into silent reaction centres by inhibition of the oxygen evolving complex and inhibited Q_A-reoxidation. The excess excitation energy is thermally dissipated by high contents of photoprotective xanthophylls.*

The increased contents of $V + A + Z$, relative to the total chlorophyll content as illustrated by Fig. 5.12 already gave an indication of the induction of the xanthophyll cycle. However, it was the xanthophyll index (Fig. 5.13), which is the ratio of the transformed xanthophyll content to the total xanthophyll content $(= (A + Z)/(V + A + Z))$, that revealed a significantly induction at 5 µM and 50 µM Cd. This was in agreement with the increased NPQ at these exposure concentrations compared to lower induction at 1 µM Cd. In fact, this could offer an explanation for the contradicting result of the better performing photosystem II at 5 µM Cd compared to the lesser performing photosystem II at 1 µM Cd. It can therefore be hypothesised that between 1 and 5 µM Cd, an increased induction of several protective processes resulted in an improved photosynthetic efficiency. The xanthophyll cycle is certainly one of those protective processes, most likely concomitantly induced with the formation of a photoprotective shield of the anthocyanins as described in chapter 4.

Another accessory carotenoid pigment (transferring its excited states to chlorophyll) is the xanthophyll lutein, which is a structural isomer of zeaxanthin, differing in the location of only one double bond. Lutein has one de-epoxidized cycle end group (analogous to antheroxanthin) and is also supposed to be involved in energy dissipation in *Arabidopsis thaliana* (Pogson *et al.*, 1996, 1998). As a consequence, the increased lutein content relative to the total chlorophyll at 5 and 50 µM Cd (Fig. 5.12) indicates a relative higher contribution to excitation energy dissipation in Cd exposed plants.

β-carotene has a photoprotective function for the light-harvesting complexes by quenching triplet state chlorophyll followed by thermal dissipation of this excitation energy and quenching of singlet oxygen (Frank & Cogdell, 1996). On the other hand, involvement of β-carotene in the xanthophyll cycle has been suggested by Depka *et al.* (1998) by the conversion of β-carotene to zeaxanthin, occurring upon the disassembly of the photodamaged photosystem II reaction centres. The β-carotene content was increased at 50 µM Cd (relative to total chlorophyll (Fig. 5.12)) again indicating increased photoprotection.

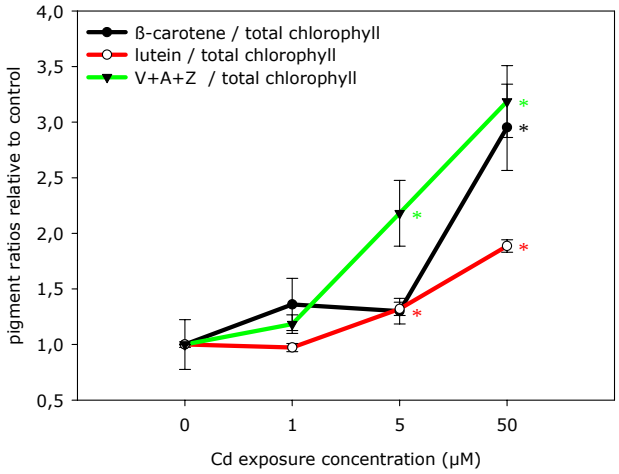

Fig. 5.12 *The effect of Cd exposure on the contents of β-carotene, lutein and the sum of the xanthophyll cycle pigments (violaxanthin, antheraxanthin, zeaxanthin) relative to total chlorophyll and presented relative to the control (0 µM Cd). The data points marked with an asterisk are significantly different (P<0.05) from the control.*

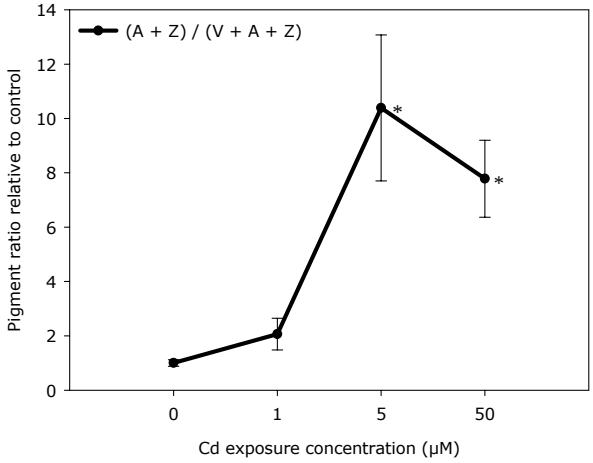

Fig. 5.13 *The effect of Cd exposure on the xanthophyll cycle as illustrated by the xanthophyll index, which is the ratio (calculated relative to the control (0 µM Cd)) of the excitation energy quenchers antheraxanthin (A) + zeaxanthin (Z) to the total xanthophyll content (violaxanthin (V) + antheraxanthin (A) + zeaxanthin (Z)). The data points marked with an asterisk are significantly different (P<0.05) from the control (0 µM Cd).*

5.4 General conclusion

The results of the chlorophyll *a* fluorescence analysis revealed no irreversible damage to photosystem II, not even at 50 µM Cd exposure. This remarkable fact could be related to the formation of silent reaction centres; protected by an induced xanthophyll cycle through increased thermal dissipation in the antennae, which can in its total be designated as photoinhibition. The protective action was confirmed by the apparently unharmed electron transport in the photochemically active reaction centres. Moreover, the formation of silent reaction centres offered an explanation as to why Cd did not result in an important decrease of φ_{P0}. However, Cd did lead to strongly decreased chlorophyll content. Therefore, by taking all these factors into account, Cd affected the performance index considerably.

The remarkable observation that at 5 µM Cd, photosynthesis had the tendency to perform better than at the less polluting 1 µM Cd concentration was most likely related to increased induction of several protective processes between 1 and 5 µM Cd. These protective processes include, apart from the induction of the xanthophyll cycle, most likely the formation of a photoprotective shield of the anthocyanins as described in chapter 4. At 50 µM however, the increased Cd-toxicity caused a further decline in photosynthesis efficiency.

5.5 Perspectives

As the results of this and previous chapter suggested the importance of antioxidative protection mechanisms, it would be of particular interest to see the effects of Cd on the photosynthetic efficiency in glutathione (GSH) and/or ascorbate (AsA) *Arabidopsis* mutant plants.

Chapter 6

The fluorimetric detection of a Cd-induced singlet oxygen burst in *Arabidopsis thaliana* cells using DanePy; a pilot study

6.1 Introduction

In chapters 4 and 5, the role of Cd in photosynthesis inhibition and some of the protection mechanisms against increased production of ROS were discussed. Inhibition of photosynthesis by adverse conditions is reported to cause an increased sensitivity to photoinhibition because of an imbalance between light capture, CO_2 assimilation and carbohydrate utilization (Foyer & Noctor, 2000; Long *et al.*, 1994). In other words, as Cd inhibits photosynthesis, the photon intensity becomes in excess of that required for CO_2 assimilation (even under normal light conditions) leading to increased photoproduction of reactive oxygen species (singlet oxygen ($^1O_2$), superoxide (O_2^-) and hydroxyl radical ($^{\cdot}OH$)). Reactive oxygen species are capable of damaging the D1 protein (PsbA) (Barber & Andersson, 1992; Foyer & Noctor, 2000), leading to suppression of the electron flow through the photosystems I and II. This results in the down-regulation of photosystem II quantum yield (photoinhibition) which is regulated by the xanthophyll cycle and the proton gradient across the thylakoid membrane leading to increased thermal dissipation of excitation energy (see chapter 5). In this way, photoinhibition decreases the light-driven formation of ROS and may serve as a strategy to counteract photooxidative processes (Anderson *et al.*, 1997). This obviously occurs in combination with scavenging of the ROS, produced in the chloroplast thylakoids.

Photoinhibition has been related to increased production of singlet oxygen ($^1O_2$) in the chloroplast thylakoid (see review by Asada, 2006). The primary source of singlet oxygen is the excitation of photosystem II chlorophyll (^{1}P680) and antenna chlorophyll (^{1}Chl). In case of photosystem II chlorophyll, the absorption of light energy raises one electron of an electron pair in the chlorophyll molecule from the (singlet) ground state ^{1}P680 to a higher energetic state P680$^+$. The lifetime of P680$^+$ is very short, because of rapid withdrawal of electrons from water to P680$^+$ and relaxation via radiative decay (fluorescence). In addition, the charge recombination of P680$^+$ with the primary electron acceptors of photosystem II pheophytin, Q_A, and Q_B forms the triplet ^{3}P680* (Fig. 6.1). This transformation occurs more frequent when the intersystem electron carriers are reduced (downregulation of photosystem II, Asada, 2006)

leading to a prolonged lifetime of $P680^+$. When the excitation energy from $^3P680^*$ is transferred to the triplet dioxygen (which is most likely $^3O_2$ evolved by the water oxidase in the lumen (Asada, 2006)), a spin reversal of one $^3O_2$ electron is induced which leads to the formation of singlet oxygen ($^1O_2$) and the relaxation of chlorophyll to its ground state $^1P680$ (see the review by Niyogi, 1999) (Fig. 6.2). The generation of singlet oxygen in the antennae chlorophyll occurs via a similar pathway, except that triplet antenna chlorophyll ($^3Chl^*$) is merely formed from $^1Chl^*$ via spontaneous intersystem crossing (reversal of the spin) (Kramer & Mathis, 1980; Rinalducci *et al.*, 2004; SantaBarbara *et al.*, 2002). In addition, $^1O_2$ may also arise as a by-product of lipoxygenase activity (Kanofsky & Axelrod, 1986).

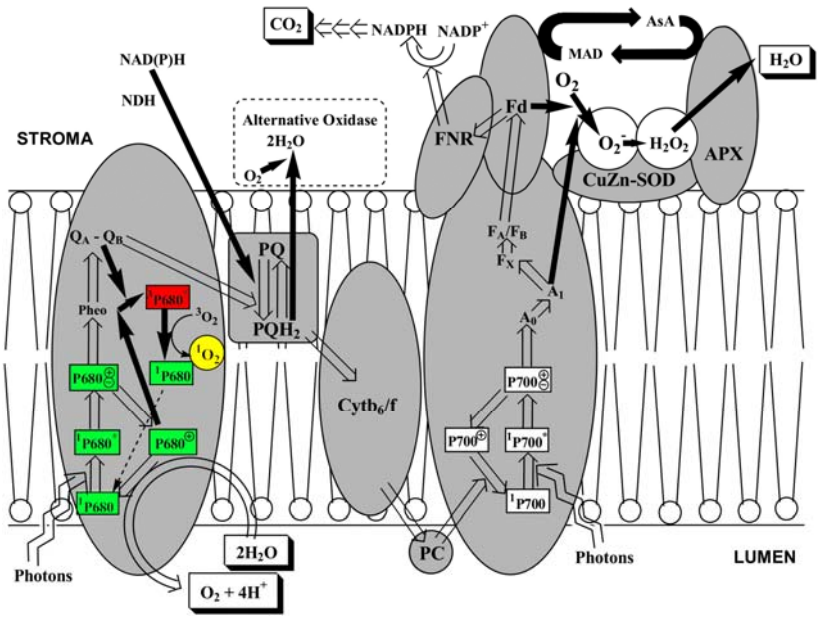

Fig. 6.1 *A simplified illustration of the generation of $^1O_2$ in photosystem II (and of O_2^- in photosystem I) in chloroplast thylakoids (adapted from Asada, 2006). The open arrows represent the photoexcitation of reaction centre chlorophyll and the electron flow under the photon intensity where all of the electrons generated are utilized for the CO_2 assimilation. Black arrows represent the electron flow when photon intensity exceeds the capacity of the flux of electron transport and the flux to CO_2 assimilation, leading to a charge recombination of $^1P680^+$ with the electron acceptors pheophytin, Q_A, and Q_B to form the triplet $^3P680^*$.*

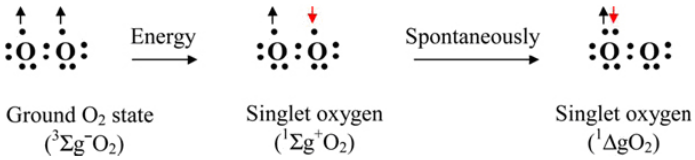

Fig. 6.2 *An illustration of the excitation energy transfer facilitating the spin reversal of one electron of triplet dioxygen ($^3O_2$); which leads to the formation of singlet oxygen ($^1O_2$) (source: Edreva, 2005).*

$^1O_2$ is highly reactive, and can add directly to the double bonds of polyunsaturated fatty acids to form lipid peroxides (LOOH) which can lead to lipid peroxidation chain reactions (Girotti & Kriska, 2004) and is further reported to modify nucleic acids (Martinez *et al.*, 2003), and proteins (Davies, 2004). As singlet oxygen is both highly reactive and quenched by water, it has a short lifetime within cells (0.1 μs) and consequently the target site is near the site of origin in the chloroplast. It is therefore most likely to affect lipids and membrane proteins located near the reaction centre of PSII, for instance the oxidation of protein D1 (PsbA) (Sharma *et al.*, 1997), consequently leading to further induction of photoinhibition (Nishiyama *et al.*, 2004). Moreover, high concentrations singlet oxygen can inactivate the *EXECUTER1* gene and trigger genetic programs that cause growth inhibition and cell death (Wagner *et al.*, 2004).

$^3Chl^*$ and $^1O_2$ are effectively quenched by β-carotenes of light-harvesting complexes (Frank & Cogdell, 1996) by transferring the excitation energy of singlet oxygen directly to β-carotene forming the triplet excited state $^3car^*$. Subsequently, $^3car^*$ returns to the ground state by thermal dissipation of the excess energy (thereby contributing to NPQ, see chapter 5). However, β-carotenes bound to photosystem II reaction centres are localized too far away from P680 to actually quench singlet oxygen (Kamiya & Shen, 2003; Krasnovsky, 1998; Loll *et al*., 2005; Telfer, 2002). In addition, the turnover of the D1 protein (PsbA) has been related to the quenching of singlet oxygen. As the D1 protein (PsbA) is oxidized by singlet oxygen (Sharma *et al.*, 1997), it actually functions as a scavenger for reactive oxygen species (Trebst, 2003).

The well-known antioxidant α-tocopherol is also an effective singlet oxygen quencher (see reviews by Munné-Bosch & Alegre, 2002 and Trebst, 2003) but at a lower rate than β-carotene (Krasnovsky, 1998). α-Tocopherol is oxidized by $^1O_2$ to α-tocopherylquinone via 8-hydroperoxy-*α*-tocopherone (Neely *et al*., 1988). In photosystem II, α-tocopherol functions primarily as a supplement in stress situations when D1 (PsbA) protein turnover becomes insufficient to quench the increased levels of singlet oxygen (Trebst, 2003). Tocopherols also play a role as an antioxidant to suppress the lipid peroxidation in thylakoids by trapping of lipid radicals (Munné-Bosch & Alegre, 2002).
In this way, singlet oxygen is an important factor for the downregulation of photosystem II, which was, according to the photosynthesis results presented in chapter 5, an important reaction towards Cd stress.
In a review, Trebst (2003) summarized all factors regulating the downregulation by singlet oxygen.

1. The redox state and redox potential of PQH_2 leading to $^3P680^*$ and $^1O_2$.
2. The rate of protein synthesis of the D1 (PsbA) protein subunit.
3. The reassembly rate of PS II, limited not only by the availability of the protein subunits, but also of cofactors, elements and pigments, to be reattached to form a new reaction centre; lack of carotene for reassembly is one example of disappearance of PS II during D1 (PsbA) protein turnover.
4. The rate of tocopherol turnover and synthesis.

6.2 Objectives

Since singlet oxygen is regarded to be one of the crucial factors for the downregulation of photosystem II, the effects of Cd on the generation of singlet oxygen is both an interesting and relevant object of study. Therefore, this chapter is dedicated to the development of a method using a fluorimetric analysis to study the generation of singlet oxygen induced by Cd in a cell culture of *Arabidopsis thaliana*.

6.3 Development of the singlet oxygen fluorescence assay

6.3.1 The fluorescent sensor DanePy

In leaf tissues, the relation between photoinhibition by excess photosynthetic active radiation (PAR) and production of singlet oxygen ($^1O_2$) in chloroplasts was demonstrated in *Arabidopsis thaliana* and spinach by Hideg *et al.* (2001, 2002) using DanePy. DanePy (3 - (*N* - diethylaminoethyl) - *N* - dansyl) aminomethyl - 2,2,5,5 – tetramethyl - 2,5 – dihydro - 1*H* - pyrrole) is a double sensor (fluorescent and spin) of singlet oxygen which penetrates into the chloroplast but does not alter the functioning of the photosynthetic electrontransport. Its strong fluorescence (well distinct from chlorophyll fluorescence) is quenched upon reaction with singlet oxygen which is the result of a conversion of its pyrrol group into nitroxide (Fig. 6.3) leading to the formation of the less fluorescent DanePyO (3 - (*N* - diethylaminoethyl) - *N* - dansyl) aminomethyl - 2,2,5,5 - tetramethyl - 2,5 – dihydro - 1*H* - pyrrol - 1 - yloxyl).

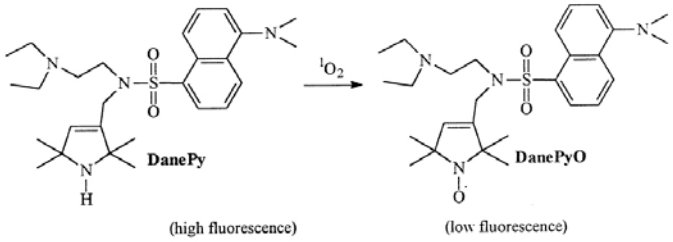

Fig. 6.3 *The conversion of DanePy into DanePyO by singlet oxygen (source: Hideg et al., 2001).*

The fluorescence is measured with a spectrofluorometer using 330 nm excitation and 530 nm emission. Currently, the best way to infiltrate the sensor into the leaf is actually a modified procedure for introducing pathogens into leaves. According to this method, the sensor (approx. 10-20 µl of 1 mM DanePy) is forced into the middle layer of the leaf tissue, using a plastic syringe without the needle through a pinhole of the tissue made at the adaxial side with a sharp pin (Hideg *et al.*, 2002). However, although this method is regarded as a milder

method for introducing sensors uniformly compared to vacuum infiltration, this method inevitable induces stress, especially in the small leaves of *Arabidopsis thaliana*. Therefore, it was regarded as not suitable for studying the effects of Cd-stress. For that reason, a cell culture of *Arabidopsis thaliana* was used instead of plants. This study has been performed in collaboration with Dr. Hideg (Biology Research Centre, Szeged, Hungary) who also kindly provided the sensor DanePy.

6.3.2 The cell culture

6.3.2.1 Subculturing

The cells of *Arabidopsis thaliana* (Columbia), kindly provided by Dr. N. Horemans (University of Antwerp, Department of Biology, Plant Physiology), were cultured in Gamborg's B5 medium (3.2 g/l) supplemented with 30 g/l sucrose, 0.1 mg/l kinetine (stock solution in 1 M NaOH) and 0.2 mg/l NAA (stock solution in 1 M NaOH) at pH 5.7 (adjusted with KOH). The cultures were maintained in 250 ml tissue culture flasks on a rotary shaker (50 rpm) at 22 °C and 50 µmol m^{-2} s light intensity. Every 7 days, 2 ml of the cell suspension culture was transferred to 18 ml fresh medium (3 flasks) and 4 ml of the cell suspension culture was transferred to 36 ml fresh medium (2 flasks).

6.3.2.2 Preparation of the cells prior to exposure to Cd

Four to 5 days after subculturing, cells from the growth medium were dried over a Büchner filter (on Whattman grade 3 filter paper), washed 3 times in 4 mM MES-buffer (β-morpholino-ethanesulfonic acid in aq. dest., pH 6.7 with KOH), dried again over a Büchner filter and resuspended in MES-buffer (~ 0.1 g cells/ml). MES-buffer was used instead of a phosphate buffer because it avoids precipitation of the added cadmium sulfate. The exposure to different concentrations of Cd occurred in the cuvette of the spectrofluorometer after loading with DanePy.

Practical remarks on the preparation:
The experiment had to be carried out on the same time every day to exclude diurnal variation. All glassware needed to be sterile before performing the experiment. When washing on the Büchner filter with MES, we had to make sure that the cells did not become dry (stress). When the cells were taken of the filter, the cells were softly dipped dry before weighing the cells. The weighing itself had to be fast. Thereafter, 1 g cells per 10 ml MES was resuspended in a sterile 50 ml falcon tube. The cell culture had on average 2 g of cells in 100 ml medium.

6.3.3 DanePy labeling

6.3.3.1 The spectrofluorometer

All experiments were performed using a PTI (Photon Technology International) QuantaMaster Model QM-6/2005 spectrofluorometer equipped with FeliX32 Software & BryteBox Interface. In order to eliminate scatter caused by the turbid cell suspension, two polarization filters were installed, one at 0° in front of the excitation beam and one at 90° in front of the photomultiplier detector. Slits were adjusted at 2 nm because sensitivity was more important than resolution. Excitation and emission spectra were taken in triplet in order to decrease the deviation (summation of the spectra). The spectra were acquired with a stepsize of 0.5 nm and an integration time of 0.1 s. In case of an emission ratio (the fluorescence measured over a period of time at a fixed excitation and emission wavelength) the measuring frequency was 1 measurement per second. The exported spectra were plotted using SigmaPlot 2004 for Windows version 9.0 (Systat Software, Inc.).

6.3.3.2 The DanePy cell loading optimization steps

Throughout the study, 1000 µl of cell suspension (20 µg cells/ml) was dispensed into a 3 ml quartz cuvette and 1000 µl of MES-buffer was added (Dr. T. Raeymaekers, PhD thesis (2007)). The suspension was mixed gently with a magnetic stirring device to avoid precipitation of the cells (thus with the lowest rotational velocity $(\vec{\omega})$ as possible).

In order to optimize (1) the amount of loaded sensor and to determine the optimal (2) excitation and (3) emission wavelengths, following excitation and emission scans were recorded.

1. The optimal DanePy concentration (*i.e.* lowest concentration delivering the highest fluorescence) was determined at 250 µM DanePy (or 10 µl of 50 mM DanePy stock solution dispensed in the 2000 µl cell suspension) and was used throughout the study.
2. An excitation scan (Fig. 6.4), with excitation ranging from 300 nm to 450 nm and emission detection at 544 nm revealed an optimum excitation at 355 nm. Exposing the cells to Cd did not shift the excitation spectrum.
3. An emission scan (Fig. 6.5), with emission detection ranging from 420 nm to 670 nm and excitation at 355 nm revealed an optimum emission at 535 nm. Exposing the cells to Cd did not shift the emission spectrum. An emission scan of cells not loaded with DanePy revealed very low background fluorescence in comparison with the loaded cells (Fig. 6.5).

The fluorescence of DanePy is much higher intracellular than extracellular. To verify that the measured fluorescence of DanePy was generated intracellular and not extracellular, an emission spectrum of the cell suspension was compared with an emission spectrum of the supernatant of the cell suspension. The marked higher fluorescence of the cell suspension compared to the supernatant designated the intracellular localization of DanePy (Fig. 6.6).

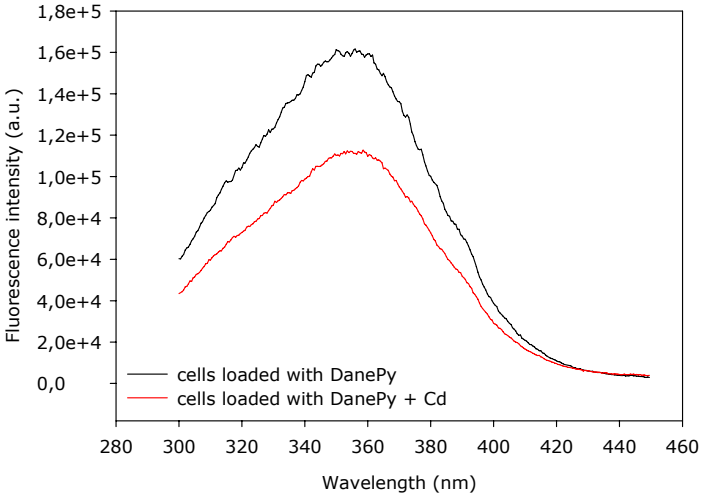

Fig. 6.4 *The excitation spectra of cells loaded with DanePy and cells loaded with DanePy which were also exposed to 50 µM Cd. The excitation wavelength ranged from 300 nm to 450 nm and emission detection was set at 544 nm.*

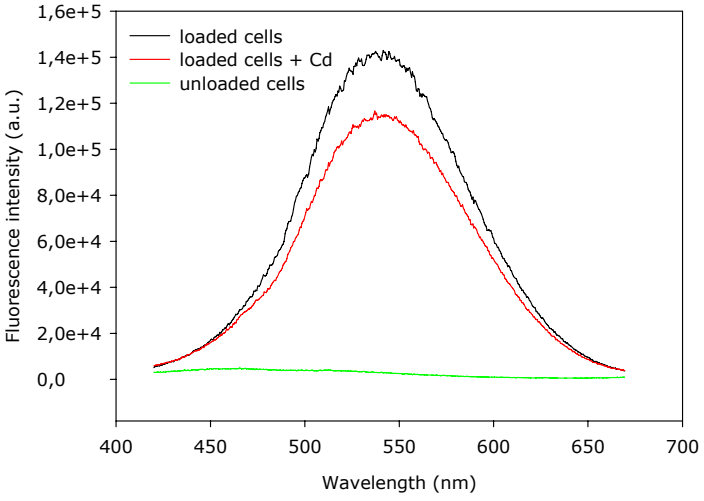

Fig. 6.5 *The emission spectra of cells loaded with DanePy and cells loaded with DanePy which are also exposed to 50 µM Cd. The emission wavelength ranged from 420 nm to 670 nm and excitation was set at 355 nm. An emission scan was also recorded with unloaded cells to illustrate background fluorescence.*

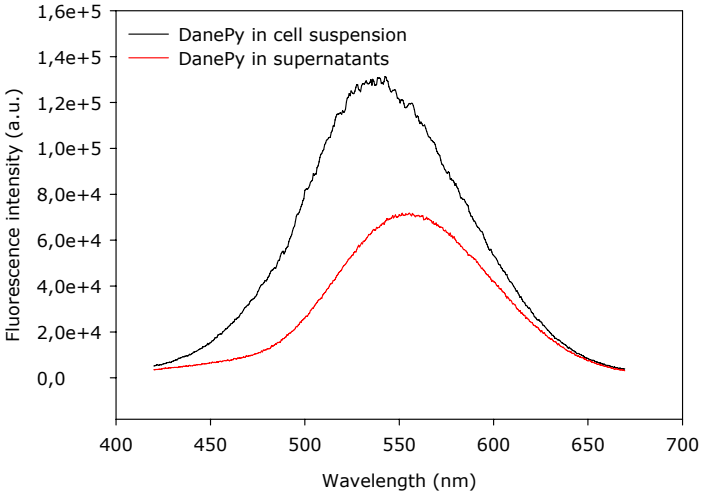

Fig. 6.6 *The spectrum of an emission scan of the stirred cell suspension loaded with DanePy and a spectrum of the supernatants (i.e. not stirred and stabilized for 10 min to allow complete sedimentation of the cells out of the excitation beam). The emission wavelength ranged from 420 nm to 670 nm and excitation was set at 355 nm.*

The penetration rate of the sensor in the cells was investigated with an emission ratio scan. The emission ratio scan measures a fixed emission (535 nm) at a fixed excitation (355 nm) during an analysis time of 1800 s (1 point/s). The signal gradually increased with time, although the steepest increase occurred in the first 10 minutes (Fig. 6.7). The intracellular localization of DanePy was further investigated by means of fluorescence microscopy. 1000 µl of cell suspension + 1000 µl MES + 10 µl DanePy were incubated in a 2 ml Eppendorf tube. 200 µl of this cell suspension was transferred to the Zeiss Axiovert 100 fluorescence microscope. The UV-excitation source was a Xenon-lamp equipped with an excitation filter of 340 nm. The emission filter was a green dichroic mirror (DF=BCELF (~520 nm) – Em = 535/40 nm + polarizer. Fig. 6.8a and Fig. 6.8b depict a transmission and fluorescence micrograph, respectively, illustrating that the fluorescence signal was located inside the cytoplasm and not in the cell wall or the vacuole.

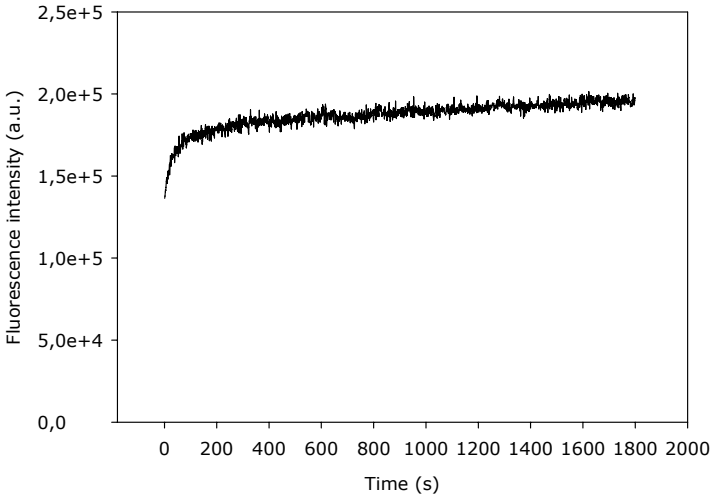

Fig. 6.7 *The spectrum of an 1800 s emission ratio scan illustrating the penetration of DanePy in the cells. Excitation was set at 355 nm, emission was 535 nm.*

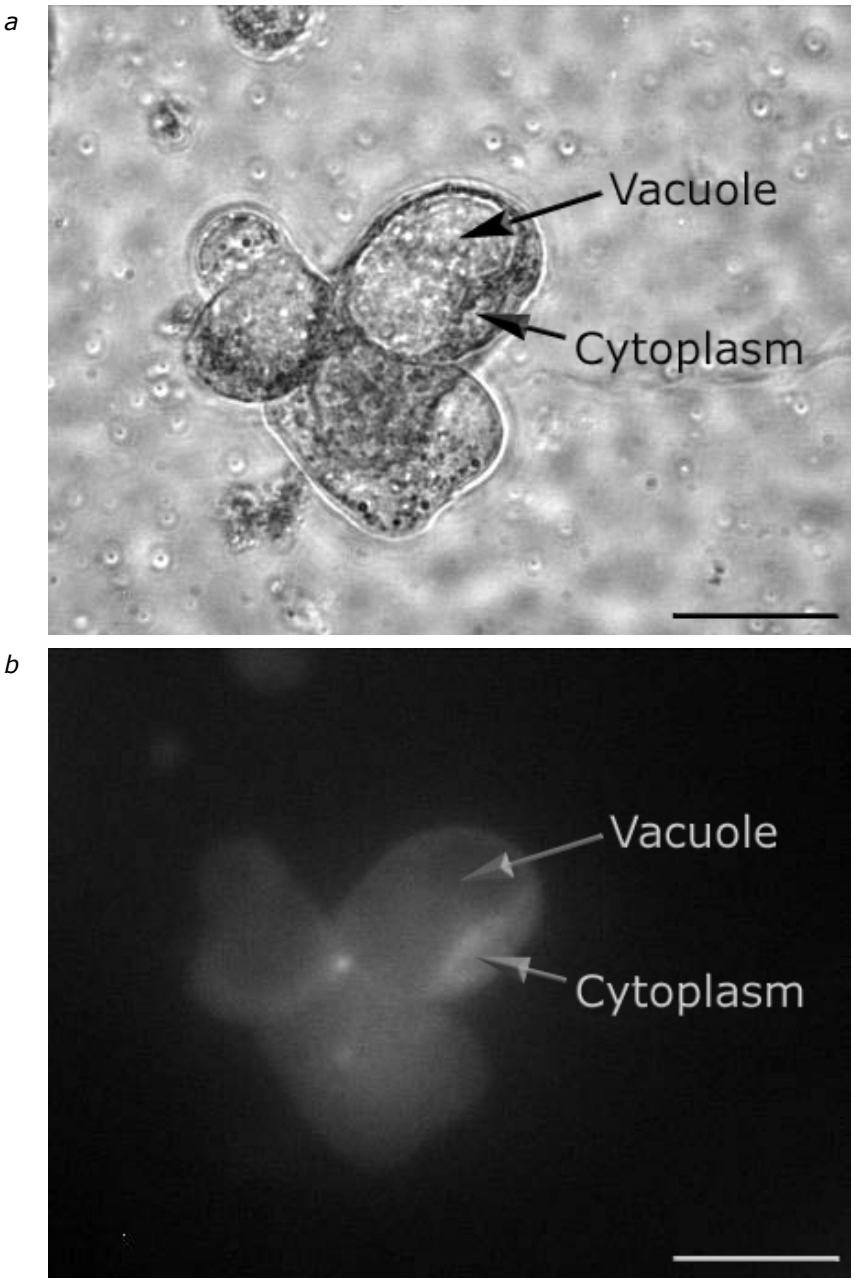

Fig. 6.8 *Two light micrographs illustrating the localization of DanePy in Arabidopsis thaliana cells (bars, 50 µm). The two micrographs are (a) a transmission micrograph and (b) a fluorescence micrograph (exc. at 340 nm, em. at 535 nm), respectively.*

The effect on cell viability was tested for all preparation steps, including the sensor loading and stirring. For the viability test, 50 µl cell culture was put inside a 500 µl Eppendorf tube, and 45 µl MES (22 °C) was added. Then 5 µl Evans blue (1 % stock solution) was added and the cells were gently homogenized (by agitation). After 15 min reaction time, 45 µl of the stained cell culture was put on a haemacytometer and covered with cover glass and the cells were counted. Evans blue penetrates death cells which can be recognized by their blue color. In a healthy population, around 5 % of the cells are death whereas a mortality of 10 % and higher indicates the presence of a toxic effect or increased stress.

According to this test none of the used preparation steps had an effect on the viability of the cells; however long-term stirring at high speed did decrease the viability considerably.

6.3.3.3 The effect of Cd on intracellular quenching of DanePy

An instantaneous generation of singlet oxygen was detected with DanePy in an *Arabidopsis thaliana* cell suspension exposed to Cd^{2+}. The singlet oxygen burst was analyzed using 0, 5, 10, 25, 50 µM $CdSO_4$ (Fig. 6.9). Cd levels starting from 10 µM Cd^{2+} delivered a detectable fluorescence quenching. For practical reasons, throughout this study, Cd was added at 250 s after addition of DanePy, although the fluorescence signal was still rising at that point, it did not influence the fluorescence quenching signal.

In order to test singlet oxygen generation (DanePy) induced by other elements, 50 µM of two redox active elements ($FeSO_4$ and $CuSO_4$) and two non redox active elements ($ZnSO_4$, $CaSO_4$) was tested. The non redox active elements Zn and Ca delivered only small or no fluorescence quenching (Fig. 6.10). On the contrary, the fluorescence quenching induced by the redox active elements Fe and Cu was considerable (Fig. 6.11). However, the kinetics of the Fe induced quenching was different compared to the quenching induced by Cd or Cu.

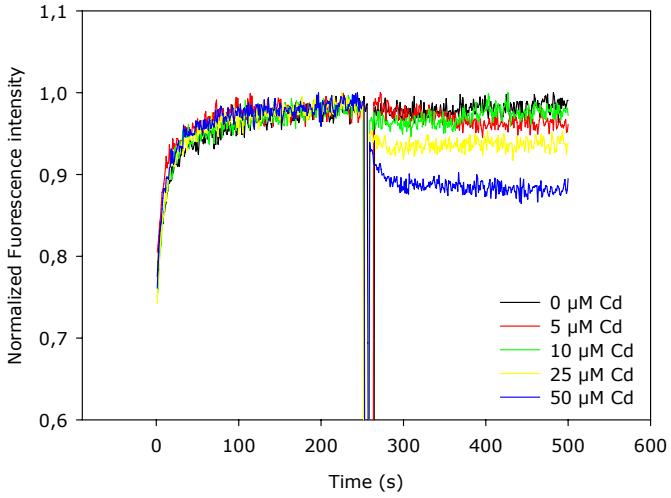

Fig. 6.9 *The effect of Cd on the singlet oxygen signal. The normalized emission ratios were measured on DanePy loaded cells exposed (at 250 s) to 0, 5, 10, 25 and 50 µM Cd. Exc = 355 nm, Em = 535 nm.*

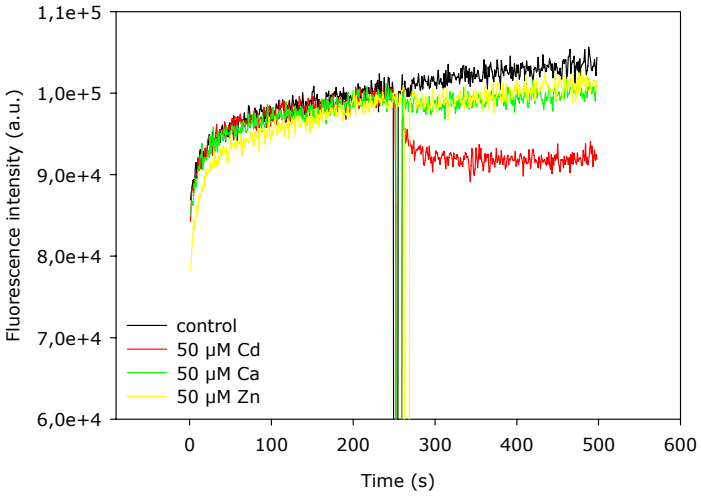

Fig. 6.10 *The effect of non redox active elements on the singlet oxygen signal in comparison with Cd. The emission ratios were measured on DanePy loaded cells exposed (at 250 s) to 50 µM of Cd and non redox active elements Ca and Zn. Exc = 355 nm, Em = 535 nm.*

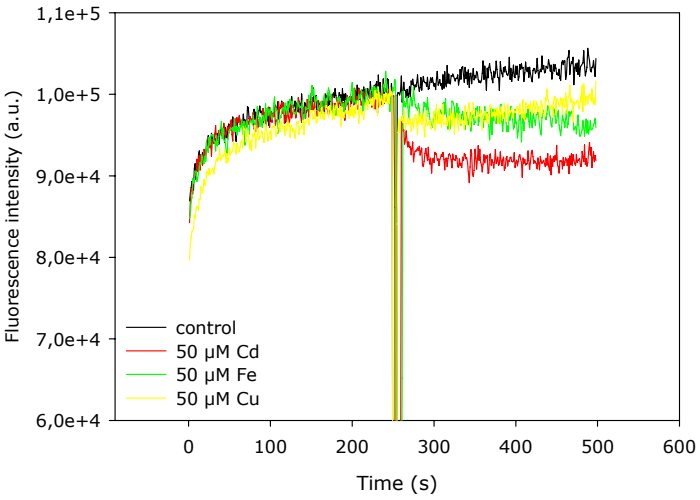

Fig. 6.11 *The effect of redox active elements on the singlet oxygen signal in comparison with Cd. The emission ratios were measured on DanePy loaded cells exposed (at 250 s) to 50 µM of Cd and the redox active elements Fe and Cu. Exc = 355 nm, Em = 535 nm.*

Although DanePy is considered to be exclusively sensitive for singlet oxygen, chemical interference with other elements is possible; therefore it was necessary to test the authenticity of the singlet oxygen signal.

1. As a negative control, the interaction with Dansylchloride (a similar fluorescent sensor as DanePy but without the electron spin trap) was tested with different elements. Cd, Zn, Cu, Ca did not interfere with Dansylchloride which is a good indication that DanePy does not react with substances other than singlet oxygen. Unfortunately, Fe strongly interacts with the fluorescent sensor Dansylchloride (Fig. 6.12). Also a test on the interaction with DanePy was tested which delivered a similar result (data not shown).
2. The signal of the sensor was tested with the singlet oxygen quencher histidine (Kim *et al.*, 2001). The addition of histidine (5 mM) resulted in a considerable inhibition of the fluorescence signal (Fig. 6.13). This result indicates that the fluorescent sensor DanePy indeed reacts with singlet oxygen.

3. Singlet oxygen is reported to be an important ROS in reactions related to ultraviolet exposition (UVA, 320-400 nm). Its toxicity is reinforced when appropriate photoexcitable compounds (sensitizers) are present with molecular oxygen. Several natural sensitizers are known to catalyze oxidative reactions with chlorophyll being particularly interesting (Lee & Min, 1990). Moreover, singlet oxygen can be generated in toluene by bare CdSe qdots, and in water when conjugated with a photosensitizer. Quantum Dots (Cadmium chalcogenide materials (CdS, CdSe, CdTe) are nonorganic nanocrystalline fluorescent probes which are in fact used for *in vivo* imaging (Tsay & Michalet, 2005). Of course, Cd used in our study is in an ionic form and not crystalline. Nevertheless, it was necessary to test the possibility of a photosensitizing effect of pigments (primarily chlorophyll) with Cd in the UV excitation beam of the PTI. In this way, the possible occurrence of a false positive signal of singlet oxygen induced by the UV-excitation beam could be designated. Therefore, an experiment was performed with different excitation slit widths (2 nm, 4 nm, 8 nm, 16 nm) to test if a variation of the UV excitation energy also generates a change in generation of singlet oxygen. No photosensitizing effect was observed on the relative quenching of DanePy (Fig. 6.14).

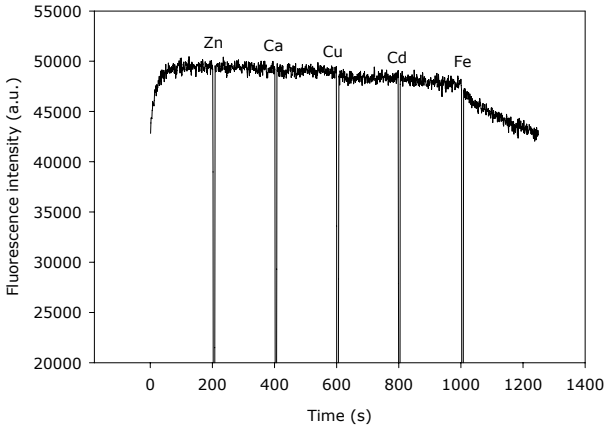

Fig. 6.12 *The interaction of all measured elements with Dansylchloride. For clarity reasons, 50 µM of all the measured elements were added to Dansylchloride loaded cells in one emission ratio scan. However, separate emission ratios were performed for each element which gave a similar result. Exc = 355 nm, Em = 535 nm.*

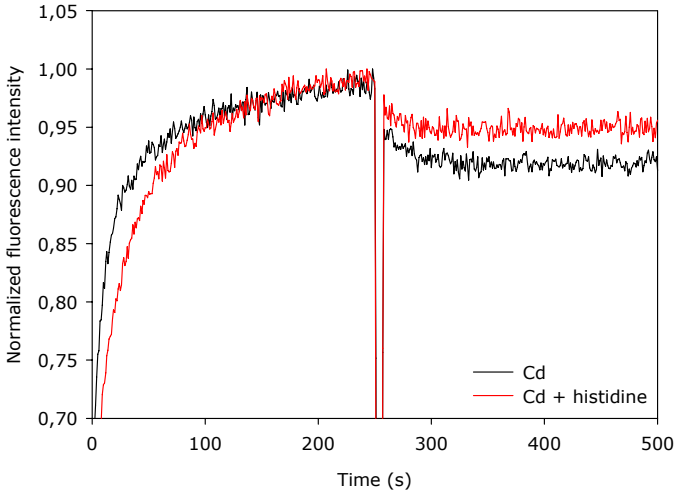

Fig. 6.13 *The effect of the singlet oxygen quencher histidine on the singlet oxygen signal. The normalized emission ratios were measured on DanePy loaded cells whether or not supplemented with 5 mM histidine and exposed to 50 µM Cd (at 250 s). Exc = 355 nm, Em = 535 nm.*

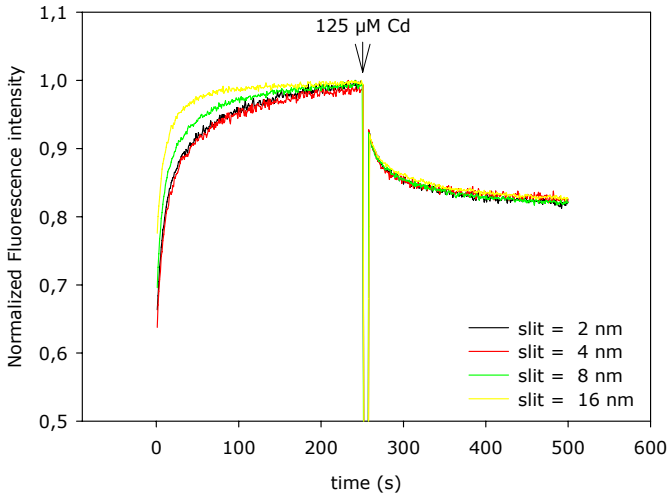

Fig. 6.14 *The effect of Cd-photosensitizing under different excitation energy levels on the singlet oxygen signal. The normalized emission ratios were measured on DanePy loaded cells exposed to 125 µM Cd (at 250 s) and subjected to different UV excitation levels by adjusting the slit widths (2 nm, 4 nm, 8 nm, 16 nm). Exc = 355 nm, Em = 535 nm.*

6.3.4 Origin of the singlet oxygen burst

6.3.4.1 The effects of high light stress

The *in vivo* generation of singlet oxygen is related to high intensity of photoactive radiation (PAR), which was successfully measured in leaves using DanePy (Hideg *et al.*, 2002). Therefore, the effect of an excitation light beam on the singlet oxygen was tested. Cells were subjected to intense PAR (> 1500 µmol m^{-2} s^{-1}) during 60 s, 120 s and 240 s in the cuvette. Both control cells as cells exposed to 50 µM Cd were tested. Yet, no additional quenching was observed neither in the control cells nor in the Cd exposed cells (Fig. 6.15). A possible explanation for this unexpected observation could be the fact that cells growing on a medium (heterotrophic) display an inhibited photosynthesis activity.

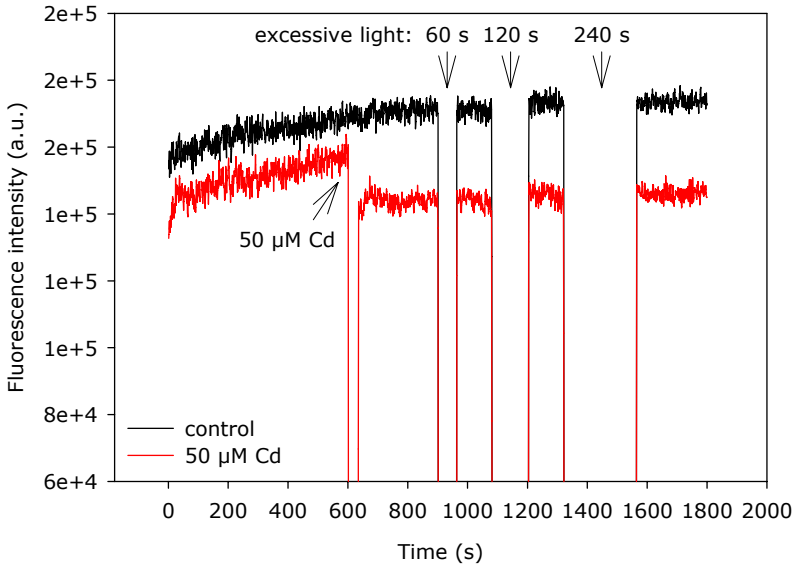

Fig. 6.15 *The effect of excessive photoactive radiation on the singlet oxygen signal. The emission ratios were measured on DanePy loaded cells unexposed and exposed to 50 µM Cd and subjected to different periods of excessive photoactive radiation (60 s, 120 s, 240 s). Exc = 355 nm, Em = 535 nm.*

6.3.4.2 Thylakoid membranes

In order to verify whether the observed singlet oxygen burst induced by Cd is originated from the pigments in the thylakoids or not, an emission ratio scan was performed on a thylakoid membrane extract suspended in HEPES-buffer (4-(2-hydroxyethyl)-1-piperazineethanesulfonic acid (no interference with DanePy)). However, Fig. 6.16 clearly illustrates that the membranes exposed to 50 µM Cd did not induce the quenching of DanePy. Also subjecting the membranes to excessive PAR did not change the singlet oxygen signal (data not shown).

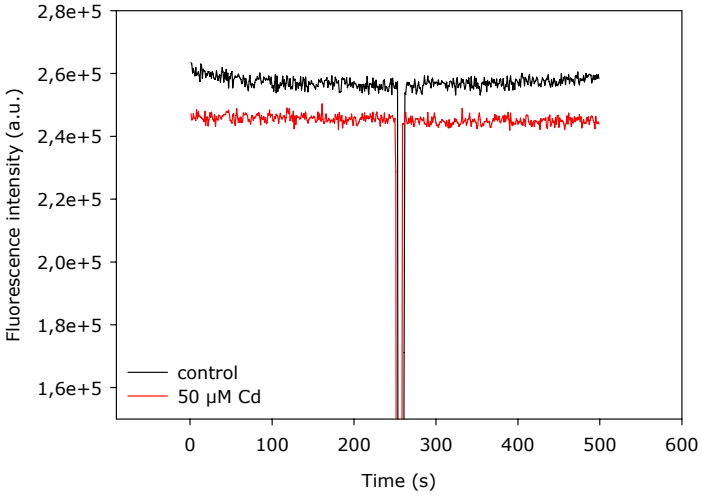

Fig. 6.16 *The effect of Cd on the singlet oxygen signal in thylakoid membranes. The emission ratios were measured on DanePy loaded thylakoid membranes (suspended in HEPES buffer) whether of not exposed to 50 µM Cd (at 250 s). Exc = 355 nm, Em = 535 nm.*

6.3.4.3 The effects of Ca channel inhibitors

Chandra *et al.* (1997) measured instantaneous Ca^{2+} fluxes (with a similar kinetics as the singlet oxygen burst observed in this study) during elicitation of oxidative stress by cold shock, hypo-osmotic stress and harpin (a protein from the pathogen *Erwinia amylovora*) in tobacco cells. These Ca^{2+} fluxes were thereby considered to be essential for transduction of the oxidative burst signals by their respective elicitors. Cd is known to enter the cell through Ca-channels and subsequently disturb the Ca-balance (Perfus-Barbeoch *et al.*, 2002). Therefore, it was interesting to study if a Ca transport channel inhibitor such as $LaCl_3$ was able to quench the singlet oxygen burst induced by Cd.

The Cd-induced quenching (50 µM Cd) of the fluorescence signal was tested after 30 min incubation of the cell suspension with $LaCl_3$ (Olmos *et al.*, 2003). Incubation with 250 µM $LaCl_3$ diminished the singlet oxygen burst whereas at 500 µM $LaCl_3$ a complete inhibition of the singlet oxygen signal was observed (Fig. 6.17). This observation is in agreement with the current opinion that Ca transport channels are important for the uptake of Cd (and consequently also for the generation of singlet oxygen). A subsequent experiment was set up to test the Cd induced singlet oxygen generation when Ca^{2+} was added in excess to the cell suspension. In this way, Ca-Cd competition was in favor of Ca leading to an inhibited uptake of Cd (Olmos *et al.*, 2003). As expected, an addition of 500 µM $CaCl_2$ inhibited the singlet oxygen burst greatly, whereas at 1000 µM $CaCl_2$ a complete inhibition was observed (Fig. 6.18). There was no difference of quenching pattern whether Ca^{2+} was added in the form of $CaCl_2$ or $CaSO_4$ (data not shown).

In conclusion, these results might suggest that a reduced Cd uptake leads to a decreased disturbance of Ca^{2+} levels consequently resulting in a decreased oxidative burst.

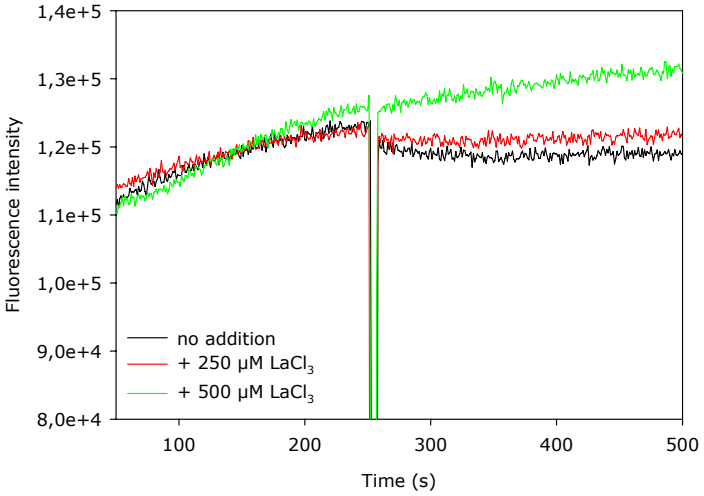

Fig. 6.17 *The effect of the Ca transport channel inhibitor $LaCl_3$ on the singlet oxygen signal. The emission ratios were measured on DanePy loaded cells supplemented with 0 µM, 250 µM and 500 µM $LaCl_3$ and exposed to 50 µM Cd (at 250 s). Exc = 355 nm, Em = 535 nm.*

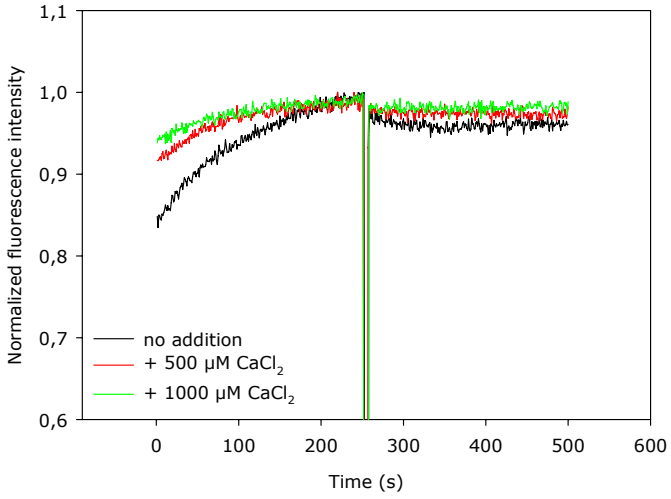

Fig. 6.18 The effect of the addition of Ca on the singlet oxygen signal. The emission ratios were measured on DanePy loaded cells supplemented with 0 µM, 500 µM and 1000 µM $CaCl_2$ and exposed to 50 µM Cd (at 250 s). Exc = 355 nm, Em = 535 nm.

6.3.4.4 Singlet oxygen generation from superoxide

Since the singlet oxygen burst generation could not be related to the photosynthesis pigments, (an)other pathway(s) must be involved. For example, Chen *et al.* (2003) have reported the induction of singlet oxygen during mechanical wounding by detecting its characteristic 1270 nm chemiluminescence emission. Earlier, Khan and Kasha (1994) have shown that singlet oxygen (detected with chemiluminescence as well) is generated in the reaction of superoxide anion with hydrogen peroxide. They demonstrated that the main reactive species is singlet oxygen generated via the Haber-Weiss reaction and not, as usually assumed, the hydroxyl radical, generated by the same reaction (Fig. 1.7).

Following reactions are considered to take place:

Haber-Weiss: $0_2^- + H_20_2 \rightarrow \mathbf{^1O_2(^1\Delta g)} + {}^{\cdot}OH + OH^-$

Electron transfer: ${}^{\cdot}OH + 0_2^- \rightarrow \mathbf{^1O_2(^1\Delta g)} + OH^-$

Dismutation: $2H^+ + 20_2^- \rightarrow \mathbf{^1O_2(^1\Delta g)} + H_20_2$

The physiological relevance of extracellular singlet oxygen production by the spontaneous dismutation of superoxide has been established for animal cells (for a review see Tarr & Valenzeno (2003)). Moreover, Lledias *et al.* (1998) stated that bacterial, fungal, plant, and animal catalases are all susceptible to modification by singlet oxygen. This means that singlet oxygen-mediated damage to superoxide dismutase (SOD) and catalase (CAT) may result in the perturbation of cellular antioxidant defence mechanisms and subsequently lead to a more oxidized environment. The inactivation of CAT and SOD by singlet oxygen was also chemically derived from a photoactivated dye (Kim *et al.,* 2001). Nevertheless, more research is needed to elucidate how singlet oxygen production influences physiologically relevant processes.
In order to investigate one possible role of superoxide in the generation of singlet oxygen of the studied cells, the effect of NADPH oxidase inhibitors, a

superoxide inhibitor (Mn^{2+}) and a superoxide dismutase inhibitor (cPTIO) was tested.

As described in chapter 4, an important group of enzymes linked to superoxide generation are NADPH oxidases. NADPH oxidases are plasma membrane bound enzymes and are crucial factors in the extracellular oxidative burst (superoxide and H_2O_2) induced by several elicitors (fungal, metallic elements, osmotic stress). Interestingly, in response to a fungal elicitor, the activation of NADPH oxidases has been reported to be concomitant with the induction of singlet oxygen generation (Xu *et al.*, 2005) which has been related to saponin synthesis. Therefore, also in this study, the effect of NADPH oxidase has been investigated by using of NADPH oxidase inhibitors. The cells were incubated for 30 min with either 20 mM imidazol (Olmos *et al.*, 2003; Xu *et al.*, 2005) or the strong NADPH oxidase inhibitor 10 µM diphenyleneiodonium (DPI) (Coelho *et al.*, 2002; Xu *et al.*, 2005; Rodriguez-Serrano *et al.*, 2006) before testing their influence on the singlet oxygen burst induced by 50 µM Cd and detected with DanePy. None of the tested inhibitors imposed any effect on the singlet oxygen burst (Fig. 6.19). Although this result suggests that NADPH oxidase is not involved in the singlet oxygen burst, these enzymes should not be ruled out immediately. Since NADPH oxidases mediate in an extracellular oxidative burst, it is possible that DanePy (being more fluorescent intracellular) does not detect extracellular formed singlet oxygen. It is also possible that NADPH oxidase induces the burst not instantaneous, but over a longer time course. However, a 3200 s during emission ratio scan did not reveal additional singlet oxygen signals (data not shown).

In order to test the involvement of superoxide, the effect of a superoxide quencher could give information whether superoxide is actually involved in the singlet oxygen burst. Mn^{2+} is a known interceptor of superoxide (Faulkner *et al.*, 1994). In this study, the addition of 200 µM $MnCl_2$ inhibited the quenching of DanePy induced by 50 µM Cd completely (Fig. 6.20). Obviously, this is a good indication that the generation of singlet oxygen depends on superoxide production.

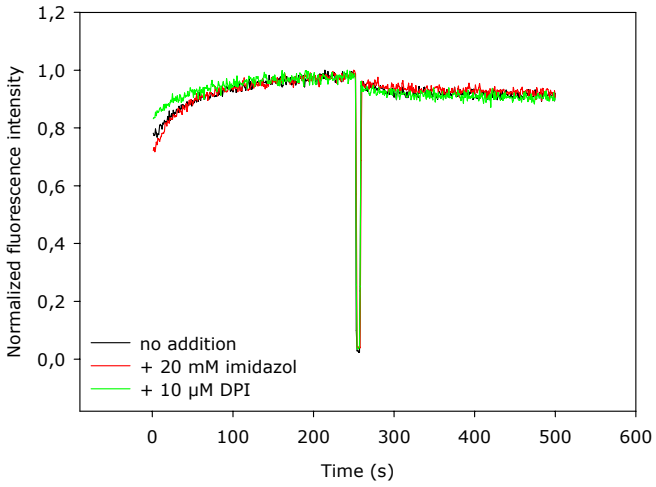

Fig. 6.19 *The effect of the addition of NADPH oxidase inhibitors imidazol and DPI on the singlet oxygen signal. The normalized emission ratios were measured on DanePy loaded cells not supplemented and supplemented with 20 mM imidazol and 10 µM DPI, respectively, and exposed to 50 µM Cd (at 250 s). Exc = 355 nm, Em = 535 nm.*

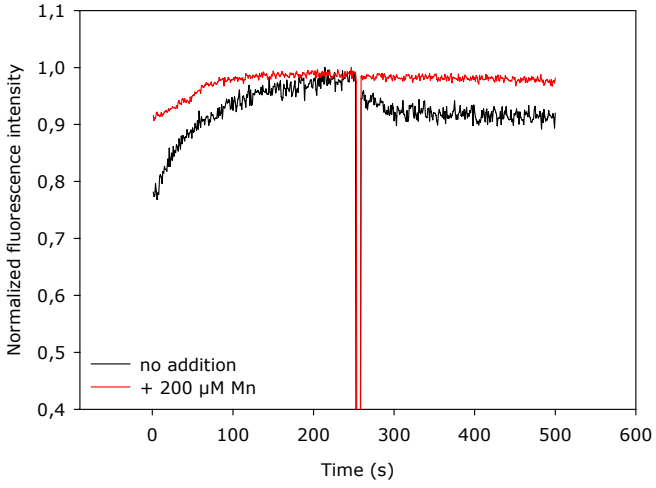

Fig. 6.20 *The effect of the addition of superoxide inhibitor Mn^{2+} on the singlet oxygen signal. The normalized emission ratios were measured on DanePy loaded cells supplemented with 200 µM Mn^{2+} and exposed to 50 µM Cd (at 250 s). Exc = 355 nm, Em = 535 nm.*

Since superoxide reacts at near diffusion limited rate with $NO^{\cdot}$, to form $ONOO^{-}$, the presence of $NO^{\cdot}$ lowers the ability of spontaneous dismutation superoxide to form singlet oxygen (Tarr & Valenzeno, 2003). To investigate whether $NO^{\cdot}$ might limit superoxide dismutation in the singlet oxygen production, the effect of a $NO^{\cdot}$ scavenger was tested. Therefore the $NO^{\cdot}$-scavenger 2-(4-carboxyphenyl)-4,4,5,5-tetramethylimidazoline-1-oxyl-3 oxide (cPTIO) in a concentration of 100 µM was used. A stronger singlet oxygen signal could be expected, however, there was no detectable effect (Fig. 6.21). Nonetheless, this result does not rule out the dismutation pathway as it is very well possible that the $NO^{\cdot}$ levels were actually too low to have a detectable effect on the singlet oxygen production because an $NO^{\cdot}$ burst could very well be not instantaneous.

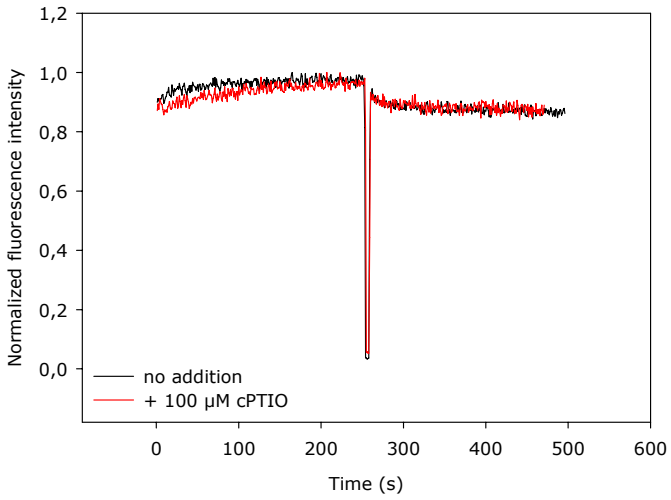

Fig. 6.21 *The effect of the addition of NO scavenger cPTIO on the singlet oxygen signal. The normalized emission ratios were measured on DanePy loaded cells supplemented with 100 µM cPTIO and exposed to 50 µM Cd (at 250 s). Exc = 355 nm, Em = 535 nm.*

Another superoxide involving mechanism for the generation singlet oxygen (together with excited carbonyls) is formed in the termination step of lipid peroxidation by a "Russell type" mechanism (Russel, 1957). This involves protonation of superoxide to produce the perhydroxyl radicals ($HO_2^{\cdot}$), these radicals subsequently react with each other to produce singlet oxygen.

Furthermore, singlet oxygen may then react with unsaturated fatty acids to produce excited carbonyls, while the quenching of triplet carbonyls by molecular oxygen may produce singlet oxygen (Halliwell & Gutteridge, 2000; Sawyer & Valentine, 1981). Lipid peroxidation has been reported to involve lipoxygenase activity and it displays different singlet oxygen generation kinetics (*i.e.* more slowly rising) compared to the singlet oxygen burst observed in this study (Kanofsky & Axelrod, 1986). Therefore, it is not likely that the lipid peroxidation pathway is involved in the instantaneous singlet oxygen burst observed in our cells.

6.4 Discussion

As pigments do not seem to be involved in this instantaneous singlet oxygen burst, other pathways are liable. The most probable explanation for the intracellular singlet oxygen burst should be the signaling function of singlet oxygen, known to trigger several stress-response pathways (op den Camp *et al.*, 2003). The results of this study did not reveal involvement of NADPH oxidase (an important factor for the extracellular singlet oxygen burst) in this early reaction. The instantaneous singlet oxygen burst also excludes the involvement of the decomposition of hydroperoxides in the singlet oxygen generation. On the other hand, superoxide seems to be an essential step in the singlet oxygen burst possibly suggesting a chemical dismutation reaction (Haber-Weiss). Additionally, also Ca^{2+} channels seem to be important for the singlet oxygen generation. Gould *et al.* (2003) observed that in cells subjected to stress (for instance hyperosmotic stress) cytoplasmic Ca^{2+} levels increased instantaneously. In fact, the involvement of Ca^{2+} levels has been related to oxidative burst signaling by Chandra *et al*. (1997). Therefore, the disturbance of the Ca^{2+} balance by Cd (Perfus-Barbeoch *et al.*, 2002) could be connected with the superoxide burst, which is eventually correlated with the singlet oxygen generation. However, additional research is necessary to confirm these results and to gather more information in order to postulate a well founded hypothesis.

6.5 Conclusion

The objective of this study was the development of a fluorescence assay for the detection of singlet oxygen in an *Arabidopsis thaliana* cell culture using the sensor DanePy. This method was tested on a Cd induced generation of singlet oxygen. Interestingly, the instantaneous singlet oxygen signal was not related to high light stress, suggesting a reaction, which is not mediated by photosensitizing. Alternatively, this singlet oxygen burst should possibly be seen as a very early signaling process dependent on both the disruption of the Ca^{2+} balance and a superoxide burst. However, additional research is necessary in order to postulate a well founded hypothesis.

Taken together, this method appears to be very promising since it is very easy to perform and delivering specific and stable fluorescence quenching signals but the results need to be verified further.

6.6 Perspectives

Obviously, as the actual investigation is in progress, more research will provide additional knowledge enabling us to postulate a founded hypothesis. Therefore, the method needs to be tested and developed further.

For instance, although the singlet oxygen signal was verified by the authenticity experiments, the only method giving absolute affirmation is the measurement of the singlet oxygen luminescence (at 1270 nm). However, this technique is challenging since the luminescence of singlet oxygen is extremely weak and single photon counting imaging equipment is needed (Kanofsky, 2000).

Using other fluorescent sensors also delivers an additional control of the obtained results and can broaden the physiological insight in this subject:

- trans -1- (2'-methoxyvinyl) pyrene could be used to investigate a possible extracellular singlet oxygen burst
- 2',7' – dichlorofluoresceindiacetate (DHCF-DA) could give an idea of the complete ROS generation (with emphasis on H_2O_2) induced by Cd
- an aequorin based Ca selective sensor could be used to study the relation of the Ca^{2+}flux with the Cd-induced singlet oxygen burst

- 2-methyl-6-(4-methoxyphenyl)-3,7-dihydroimidazo[1,2-a]pyrazin-3-one, hydrochloride (MCLA) (Molecular Probes) can be used to measure superoxide specifically.

The pH of the suspension was optimized for measuring an H_2O_2 burst induced by Cd (Dr. Tine Raeymaekers, pers. comm.). However, the effect of pH on the generation of singlet oxygen should be tested.

Considerable cytoplasmic shrinkage was observed in cells under Cd exposure (data not shown), therefore the cell viability should be assessed as a dose response to the applied Cd exposure concentration.

Other stress factors as for instance sorbitol (osmotic stress) and NaCl (salinity) which are known to have an instantaneous effect on the Ca^{2+} level (Gould *et al.*, 2003) should be tested in order to examine whether these stress factors also induce the singlet oxygen burst.

Using autotrophic cells of *Arabidopsis thaliana* in addition to the currently studied heterotrophic cells should be interesting because it can be expected that the increased photosynthetic activity has an influence on the pigment induced singlet oxygen generation. It would also enable the correlation of the photosystem II efficiency (by fast chlorophyll a fluorescence and quenching analysis) with the singlet oxygen generation.

Chapter 7

General discussion and conclusion

7.1 General discussion

The main objective of this study was the investigation of the effects of low to intermediate Cd concentrations on *Arabidopsis thaliana*. This thesis consists of four diverse studies: (1) an EDXMA localization study, (2) a cytological/gene expression study, (3) a photosynthesis study and (4) a fluorimetric quantification study. Nevertheless, as all exposure conditions were kept constant, the results could be compared and a general pattern of response to Cd exposure emerged from the separate studies. This general discussion combines the result of the separate studies, which are described per exposure concentration.

When *Arabidopsis thaliana* plants were exposed to the relatively low Cd concentration of 1 µM, the EDXMA localization study revealed only apoplastic accumulation. Although some small granules (no Cd detected) were present in the symplast of the central cortex, no effective symplastic accumulation was detected in the cytoplasm of the central cortex and the endodermis (only in the cytoplasm and cell walls of the xylem). This result suggested that for *Arabidopsis thaliana*, the sequestration processes were not fully operational at this Cd exposure concentration. However, in comparison with the control plants, 1 µM Cd did induce perceptible effects in leaves such as chlorosis and growth and photosynthesis rate inhibition. Nevertheless, the ultrastructural cytological study revealed that at this exposure concentration, there was no effective membrane damage. Also the measured genes of the antioxidant defence system were not upregulated, which suggested a relatively undisturbed redox-balance. It was hypothesised that the morphological and physiological effects were in fact common symptoms that, at least partly, resulted from the NADPH-mediated signaling mechanism (leading to increased H_2O_2 generation in the leaves) which was related with the Cd induced disturbance of the water balance. In addition, on the basis of the results of chapter 6, it could also be hypothesised that the Cd-induced generation of singlet oxygen (independent from chlorophyll) could also play a role in the ROS-mediated responses. Although oxidative stress was apparently under control, the inhibition of photosynthesis (which was most likely

decreased because of the decreased uptake of CO_2) had a strong effect on photosystem II. Chlorophyll *a* fluorescence analysis revealed a strong downregulation of photosystem II, which was detected by the JIP-test as an increase of silent reaction centres.

In conclusion, at this exposure concentration *Arabidopsis thaliana* was subjected to mild stress, which was most likely related with the Cd-induced disturbance of the water balance. However, although photosynthesis was downregulated to a great extent, the plant was apparently able to adapt to this stress without fully activating the extensive range of protection mechanisms.

The intermediate 5 µM Cd exposure concentration, revealed a situation that was much more interesting since it demonstrated the adaptation of a plant under stress with a fully operational protection system that was able to prevent the destruction of the cellular structure and physiological functions. One of the well-known defence mechanisms of *Arabidopsis thaliana*, the excluder strategy, was clearly observable by the presence of symplastic accumulation in both the endodermis and pericycle (reducing the apoplastic transport to the xylem) and the retranslocation of Cd from the leaves back to the roots. In the shoot, the leaf growth was completely inhibited and the water content and photosynthetic rate were strongly decreased, which was most likely primarily related to severe Cd-induced water stress. The severe stress was also reflected in the membrane damage observed at the ultrastructural level in the chloroplast, which was in all probability related to increased oxidative stress caused (at least to some extent) by the strongly induced NADPH oxidases and lipoxygenases. Nevertheless, as already mentioned, the plant adapted to this adverse situation by excluding Cd from the shoot, by the upregulation of the antioxidative defence mechanisms, by the accumulation of anthocyanins in the peripheral tissues and last but not least by the induced xanthophyll mediated dissipation of excess excitation energy. The latter two protection mechanisms were probably responsible for the remarkable fact that at 5 µM Cd, the active reaction centres of photosystem II were actually performing better than at 1 µM Cd. Consequently, this fact should be seen as an adaptation strategy to maximize the energy efficiency so as to deal with adverse conditions. As this phenomenon most likely varies among plant species (*i.e.* occurs at different concentrations), and possibly even varies

for the same plant species but in other environmental conditions, this could offer an explanation for the sometimes contradictory results between various studies.

In conclusion, at the 5 µM Cd exposure concentration, Cd-induced stress was considerable but the plant remained its ability to adapt to this stress situation by the activation of several protection mechanisms.

The low and intermediate exposure concentrations were compared with the high 50 µM Cd exposure concentration. At that concentration, the plant was evidently subjected to severe Cd-stress. The symplastic accumulation of Cd was omnipresent across the root but the cellular structure was severely damaged and the cells suffered from plasmolytic shrinkage, which was actually hindering precise localization of Cd accumulation. Likewise, the cytological study of the chloroplasts revealed substantial membrane damage indicating severe oxidative stress. This was most likely related to severe Cd-induced water stress, probably in addition to the Cd-related inhibition of the antioxidative defence system. However, even at this high level of damage, chlorophyll *a* fluorescence analysis indicated that the observed membrane (thylakoid) damage was not irreversible, which suggests a strong ability of adaptation.

In conclusion, at the 50 µM Cd exposure concentration, Cd-induced stress was severe as judged by the deteriorated cell structure and physiological functions. However, the plant still managed to survive thanks to potent adaptation abilities.

7.2 Conclusion

The main objective of this study was to investigate the responses of low to intermediate Cd concentrations in *Arabidopsis thaliana* at different fields of research.

The results of this study have demonstrated that, at the 1 µM and 5 µM Cd exposure concentrations, much of the morphological and ultrastructural effects caused by Cd toxicity are related to the disturbance of the water balance leading to nonspecific symptoms of Cd-induced water stress. The strongly induced NADPH-oxidase and lipoxygenase signaling was thereby considered as an important contributor of oxidative stress, leading to lipid peroxidation and

membrane damage. However, at 50 µM Cd, the inhibition of the antioxidative defence system seemed to be more important. It was also suggested that Cd-induced generation of singlet oxygen could actually contribute to the Cd-induced oxidative stress. Despite the fact that Cd induced severe membrane damage at the highest exposure concentration (50 µM Cd), there was no irreversible damage to photosystem II, which emphasizes the adaptive ability of the nontolerant *Arabidopsis thaliana* to Cd stress. This was almost certainly attributable to activation of an extensive range of protective mechanisms of which the apoplastic- and symplastic sequestration of Cd in the root combined with retranslocation via the phloem (the excluder strategy) could be considered as the first line of defence.

References

Adriano DC. **2001.** *Trace elements in terrestrial environments. Biogeochemistry, Bioavailability, and Risks of Metals*. New York: Springer-Verlag.

Ager FJ, Ynsa MD, Dominguez-Solis JR, Lopez-Martin MC, Gotor C, Romero LC. **2003.** Nuclear micro-probe analysis of *Arabidopsis thaliana* leaves. *Nuclear Instruments & Methods in Physics Research Section B-Beam Interactions with Materials and Atoms* **210:** 401-406.

Allen JF, Forsberg J. **2001.** Molecular recognition in thylakoid structure and function. *Trends in Plant Science* **6:** 317-326.

Anderson JM, Osmond CB. **1987.** Shade-sun responses: compromises between acclimation and photoinhibition. In: Kyle DJ, Osmond CB, Arntzen DJ, eds. *Photoinhibition, Topics in Photosynthesis*. Amsterdam: Elsevier, 1-38.

Anderson JM, Park YI, Chow WS. **1997.** Photoinactivation and photoprotection of photosystem II in nature. *Physiologia Plantarum* **100:** 214-223.

Antosiewicz D, Wierzbicka M. **1999.** Localization of lead in *Allium cepa* L. cells by electron microscopy. *Journal of Microscopy-Oxford* **195:** 139-146.

Apel K, Hirt H. **2004.** Reactive oxygen species: Metabolism, oxidative stress, and signal transduction. *Annual Review of Plant Biology* **55:** 373-399.

Appenroth KJ, Stockel J, Srivastava A, Strasser RJ. **2001.** Multiple effects of chromate on the photosynthetic apparatus of *Spirodela polyrhiza* as probed by OJIP chlorophyll *a* fluorescence measurements. *Environmental Pollution* **115:** 49-64.

Arguello JM. **2003.** Identification of ion-selectivity determinants in heavy-metal transport P-1B-type ATPases. *Journal of Membrane Biology* **195:** 93-108.

Arora A, Sairam RK, Srivastava GC. **2002.** Oxidative stress and antioxidative system in plants. *Current Science* **82:** 1227-1238.

Asada K. **1999.** The water-water cycle in chloroplasts: Scavenging of active oxygens and dissipation of excess photons. *Annual Review of Plant Physiology and Plant Molecular Biology* **50:** 601-639.

Asada K. **2006.** Production and scavenging of reactive oxygen species in chloroplasts and their functions. *Plant Physiology* **141:** 391-396.

Atal N, Saradhi PP, Mohanty P. **1991.** Inhibition of the chloroplast photochemical-Reactions by treatment of wheat seedlings with low concentrations of cadmium - analysis of electron-transport activities and changes in fluorescence yield. *Plant and Cell Physiology* **32:** 943-951.

ATSDR. Toxicologic profile for cadmium. Agency for Toxic Substances and Disease Registry. 1999. Atlanta.

Azevedo H, Pinto CGG, Fernandes J, Loureiro S, Santos C. **2005.** Cadmium effects on sunflower growth and photosynthesis. *Journal of Plant Nutrition* **28:** 2211-2220.

Babani F, Lichtenthaler HK. **1996.** Light-induced and age-dependent development of chloroplasts in etiolated barley leaves as visualized by determination of photosynthetic pigments, CO_2 assimilation rates and different kinds of chlorophyll fluorescence ratios. *Journal of Plant Physiology* **148:** 555-566.

Balakhnina TI, Kosobryukhov AA, Ivanov AA, Kreslavskii VD. **2005.** The effect of cadmium on CO_2 exchange, variable fluorescence of chlorophyll, and the level of antioxidant enzymes in pea leaves. *Russian Journal of Plant Physiology* **52:** 15-20.

Balestrasse KB, Benavides MP, Gallego SM, Tomaro ML. **2003.** Effect of cadmium stress on nitrogen metabolism in nodules and roots of soybean plants. *Functional Plant Biology* **30:** 57-64.

Barber J, Andersson B. **1992.** Too much of a good thing - light can be bad for photosynthesis. *Trends in Biochemical Sciences* **17:** 61-66.

Barber J, De las Rivas JD. **1993.** A functional-model for the role of cytochrome-B(559) in the protection against donor and acceptor side photoinhibition. *Proceedings of the National Academy of Sciences of the United States of America* **90:** 10942-10946.

Barcelo AR. **2005.** Xylem parenchyma cells deliver the H_2O_2 necessary for lignification in differentiating xylem vessels. *Planta* **220:** 747-756.

Barceló J, Poschenrieder C. **1990.** Plant water relations as affected by heavy-metal stress - a review. *Journal of Plant Nutrition* **13:** 1-37.

Baryla A, Carrier P, Franck F, Coulomb C, Sahut C, Havaux M. **2001.** Leaf chlorosis in oilseed rape plants (*Brassica napus*) grown on cadmium-polluted soil: causes and consequences for photosynthesis and growth. *Planta* **212:** 696-709.

Becher M, Talke IN, Krall L, Kramer U. **2004.** Cross-species microarray transcript profiling reveals high constitutive expression of metal homeostasis genes in shoots of the zinc hyperaccumulator *Arabidopsis halleri*. *Plant Journal* **37:** 251-268.

Bell E, Creelman RA, Mullet JE. **1995.** A chloroplast lipoxygenase is required for wound-induced jasmonic acid accumulation in *Arabidopsis*. *Proceedings of the National Academy of Sciences of the United States of America* **92:** 8675-8679.

Benavides MP, Gallego SM, Tomaro ML. **2005.** Cadmium toxicity in plants. *Brazilian Journal of Plant Physiology* **17:** 21-34.

Bovet L, Eggmann T, Meylan-Bettex M, Polier J, Kammer P, Marin E, Feller U, Martinoia E. **2003.** Transcript levels of AtMRPs after cadmium treatment: induction of AtMRP3. *Plant Cell and Environment* **26:** 371-381.

Branco-Price C, Kawaguchi R, Ferreira RB, Bailey-Serres J. **2005.** Genome-wide analysis of transcript abundance and translation in *Arabidopsis* seedlings subjected to oxygen deprivation. *Annals of Botany* **96:** 647-660.

Briat JF, Lebrun M. **1999.** Plant responses to metal toxicity. *Comptes Rendus de l Academie des Sciences Serie III-Sciences de la Vie-Life Sciences* **322:** 43-54.

Bright J, Desikan R, Hancock JT, Weir IS, Neill SJ. **2006.** ABA-induced NO generation and stomatal closure in *Arabidopsis* are dependent on H_2O_2 synthesis. *Plant Journal* **45:** 113-122.

Buchet JP, Lauwerys R, Roels H, Bernard A, Bruaux P, Claeys F, Ducoffre G, Deplaen P, Staessen J, Amery A, Lijnen P, Thijs L, Rondia D, Sartor F, Saintremy A, Nick L. **1990.** Renal effects of cadmium body burden of the general population. *Lancet* **336:** 699-702.

Buckingham DA, Plachy J. 2004. Cd statistics. Reston, Virginia, USA, United States Geological Survey (USGS).

Burzynski M, Klobus G. **2004.** Changes of photosynthetic parameters in cucumber leaves under Cu, Cd, and Pb stress. *Photosynthetica* **42:** 505-510.

Bussotti F, Agati G, Desotgiu R, Matteini P, Tani C. **2005.** Ozone foliar symptoms in woody plant species assessed with ultrastructural and fluorescence analysis. *New Phytologist* **166:** 941-955.

Cakmak I, Welch RM, Hart J, Norvell WA, Ozturk L, Kochian LV. **2000.** Uptake and retranslocation of leaf-applied cadmium (Cd-109) in diploid, tetraploid and hexaploid wheats. *Journal of Experimental Botany* **51:** 221-226.

Cameron KD, Teece MA, Smart LB. **2006.** Increased accumulation of cuticular wax and expression of lipid transfer protein in response to periodic drying events in leaves of tree tobacco. *Plant Physiology* **140:** 176-183.

Cardol P, Gloire G, Havaux M, Remacle C, Matagne R, Franck F. **2003.** Photosynthesis and state transitions in mitochondrial mutants of *Chlamydomonas reinhardtii* affected in respiration. *Plant Physiology* **133:** 2010-2020.

Carol RJ, Takeda S, Linstead P, Durrant MC, Kakesova H, Derbyshire P, Drea S, Zarsky V, Dolan L. **2005.** A RhoGDP dissociation inhibitor spatially regulates growth in root hair cells. *Nature* **438:** 1013-1016.

Cataldo DA, McFadden KM, Garland TR, Wildung RE. **1988.** Organic-constituents and complexation of Nickel(II), Iron(III), Cadmium(II), and Plutonium(IV) in soybean xylem exudates. *Plant Physiology* **86:** 734-739.

Chandra S, Stennis M, Low PS. **1997.** Measurement of Ca^{2+} fluxes during elicitation of the oxidative burst in aequorin-transformed tobacco cells. *Journal of Biological Chemistry* **272:** 28274-28280.

Chen WL, Xing D, Tan SC, Tang YH, He YH. **2003.** Imaging of ultra-weak bio-chemiluminescence and singlet oxygen generation in germinating soybean in response to wounding. *Luminescence* **18:** 37-41.

Chen XY, Kim JY. **2006.** Transport of macromolecules through plasmodesmata and the phloem. *Physiologia Plantarum* **126:** 560-571.

Cholewa E, Peterson CA. **2004.** Evidence for symplastic involvement in the radial movement of calcium in onion roots. *Plant Physiology* **134:** 1793-1802.

Ciscato M, Vangronsveld J, Valcke R. **1999.** Effects of heavy metals on the fast chlorophyll fluorescence induction kinetics of photosystem II: a comparative study. *Zeitschrift fur Naturforschung C-A Journal of Biosciences* **54:** 735-739.

Ciscato M. **2000.** Development of a fluorescence imaging system for the quality assessment of fruits and vegetables. Limburgs Universitair Centrum.

Clemens S, Kim EJ, Neumann D, Schroeder JI. **1999.** Tolerance to toxic metals by a gene family of phytochelatin synthases from plants and yeast. *EMBO Journal* **18:** 3325-3333.

Clemens S. **2001.** Molecular mechanisms of plant metal tolerance and homeostasis. *Planta* **212:** 475-486.

Clemens S. **2006.** Toxic metal accumulation, responses to exposure and mechanisms of tolerance in plants. *Biochimie* **88:** 1707-1719.

Clijsters H, Van Assche F. **1985.** Inhibition of photosynthesis by heavy-metals. *Photosynthesis Research* **7:** 31-40.

Cobbett CS, Goldsbrough P. **2002.** Phytochelatins and metallothioneins: roles in heavy metal detoxification and homeostasis. *Annual Review of Plant Biology* **53:** 159-182.

Cobbett CS, May MJ, Howden R, Rolls B. **1998.** The glutathione-deficient, cadmium-sensitive mutant, cad2-1, of *Arabidopsis thaliana* is deficient in gamma-glutamylcysteine synthetase. *Plant Journal* **16:** 73-78.

Coelho SM, Taylor AR, Ryan KP, Sousa-Pinto I, Brown MT, Brownlee C. **2002.** Spatiotemporal patterning of reactive oxygen production and Ca^{2+} wave propagation in fucus rhizoid cells. *Plant Cell* **14:** 2369-2381.

Connolly EL, Fett JP, Guerinot ML. **2002.** Expression of the IRT1 metal transporter is controlled by metals at the levels of transcript and protein accumulation. *Plant Cell* **14:** 1347-1357.

Costa G, Morel JL. **1993.** Cadmium uptake by *Lupinus albus* (L) - cadmium excretion, a possible mechanism of cadmium tolerance. *Journal of Plant Nutrition* **16:** 1921-1929.

Crofts J, Horton P. **1991.** Dissipation of excitation-energy by photosystem II particles at low pH. *Biochimica et Biophysica Acta* **1058:** 187-193.

Curie C, Alonso JM, Le Jean M, Ecker JR, Briat JF. **2000.** Involvement of NRAMP1 from *Arabidopsis thaliana* in iron transport. *Biochemical Journal* **347:** 749-755.

Cuypers A, Vangronsveld J, Clijsters H. **2001.** The redox status of plant cells (AsA and GSH) is sensitive to zinc imposed oxidative stress in roots and primary leaves of *Phaseolus vulgaris*. *Plant Physiology and Biochemistry* **39:** 657-664.

Das P, Samantaray S, Rout GR. **1997.** Studies on cadmium toxicity in plants: a review. *Environmental Pollution* **98:** 29-36.

Dau H. **1994.** Molecular mechanisms and quantitative models of variable photosystem II fluorescence. *Photochemistry and Photobiology* **60:** 1-23.

Davies KL, Davies MS, Francis D. **1991.** Zinc-induced vacuolation in root meristematic cells of *Festuca rubra* L. *Plant Cell and Environment* **14:** 399-406.

Davies MJ. **2004.** Reactive species formed on proteins exposed to singlet oxygen. *Photochemical & Photobiological Sciences* **3:** 17-25.

Deckert J. **2005.** Cadmium toxicity in plants: Is there any analogy to its carcinogenic effect in mammalian cells? *Biometals* **18:** 475-481.

De Knecht JA, Koevoets PLM, Verkleij JAC, Ernst WHO. **1992.** Evidence against a role for phytochelatins in naturally selected increased cadmium tolerance in *Silene vulgaris* (Moench) Garcke. *New Phytologist* **122:** 681-688.

De Knecht JA, Vandillen M, Koevoets PLM, Schat H, Verkleij JAC, Ernst WHO. **1994.** Phytochelatins in cadmium-sensitive and cadmium-tolerant *Silene vulgaris* - chain-length distribution and sulfide incorporation. *Plant Physiology* **104:** 255-261.

Demidchik V, Davenport RJ, Tester M. **2002.** Nonselective cation channels in plants. *Annual Review of Plant Biology* **53:** 67-107.

Demmig-Adams B, Adams WW, Heber U, Neimanis S, Winter K, Kruger A, Czygan FC, Bilger W, Bjorkman O. **1990.** Inhibition of zeaxanthin formation and of rapid changes in radiationless energy-dissipation by dithiothreitol in spinach leaves and chloroplasts. *Plant Physiology* **92:** 293-301.

Demmig-adams B, Adams WW. **1992.** Photoprotection and other responses of plants to high light stress. *Annual Review of Plant Physiology and Plant Molecular Biology* **43:** 599-626.

Demmig-Adams B, Adams WW. **1996.** The role of xanthophyll cycle carotenoids in the protection of photosynthesis. *Trends in Plant Science* **1:** 21-26.

Depka B, Jahns P, Trebst A. **1998.** Beta-carotene to zeaxanthin conversion in the rapid turnover of the D1 protein of photosystem II. *FEBS Letters* **424:** 267-270.

Di Cagno R, Guidi L, De Gara L, Soldatini GF. **2001.** Combined cadmium and ozone treatments affect photosynthesis and ascorbate-dependent defences in sunflower. *New Phytologist* **151:** 627-636.

Djebali W, Zarrouk M, Brouquisse R, El Kahoui S, Limam F, Ghorbel MH, Chaibi W. **2005.** Ultrastructure and lipid alterations induced by cadmium in tomato (*Lycopersicon esculentum*) chloroplast membranes. *Plant Biology* **7:** 358-368.

Duysens LNM, Sweers HE. **1963.** Mechanisms of the two photochemical reactions in algae as studied by means of fluorescence. In: Japanese Society of Plant Physiologists, ed. *Studies on Microalgae and Photosynthetic Bacteria*. Tokyo: University of Tokyo Press, 353-372.

Ebbs S, Lau I, Ahner B, Kochian L. **2002.** Phytochelatin synthesis is not responsible for Cd tolerance in the Zn/Cd hyperaccumulator *Thlaspi caerulescenes* (J. and C. Presl). *Planta* **214:** 635-640.

Edreva A. **2005.** Generation and scavenging of reactive oxygen species in chloroplasts: a submolecular approach. *Agriculture Ecosystems & Environment* **106:** 119-133.

Eren E, Arguello JM. **2004.** *Arabidopsis* HMA2, a divalent heavy metal-transporting P-IB-type ATPase, is involved in cytoplasmic Zn2+ homeostasis. *Plant Physiology* **136:** 3712-3723.

Faller P, Kienzler K, Krieger-Liszkay A. **2005.** Mechanism of Cd^{2+} toxicity: Cd^{2+} inhibits photoactivation of photosystem II by competitive binding to the essential Ca^{2+} site. *Biochimica et Biophysica Acta-Bioenergetics* **1706:** 158-164.

Faulkner KM, Liochev SI, Fridovich I. **1994.** Stable Mn(III) porphyrins mimic Superoxide dismutase *invitro* and substitute for it *invivo*. *Journal of Biological Chemistry* **269:** 23471-23476.

Fojtova M, Kovarik A. **2000.** Genotoxic effect of cadmium is associated with apoptotic changes in tobacco cells. *Plant Cell and Environment* **23:** 531-537.

Foreman J, Demidchik V, Bothwell JHF, Mylona P, Miedema H, Torres MA, Linstead P, Costa S, Brownlee C, Jones JDG, Davies JM, Dolan L. **2003.** Reactive oxygen species produced by NADPH oxidase regulate plant cell growth. *Nature* **422:** 442-446.

Foyer CH, Noctor G. **2000.** Oxygen processing in photosynthesis: regulation and signalling. *New Phytologist* **146:** 359-388.

Foyer CH, Noctor G. **2003.** Redox sensing and signalling associated with reactive oxygen in chloroplasts, peroxisomes and mitochondria. *Physiologia Plantarum* **119:** 355-364.

Foyer CH, Noctor G. **2005.** Oxidant and antioxidant signalling in plants: a re-evaluation of the concept of oxidative stress in a physiological context. *Plant Cell and Environment* **28:** 1056-1071.

Frank HA, Cogdell RJ. **1996.** Carotenoids in photosynthesis. *Photochemistry and Photobiology* **63:** 257-264.

Fusco N, Micheletto L, Dal Corso G, Borgato L, Furini A. **2005.** Identification of cadmium-regulated genes by cDNA-AFLP in the heavy metal accumulator *Brassica juncea* L. *Journal of Experimental Botany* **56:** 3017-3027.

Gao XP, Wang XF, Lu YF, Zhang LY, Shen YY, Liang Z, Zhang DP. **2004.** Jasmonic acid is involved in the water-stress-induced betaine accumulation in pear leaves. *Plant Cell and Environment* **27:** 497-507.

Gapper C, Dolan L. **2006.** Control of plant development by reactive oxygen species. *Plant Physiology* **141:** 341-345.

Garstka M, Kaniuga Z. **1988.** Linolenic acid-induced release of Mn, polypeptides and inactivation of oxygen evolution in photosystem II particles. *FEBS Letters* **232:** 372-376.

Geiken B, Masojidek J, Rizzuto M, Pompili ML, Giardi MT. **1998.** Incorporation of [S-35] methionine in higher plants reveals that stimulation of the D1 reaction centre II protein turnover accompanies tolerance to heavy metal stress. *Plant Cell and Environment* **21:** 1265-1273.

Gichner T, Patkova Z, Szakova J, Demnerova K. **2004.** Cadmium induces DNA damage in tobacco roots, but no DNA damage, somatic mutations or homologous recombination in tobacco leaves. *Mutation Research-Genetic Toxicology and Environmental Mutagenesis* **559:** 49-57.

Gilmore AM, Yamamoto HY. **1993.** Linear-models relating xanthophylls and lumen acidity to nonphotochemical fluorescence quenching - evidence that antheraxanthin explains zeaxanthin-independent quenching. *Photosynthesis Research* **35:** 67-78.

Girotti AW, Kriska T. **2004.** Role of lipid hydroperoxides in photo-oxidative stress signaling. *Antioxidants & Redox Signaling* **6:** 301-310.

Golan T, Muller-Moule P, Niyogi KK. **2006.** Photoprotection mutants of *Arabidopsis thaliana* acclimate to high light by increasing photosynthesis and specific antioxidants. *Plant Cell and Environment* **29:** 879-887.

Gong JM, Lee DA, Schroeder JI. **2003.** Long-distance root-to-shoot transport of phytochelatins and cadmium in *Arabidopsis*. *Proceedings of the National Academy of Sciences of the United States of America* **100:** 10118-10123.

Gould KS, Lamotte O, Klinguer A, Pugin A, Wendehenne D. **2003.** Nitric oxide production in tobacco leaf cells: a generalized stress response? *Plant Cell and Environment* **26:** 1851-1862.

Govindjee. **1995.** 63 years since Kautsky – chlorophyll *a* fluorescence. *Australian Journal of Plant Physiology* **22:** 131-160.

Greer DH, Ottander C, Öquist G. **1991.** Photoinhibition and recovery of photosynthesis in intact barley leaves at 5 and 20-Degrees-C. *Physiologia Plantarum* **81:** 203-210.

Greger M, Ogren E. **1991.** Direct and indirect effects of Cd^{2+} on photosynthesis in sugar-Beet (*Beta vulgaris*). *Physiologia Plantarum* **83:** 129-135.

Grill E, Zenk MH, Winnacker EL. **1985.** Induction of heavy metal-sequestering phytochelatin by cadmium in cell-cultures of *Rauvolfia serpentina*. *Naturwissenschaften* **72:** 432-433.

Grill E, Winnacker EL, Zenk MH. **1987.** Phytochelatins, a class of heavy-metal-binding peptides from plants, are functionally analogous to metallothioneins. *Proceedings of the National Academy of Sciences of the United States of America* **84:** 439-443.

Guerinot ML. **2000.** The ZIP family of metal transporters. *Biochimica et Biophysica Acta-Biomembranes* **1465:** 190-198.

Ha SB, Smith AP, Howden R, Dietrich WM, Bugg S, O'Connell MJ, Goldsbrough PB, Cobbett CS. **1999.** Phytochelatin synthase genes from *Arabidopsis* and the yeast *Schizosaccharomyces pombe*. *Plant Cell* **11:** 1153-1163.

Hall JL. **2002.** Cellular mechanisms for heavy metal detoxification and tolerance. *Journal of Experimental Botany* **53:** 1-11.

Halliwell B, Gutteridge JMC. **2000.** *Free radicals in biology and medicine*. New York: Oxford University Press, Inc.

Hartwig A, Schwerdtle T. **2002.** Interactions by carcinogenic metal compounds with DNA repair processes: toxicological implications. *Toxicology Letters* **127:** 47-54.

Havaux M, Strasser RJ, Greppin H. **1991.** A theoretical and experimental-analysis of the q_p and q_n coefficients of chlorophyll fluorescence quenching and their relation to photochemical and nonphotochemical events. *Photosynthesis Research* **27:** 41-55.

Heber U, Wiese C, Neimanis S, Savchenko G, Bukhov NG, Hedrich R. **2002.** Energy-dependent solute transport from the apoplast into the symplast of leaves during transpiration. *Russian Journal of Plant Physiology* **49:** 32-43.

Heckenberger U, Roggatz U, Schurr U. **1998.** Effect of drought stress on the cytological status in *Ricinus communis*. *Journal of Experimental Botany* **49:** 181-189.

Hetherington SE, He J, Smillie RM. **1989.** Photoinhibition at low-temperature in chilling-sensitive and chilling-resistant plants. *Plant Physiology* **90:** 1609-1615.

Hideg E, Ogawa K, Kalai T, Hideg K. **2001.** Singlet oxygen imaging in *Arabidopsis thaliana* leaves under photoinhibition by excess photosynthetically active radiation. *Physiologia Plantarum* **112:** 10-14.

Hideg E, Barta C, Kalai T, Vass I, Hideg K, Asada K. **2002.** Detection of singlet oxygen and superoxide with fluorescent sensors in leaves under stress by photoinhibition or UV radiation. *Plant and Cell Physiology* **43:** 1154-1164.

Hill R, Larkum AWD, Frankart C, Kuhl M, Ralph PJ. **2004.** Loss of functional photosystem II reaction centres in zooxanthellae of corals exposed to bleaching conditions: using fluorescence rise kinetics. *Photosynthesis Research* **82:** 59-72.

Hogervorst J, Plusquin M, Vangronsveld J, Nawrot T, Cuypers A, Van Hecke E, Roels HA, Carleer R, Staessen JA. **2007.** House dust as possible route of environmental exposure to cadmium and lead in the adult general population. *Environmental Research* **103:** 30-37.

Hollenbach B, Schreiber L, Hartung W, Dietz KJ. **1997.** Cadmium leads to stimulated expression of the lipid transfer protein genes in barley: implications for the involvement of lipid transfer proteins in wax assembly. *Planta* **203:** 9-19.

Howden R, Goldsbrough PB, Andersen CR, Cobbett CS. **1995.** Cadmium-sensitive, *cad1* mutants of *Arabidopsis thaliana* are phytochelatin deficient. *Plant Physiology* **107:** 1059-1066.

Hsu BD. **1993.** Evidence for the contribution of the s-state transitions of oxygen evolution to the initial phase of fluorescence induction. *Photosynthesis Research* **36:** 81-88.

IARC. 1993. Berrylium, cadmium, mercury and exposures in the glass manufacturing industry, International Agency for Research on Cancer Monographs on the Evaluation of Carcinogenic Risks to Humans. [58]. Lyon, IARC Scientific Publications.

Isaure M, Bourguignon J, Fayard B. 2005. Localization and speciation of cadmium in *Arabidopsis thaliana* plants. [Metal fluxes and stresses in terrestrial ecosystems. Abstracts. Birmensdorf, Swiss Federal Institute for Forest, Snow and Landscape Research WSL.], 46.

Jarup L, Berglund M, Elinder CG, Nordberg G, Vahter M. **1998.** Health effects of cadmium exposure - a review of the literature and a risk estimate - Preface. *Scandinavian Journal of Work Environment & Health* **24**.

Jiang MY, Zhang JH. **2002.** Involvement of plasma-membrane NADPH oxidase in abscisic acid- and water stress-induced antioxidant defence in leaves of maize seedlings. *Planta* **215:** 1022-1030.

Jimenez A, Hernandez JA, delRio LA, Sevilla F. **1997.** Evidence for the presence of the ascorbate-glutathione cycle in mitochondria and peroxisomes of pea leaves. *Plant Physiology* **114:** 275-284.

Jin TY, Lu J, Nordberg M. **1998.** Toxicokinetics and biochemistry of cadmium with special emphasis on the role of metallothionein. *Neurotoxicology* **19:** 529-535.

Jones HG. **1998.** Stomatal control of photosynthesis and transpiration. *Journal of Experimental Botany* **49:** 387-398.

Kacperska A. **2004.** Sensor types in signal transduction pathways in plant cells responding to abiotic stressors: do they depend on stress intensity? *Physiologia Plantarum* **122:** 159-168.

Kamiya N, Shen JR. **2003.** Crystal structure of oxygen-evolving photosystem II from *Thermosynechococcus vulcanus* at 3.7-angstrom resolution. *Proceedings of the National Academy of Sciences of the United States of America* **100:** 98-103.

Kanofsky JR, Axelrod B. **1986.** Singlet oxygen production by soybean lipoxygenase isozymes. *Journal of Biological Chemistry* **261:** 1099-1104.

Kanofsky JR. **2000.** Assay for singlet-oxygen generation by peroxidases using 1270-nm chemiluminescence. *Singlet Oxygen, UV-A, and Ozone* **319:** 59-67.

Kautsky H, Hirsch A. **1931.** Neue versuche zur kohlensäureassimilation. *Naturwissenschaften* **19:** 964.

Keller F, Ludlow MM. **1993.** Carbohydrate-metabolism in drought-stressed leaves of pigeonpea (*Cajanus cajan*). *Journal of Experimental Botany* **44:** 1351-1359.

Kevresan S, Kirsek S, Kandrac J, Petrovic N, Kelemen D. **2003.** Dynamics of cadmium distribution in the intercellular space and inside cells in soybean roots, stems and leaves. *Biologia Plantarum* **46:** 85-88.

Khan AU, Kasha M. **1994.** Singlet molecular-oxygen in the Haber-Weiss reaction. *Proceedings of the National Academy of Sciences of the United States of America* **91:** 12365-12367.

Khan DH, Duckett JG, Frankland B, Kirkham JB. **1984.** An X-ray microanalytical study of the distribution of cadmium in roots of *Zea mays* L. *Journal of Plant Physiology* **115:** 19-28.

Kim CG, Power SA, Bell JNB. **2003.** Effects of cadmium and soil type on mineral nutrition and carbon partitioning in seedlings of *Pinus sylvestris*. *Water Air and Soil Pollution* **145:** 253-266.

Kim SY, Kwon OJ, Park JW. **2001.** Inactivation of catalase and superoxide dismutase by singlet oxygen derived from photoactivated dye. *Biochimie* **83:** 437-444.

Kliebenstein DJ, Monde RA, Last RL. **1998.** Superoxide dismutase in *Arabidopsis*: An eclectic enzyme family with disparate regulation and protein localization. *Plant Physiology* **118:** 637-650.

Korshunova YO, Eide D, Clark WG, Guerinot ML, Pakrasi HB . **1999.** The IRT1 protein from *Arabidopsis thaliana* is a metal transporter with a broad substrate range. *Plant Molecular Biology* **40:** 37-44.

Kramer H, Mathis P. **1980.** Quantum yield and rate of formation of the carotenoid triplet-state in photosynthetic structures. *Biochimica et Biophysica Acta* **593:** 319-329.

Kramer U, Cotter-Howells JD, Charnock JM, Baker AJM, Smith JAC. **1996.** Free histidine as a metal chelator in plants that accumulate nickel. *Nature* **379:** 635-638.

Krasnovsky AA. **1998.** Phosphorescence analysis of singlet molecular oxygen in photobiochemical systems. *Biologicheskie Membrany* **15:** 530-548.

Krause GH. **1988.** Photoinhibition of photosynthesis - an evaluation of damaging and protective mechanisms. *Physiologia Plantarum* **74:** 566-574.

Krause GH, Weis E. **1991.** Chlorophyll fluorescence and photosynthesis - the basics. *Annual Review of Plant Physiology and Plant Molecular Biology* **42:** 313-349.

Kriedemann PE, Graham RD, Wiskich JT. **1985.** Photosynthetic dysfunction and invivo changes in chlorophyll *a* fluorescence from Manganese-deficient wheat leaves. *Australian Journal of Agricultural Research* **36:** 157-169.

Krieger A, Moya I, Weis E. **1992.** Energy-dependent quenching of chlorophyll-*a* fluorescence - effect of pH on stationary fluorescence and picosecond-relaxation

kinetics in thylakoid membranes and photosystem II preparations. *Biochimica et Biophysica Acta* **1102:** 167-176.

Krotz RM, Evangelou BP, Wagner GJ. **1989.** Relationships between cadmium, zinc, Cd-peptide, and organic-acid in tobacco suspension cells. *Plant Physiology* **91:** 780-787.

Krupa Z, Baszynski T. **1985.** Effects of cadmium on the acyl lipid-content and fatty-acid composition in thylakoid membranes isolated from tomato leaves. *Acta Physiologiae Plantarum* **7:** 55-64.

Krupa Z, Baszynski T. **1989.** Acyl lipid-composition of thylakoid membranes of cadmium-treated tomato plants. *Acta Physiologiae Plantarum* **11:** 111-116.

Krupa Z, Öquist G, Huner NPA. **1993.** The effects of cadmium on photosynthesis of *Phaseolus vulgaris* - a fluorescence analysis. *Physiologia Plantarum* **88:** 626-630.

Kumar PBAN, Dushenkov V, Motto H, Raskin I. **1995.** Phytoextraction - the use of plants to remove heavy-metals from soils. *Environmental Science & Technology* **29:** 1232-1238.

Kupper H, Kupper F, Spiller M. **1998.** In situ detection of heavy metal substituted chlorophylls in water plants. *Photosynthesis Research* **58:** 123-133.

Kupper H, Lombi E, Zhao FJ, McGrath SP. **2000.** Cellular compartmentation of cadmium and zinc in relation to other elements in the hyperaccumulator *Arabidopsis halleri*. *Planta* **212:** 75-84.

Kwak JM, Mori IC, Pei ZM, Leonhardt N, Torres MA, Dangl JL, Bloom RE, Bodde S, Jones JDG, Schroeder JI. **2003.** NADPH oxidase AtrbohD and AtrbohF genes function in ROS-dependent ABA signaling in *Arabidopsis*. *EMBO Journal* **22:** 2623-2633.

Kwak JM, Nguyen V, Schroeder JI. **2006.** The role of reactive oxygen species in hormonal responses. *Plant Physiology* **141:** 323-329.

Lamkemeyer P, Laxa M, Collin V, Li W, Finkemeier I, Schottler MA, Holtkamp V, Tognetti VB, Issakidis-Bourguet E, Kandlbinder A, Weis E, Miginiac-Maslow M, Dietz KJ. **2006.** Peroxiredoxin Q of *Arabidopsis thaliana* is attached to the thylakoids and functions in context of photosynthesis. *Plant Journal* **45:** 968-981.

Lasat MM, Pence NS, Garvin DF, Ebbs SD, Kochian LV. **2000.** Molecular physiology of zinc transport in the Zn hyperaccumulator *Thlaspi caerulescens*. *Journal of Experimental Botany* **51:** 71-79.

Layne DR, Flore JA. **1993.** Physiological-responses of *Prunus cerasus* to whole-plant source manipulation - leaf gas-exchange, chlorophyll fluorescence, water relations and carbohydrate concentrations. *Physiologia Plantarum* **88:** 44-51.

Lazar D. **2003.** Chlorophyll *a* fluorescence rise induced by high light illumination of dark-adapted plant tissue studied by means of a model of photosystem II and considering photosystem II heterogeneity. *Journal of Theoretical Biology* **220:** 469-503.

Lee SH, Min DB. **1990.** Effects, quenching mechanisms, and kinetics of carotenoids in chlorophyll-sensitized photooxidation of soybean oil. *Journal of Agricultural and Food Chemistry* **38:** 1630-1634.

Lehmann EL. **1975.** *Nonparametrics, statistical methods based on ranks*. San Francisco: Holden-day Inc.

Leita L, DeNobili M, Cesco S, Mondini C. **1996.** Analysis of intercellular cadmium forms in roots and leaves of bush bean. *Journal of Plant Nutrition* **19:** 527-533.

Li XP, Bjorkman O, Shih C, Grossman AR, Rosenquist M, Jansson S, Niyogi KK. **2000.** A pigment-binding protein essential for regulation of photosynthetic light harvesting. *Nature* **403:** 391-395.

Li XP, Gilmore AM, Caffarri S, Bassi R, Golan T, Kramer D, Niyogi KK. **2004.** Regulation of photosynthetic light harvesting involves intrathylakoid lumen pH sensing by the PsbS protein. *Journal of Biological Chemistry* **279:** 22866-22874.

Lichtenthaler HK, Wellburn AR. **1983.** Determinations of total carotenoids and chlorophylls *a* and *b* of leaf extracts in different solvents. *Biochemical Society Transactions* **11:** 591-592.

Lichtenthaler HK. **1996.** Vegetation stress: An introduction to the stress concept in plants. *Journal of Plant Physiology* **148:** 4-14.

Linger P, Ostwald A, Haensler J. **2005.** *Cannabis sativa* L. growing on heavy metal contaminated soil: growth, cadmium uptake and photosynthesis. *Biologia Plantarum* **49:** 567-576.

Liu DH, Kottke I. **2003.** Subcellular localization of Cd in the root cells of *Allium sativum* by electron energy loss spectroscopy. *Journal of Biosciences* **28:** 471-478.

Livak KJ, Schmittgen TD. **2001.** Analysis of relative gene expression data using real-time quantitative PCR and the 2(T)(-Delta Delta C) method. *Methods* **25:** 402-408.

Lledias F, Rangel P, Hansberg W. **1998.** Oxidation of catalase by singlet oxygen. *Journal of Biological Chemistry* **273:** 10630-10637.

Loll B, Kern J, Saenger W, Zouni A, Biesiadka J. **2005.** Towards complete cofactor arrangement in the 3.0 angstrom resolution structure of photosystem II. *Nature* **438:** 1040-1044.

Long SP, Humphries S, Falkowski PG. **1994.** Photoinhibition of photosynthesis in nature. *Annual Review of Plant Physiology and Plant Molecular Biology* **45:** 633-662.

Lozano-Rodriguez E, Hernandez LE, Bonay P, Carpena-Ruiz RO. **1997.** Distribution of cadmium in shoot and root tissues of maize and pea plants: physiological disturbances. *Journal of Experimental Botany* **48:** 123-128.

Ma FS, Peterson CA. **2003.** Current insights into the development, structure, and chemistry of the endodermis and exodermis of roots. *Canadian Journal of Botany-Revue Canadienne de Botanique* **81:** 405-421.

Maitani T, Kubota H, Sato K, Yamada T. **1996.** The composition of metals bound to class III metallothionein (phytochelatin and its desglycyl peptide) induced by various metals in root cultures of *Rubia tinctorum*. *Plant Physiology* **110:** 1145-1150.

Mallick N, Mohn FH. **2003.** Use of chlorophyll fluorescence in metal-stress research: a case study with the green microalga *Scenedesmus*. *Ecotoxicology and Environmental Safety* **55:** 64-69.

Marschner H. **1995.** *Mineral Nutrition of Higher Plants*. London: Academic Press.

Martinez GR, Loureiro APM, Marques SA, Miyamoto S, Yamaguchi LF, Onuki J, Almeida EA, Garcia CCM, Barbosa LF, Medeiros MHG, Di Mascio P. **2003.** Oxidative and alkylating damage in DNA. *Mutation Research-Reviews in Mutation Research* **544:** 115-127.

Maxwell K, Johnson GN. **2000.** Chlorophyll fluorescence - a practical guide. *Journal of Experimental Botany* **51:** 659-668.

Melan MA, Dong XN, Endara ME, Davis KR, Ausubel FM, Peterman TK. **1993.** An *Arabidopsis thaliana* lipoxygenase gene can be induced by pathogens, abscisic acid, and methyl jasmonate. *Plant Physiology* **101:** 441-450.

Mittler R, Vanderauwera S, Gollery M, Van Breusegem F. **2004.** Reactive oxygen gene network of plants. *Trends in Plant Science* **9:** 490-498.

Montillet JL, Cacas JL, Garnier L, Montane MH, Douki T, Bessoule JJ, Polkowska-Kowalczyk L, Maciejewska U, Agnel JP, Vial A, Triantaphylides C. **2004.** The upstream oxylipin profile of *Arabidopsis thaliana*: a tool to scan for oxidative stresses. *Plant Journal* **40:** 439-451.

Mullet JE, Whitsitt MS. **1996.** Plant cellular responses to water deficit. *Plant Growth Regulation* **20:** 119-124.

Munné-Bosch S, Jubany-Mari T, Alegre L. **2001.** Drought-induced senescence is characterized by a loss of antioxidant defences in chloroplasts. *Plant Cell and Environment* **24:** 1319-1327.

Munné-Bosch S, Alegre L. **2002.** The function of tocopherols and tocotrienols in plants. *Critical Reviews in Plant Sciences* **21:** 31-57.

Nassiri Y, Mansot JL, Wery J, Ginsburger-Vogel T, Amiard JC. **1997.** Ultrastructural and electron energy loss spectroscopy studies of sequestration mechanisms of Cd and Cu in the marine diatom *Skeletonema costatum*. *Archives of Environmental Contamination and Toxicology* **33:** 147-155.

Nawrot T, Plusquin M, Hogervorst J, Roels HA, Celis H, Thijs L, Vangronsveld J, Van Hecke E, Staessen JA. **2006.** Environmental exposure to cadmium and risk of cancer: a prospective population-based study. *Lancet Oncology* **7:** 119-126.

Neely WC, Martin JM, Barker SA. **1988.** Products and relative reaction-rates of the oxidation of tocopherols with singlet molecular-oxygen. *Photochemistry and Photobiology* **48:** 423-428.

Neter J, Kutner MH, Nachtsheim CJ, Wasserman W. **1996.** *Applied Linear Statistics Models*. The McGraw-Hill Companies, Inc.

Neubauer C, Schreiber U. **1987.** The polyphasic rise of chlorophyll fluorescence upon onset of strong continuous illumination .1. Saturation characteristics and partial control by the photosystem II acceptor side. *Zeitschrift fur Naturforschung C-A Journal of Biosciences* **42:** 1246-1254.

Nieboer E, Richardson DHS. **1980.** The replacement of the non-descript term heavy-metals by a biologically and chemically significant classification of metal-ions. *Environmental Pollution Series B-Chemical and Physical* **1:** 3-26.

Nies DH, Silver S. **1989.** Plasmid-determined inducible efflux is responsible for resistance to cadmium, zinc, and cobalt in *Alcaligenes eutrophus*. *Journal of Bacteriology* **171:** 896-900.

Nishiyama Y, Allakhverdiev SI, Yamamoto H, Hayashi H, Murata N. **2004.** Singlet oxygen inhibits the repair of photosystem II by suppressing the translation elongation of the D1 protein in *Synechocystis* sp PCC 6803. *Biochemistry* **43:** 11321-11330.

Niyogi KK, Grossman AR, Bjorkman O. **1998.** *Arabidopsis* mutants define a central role for the xanthophyll cycle in the regulation of photosynthetic energy conversion. *Plant Cell* **10:** 1121-1134.

Niyogi KK. **1999.** Photoprotection revisited: Genetic and molecular approaches. *Annual Review of Plant Physiology and Plant Molecular Biology* **50:** 333-359.

Niyogi KK, Shih C, Chow WS, Pogson BJ, DellaPenna D, Bjorkman O. **2001.** Photoprotection in a zeaxanthin- and lutein-deficient double mutant of *Arabidopsis*. *Photosynthesis Research* **67:** 139-145.

Olmos E, Martinez-Solano JR, Piqueras A, Hellin E. **2003.** Early steps in the oxidative burst induced by cadmium in cultured tobacco cells (BY-2 line). *Journal of Experimental Botany* **54:** 291-301.

op den Camp RGL, Przybyla D, Ochsenbein C, Laloi C, Kim CH, Danon A, Wagner D, Hideg E, Gobel C, Feussner I, Nater M, Apel K. **2003.** Rapid induction of distinct stress responses after the release of singlet oxygen in *Arabidopsis*. *Plant Cell* **15:** 2320-2332.

Öquist G, Chow WS, Anderson JM. **1992.** Photoinhibition of photosynthesis represents a mechanism for the long-term regulation of photosystem II. *Planta* **186:** 450-460.

Öquist G, Hurry VM, Huner NPA. **1993.** The temperature-dependence of the redox state of Q(A) and susceptibility of photosynthesis to photoinhibition. *Plant Physiology and Biochemistry* **31:** 683-691.

Orlovich DA, Ashford AE. **1995.** X-ray-microanalysis of ion distribution in frozen salt dextran droplets after freeze-substitution and embedding in anhydrous conditions. *Journal of Microscopy-Oxford* **180:** 117-126.

Orozco-Cardenas ML, Narvaez-Vasquez J, Ryan CA. **2001.** Hydrogen peroxide acts as a second messenger for the induction of defense genes in tomato plants in response to wounding, systemin, and methyl jasmonate. *Plant Cell* **13:** 179-191.

Ortiz DF, Kreppel L, Speiser DM, Scheel G, McDonald G, Ow DW. **1992.** Heavy-metal tolerance in the fission yeast requires an ATP-binding cassette-type vacuolar membrane transporter. *EMBO Journal* **11:** 3491-3499.

Ortiz DF, Ruscitti T, Mccue KF, Ow DW. **1995.** Transport of metal-binding peptides by Hmt1, A fission yeast ABC-type vacuolar membrane-protein. *Journal of Biological Chemistry* **270:** 4721-4728.

Ottander C, Campbell D, Öquist G. **1995.** Seasonal-changes in photosystem II organization and pigment composition in *Pinus sylvestris*. *Planta* **197:** 176-183.

Ouzounidou G. **1993.** Changes in variable chlorophyll fluorescence as a result of Cu-treatment - dose-response relations in *Silene* and *Thlasp*i. *Photosynthetica* **29:** 455-462.

Ouzounidou G, Moustakas M, Eleftheriou EP. **1997.** Physiological and ultrastructural effects of cadmium on wheat (*Triticum aestivum* L) leaves. *Archives of Environmental Contamination and Toxicology* **32:** 154-160.

Papageorgiou G. **1975.** Mechanism of PMS-effected quenching of chloroplast fluorescence. *Archives of Biochemistry and Biophysics* **166:** 390-399.

Pelleschi S, Rocher JP, Prioul JL. **1997.** Effect of water restriction on carbohydrate metabolism and photosynthesis in mature maize leaves. *Plant Cell and Environment* **20:** 493-503.

Pence NS, Larsen PB, Ebbs SD, Letham DLD, Lasat MM, Garvin DF, Eide D, Kochian LV. **2000.** The molecular physiology of heavy metal transport in the Zn/Cd hyperaccumulator *Thlaspi caerulescens*. *Proceedings of the National Academy of Sciences of the United States of America* **97:** 4956-4960.

Perfus-Barbeoch L, Leonhardt N, Vavasseur A, Forestier C . **2002.** Heavy metal toxicity: cadmium permeates through calcium channels and disturbs the plant water status. *Plant Journal* **32:** 539-548.

Peterson CA, Enstone DE. **1996.** Functions of passage cells in the endodermis and exodermis of roots. *Physiologia Plantarum* **97:** 592-598.

Pich A, Scholz G. **1996.** Translocation of copper and other micronutrients in tomato plants (*Lycopersicon esculentum* Mill): nicotianamine-stimulated copper transport in the xylem. *Journal of Experimental Botany* **47:** 41-47.

Pietrini F, Iannelli MA, Pasqualini S, Massacci A. **2003.** Interaction of cadmium with glutathione and photosynthesis in developing leaves and chloroplasts of *Phragmites australis* (Cav.) Trin. ex steudel. *Plant Physiology* **133:** 829-837.

Pogson B, McDonald KA, Truong M, Britton G, DellaPenna D. **1996.** *Arabidopsis* carotenoid mutants demonstrate that lutein is not essential for photosynthesis in higher plants. *Plant Cell* **8:** 1627-1639.

Pogson BJ, Niyogi KK, Bjorkman O, DellaPenna D. **1998.** Altered xanthophyll compositions adversely affect chlorophyll accumulation and nonphotochemical quenching in *Arabidopsis* mutants. *Proceedings of the National Academy of Sciences of the United States of America* **95:** 13324-13329.

Porta H, Rueda-Benitez P, Campos F, Colmenero-Flores JM, Colorado JM, Carmona MJ, Covarrubias AA, Rocha-Sosa M. **1999.** Analysis of lipoxygenase mRNA accumulation in the common bean (*Phaseolus vulgaris* L.) during development and under stress conditions. *Plant and Cell Physiology* **40:** 850-858.

Porta H, Rocha-Sosa M. **2002.** Plant lipoxygenases. Physiological and molecular features. *Plant Physiology* **130:** 15-21.

Pospisil P, Dau H. **2000.** Chlorophyll fluorescence transients of photosystem II membrane particles as a tool for studying photosynthetic oxygen evolution. *Photosynthesis Research* **65:** 41-52.

Poulson M, Samson G, Whitmarsh J. **1995.** Evidence that cytochrome B(559) protects photosystem II against photoinhibition. *Biochemistry* **34:** 10932-10938.

Prasad MNV. **1995.** Cadmium toxicity and tolerance in vascular plants. *Environmental and Experimental Botany* **35:** 525-545.

Raeymaekers T. **2007.** *Oxygen radical production and redox changes induced in plant cell cultures by metal stress*. Universiteit Antwerpen.

Rascio N, Dallavecchia F, Ferretti M, Merlo L, Ghisi R. **1993.** Some effects of cadmium on maize plants. *Archives of Environmental Contamination and Toxicology* **25:** 244-249.

Rauser WE, Ackerley CA. **1987.** Localization of cadmium in granules within differentiating and mature root-cells. *Canadian Journal of Botany-Revue Canadienne de Botanique* **65:** 643-646.

Reese RN, White CA, Winge DR. **1992.** Cadmium-sulfide crystallites in Cd-$(\gamma EC)_n$G peptide complexes from tomato. *Plant Physiology* **98:** 225-229.

Reid RJ, Dunbar KR, McLaughlin MJ. **2003.** Cadmium loading into potato tubers: the roles of the periderm, xylem and phloem. *Plant Cell and Environment* **26:** 201-206.

Ribeiro KC, Benchimol M, Farina M. **2001.** Contribution of cryofixation and freeze-substitution to analytical microscopy: a study of *Tritrichomonas foetus* hydrogenosomes. *Microscopy Research and Technique* **53:** 87-92.

Rinalducci S, Pedersen JZ, Zolla L. **2004.** Formation of radicals from singlet oxygen produced during photoinhibition of isolated light-harvesting proteins of photosystem II. *Biochimica et Biophysica Acta-Bioenergetics* **1608:** 63-73.

Rodriguez-Serrano M, Romero-Puertas MC, Zabalza A, Corpas FJ, Gomez M, del Rio LA, Sandalio LM. **2006.** Cadmium effect on oxidative metabolism of pea (*Pisum sativum* L.) roots. Imaging of reactive oxygen species and nitric oxide accumulation in vivo. *Plant Cell and Environment* **29:** 1532-1544.

Romero-Puertas MC, Rodriguez-Serrano M, Corpas FJ, Gomez M, del Rio LA, Sandalio LM. **2004.** Cadmium-induced subcellular accumulation of $O_2^{\cdot-}$and H_2O_2 in pea leaves. *Plant Cell and Environment* **27:** 1122-1134.

Russell GA. **1957.** Deuterium-isotope effects in the autoxidation of aralkyl hydrocarbons. Mechanism of the interaction of peroxy radicals. *Journal of the American Chemical Society* **79:** 3871-3877.

Sagi M, Fluhr R. **2001.** Superoxide production by plant homologues of the gp91(phox) NADPH oxidase. Modulation of activity by calcium and by tobacco mosaic virus infection. *Plant Physiology* **126:** 1281-1290.

Salt DE, Wagner GJ. **1993.** Cadmium transport across tonoplast of vesicles from oat roots - evidence for a Cd^{2+}/H^{+} antiport activity. *Journal of Biological Chemistry* **268:** 12297-12302.

Salt DE, Rauser WE. **1995.** MgATP-dependent transport of phytochelatins across the tonoplast of oat roots. *Plant Physiology* **107:** 1293-1301.

Salt DE, Prince RC, Pickering IJ, Raskin I. **1995.** Mechanisms of cadmium mobility and accumulation in Indian mustard. *Plant Physiology* **109:** 1427-1433.

Sanità di Toppi LS, Gabbrielli R. **1999.** Response to cadmium in higher plants. *Environmental and Experimental Botany* **41:** 105-130.

Santabarbara S, Bordignon E, Jennings RC, Carbonera D. **2002.** Chlorophyll triplet states associated with photosystem II of thylakoids. *Biochemistry* **41:** 8184-8194.

Sawyer DT, Valentine JS. **1981.** How super is superoxide. *Accounts of Chemical Research* **14:** 393-400.

Sayed OH. **1998.** Analysis of photosynthetic responses and adaptation to nitrogen starvation in Chlorella using in vivo chlorophyll fluorescence. *Photosynthetica* **35:** 611-619.

Scandalios JG. **2005.** Oxidative stress: molecular perception and transduction of signals triggering antioxidant gene defenses. *Brazilian Journal of Medical and Biological Research* **38:** 995-1014.

Schansker G, Toth SZ, Strasser RJ. **2005.** Methylviologen and dibromothymoquinone treatments of pea leaves reveal the role of photosystem I in the Chl a fluorescence rise OJIP. *Biochimica et Biophysica Acta-Bioenergetics* **1706:** 250-261.

Schat H, Llugany M, Vooijs R, Hartley-Whitaker J, Bleeker PM. **2002.** The role of phytochelatins in constitutive and adaptive heavy metal tolerances in hyperaccumulator and non-hyperaccumulator metallophytes. *Journal of Experimental Botany* **53:** 2381-2392.

Schindler C, Lichtenthaler HK. **1994.** Is There A Correlation Between Light-Induced Zeaxanthin Accumulation and Quenching of Variable Chlorophyll-*a* Fluorescence. *Plant Physiology and Biochemistry* **32:** 813-823.

Schreiber U, Neubauer C. **1987.** The Polyphasic Rise of Chlorophyll Fluorescence Upon Onset of Strong Continuous Illumination .2. Partial Control by the Photosystem II Donor Side and Possible Ways of Interpretation. *Zeitschrift fur Naturforschung C-A Journal of Biosciences* **42:** 1255-1264.

Schreiber U, Neubauer C. **1990.** O_2-Dependent Electron Flow, Membrane Energization and the Mechanism of Nonphotochemical Quenching of Chlorophyll Fluorescence. *Photosynthesis Research* **25:** 279-293.

Schreiber U. **2004.** Pulse-amplitude-modulation (PAM) fluorometry and saturation pulse method: an overview. In: Papageorgiou G, Govindjee, eds. *Chlorophyll Fluorescence: a Signature of Photosynthesis*. Dordrecht, The Netherlands: Springer, 279-319.

Schützendübel A, Polle A. **2002.** Plant responses to abiotic stresses: heavy metal-induced oxidative stress and protection by mycorrhization. *Journal of Experimental Botany* **53:** 1351-1365.

Sela M, Fritz E, Huttermann A, Telor E. **1990.** Studies on cadmium localization in the water fern *Azolla*. *Physiologia Plantarum* **79:** 547-553.

Semane B, Cuypers A, Smeets K, Van Belleghem F, Horemans N, Schat H, Vangronsveld J. **2007.** Cadmium responses in *Arabidopsis thaliana*: glutathione metabolism and antioxidative defence system. *Physiologia Plantarum* **129:** 519-528.

Senden MHMN, Van Paassen FJM, Van Der Meer AJGM, Wolterbeek HT. **1992.** Cadmium citric-acid xylem cell-wall interactions in tomato plants. *Plant Cell and Environment* **15:** 71-79.

Seregin IV, Ivanov VB. **1997.** Histochemical investigation of cadmium and lead distribution in plants. *Russian Journal of Plant Physiology* **44:** 791-796.

Seregin IV, Ivanov VB. **2001.** Physiological aspects of cadmium and lead toxic effects on higher plants. *Russian Journal of Plant Physiology* **48:** 523-544.

Sharma J, Panico M, Barber J, Morris HR. **1997.** Characterization of the low molecular weight photosystem II reaction center subunits and their light-induced modifications by mass spectrometry. *Journal of Biological Chemistry* **272:** 3935-3943.

Sharma RP, Street JC, Verma MP, Shupe JL. **1979.** Cadmium uptake from feed and its distribution to food-products of livestock. *Environmental Health Perspectives* **28:** 59-66.

Shimoni E, Müller M. **1998.** On optimizing high-pressure freezing: from heat transfer theory to a new microbiopsy device. *Journal of Microscopy-Oxford* **192:** 236-247.

Simon-Plas F, Elmayan T, Blein JP. **2002.** The plasma membrane oxidase NtrbohD is responsible for AOS production in elicited tobacco cells. *Plant Journal* **31:** 137-147.

Skórzyńska-Polit E, Baszynski T. **2000.** Does Cd^{2+} use Ca^{2+} channels to penetrate into chloroplasts? - a preliminary study. *Acta Physiologiae Plantarum* **22:** 171-178.

Skórzyńska-Polit E, Drazkiewicz M, Krupa Z. **2003.** The activity of the antioxidative system in cadmium-treated *Arabidopsis thaliana*. *Biologia Plantarum* **47:** 71-78.

Skórzyńska-Polit E, Pawlikowska-Pawlega B, Szczuka E, Drazkiewicz M, Krupa Z. **2006.** The activity and localization of lipoxygenases in *Arabidopsis thaliana* under cadmium and copper stresses. *Plant Growth Regulation* **48:** 29-39.

Skórzyńska-Polit E, Krupa Z. **2006.** Lipid peroxidation in cadmium-treated *Phaseolus coccineus* plants. *Archives of Environmental Contamination and Toxicology* **50:** 482-487.

Skórzyńska-Polit E, Bednara J, Baszynski T. **1995.** Some aspects of runner bean plant-response to cadmium at different stages of the primary leaf growth. *Acta Societatis Botanicorum Poloniae* **64:** 165-170.

Skórzyńska-Polit E, Baszynski T. **1997.** Differences in sensitivity of the photosynthetic apparatus in Cd-stressed runner bean plants in relation to their age. *Plant Science* **128:** 11-21.

Smeets K, Cuypers A, Lambrechts A, Semane B, Hoet P, Van Laere A, Vangronsveld J. **2005.** Induction of oxidative stress and antioxidative mechanisms in *Phaseolus vulgaris* after Cd application. *Plant Physiology and Biochemistry* **43:** 437-444.

Solioz M, Vulpe C. **1996.** CPx-type ATPases: A class of p-type ATPases that pump heavy metals. *Trends in Biochemical Sciences* **21:** 237-241.

Spiteller G. **2003.** The relationship between changes in the cell wall, lipid peroxidation, proliferation, senescence and cell death. *Physiologia Plantarum* **119:** 5-18.

Srivastava A, Strasser RJ, Govindjee. **1999.** Greening of peas: parallel measurements of 77 K emission spectra, OJIP chlorophyll *a* fluorescence transient, period four oscillation of the initial fluorescence level, delayed light emission, and P700. *Photosynthetica* **37:** 365-392.

Staessen JA, Vyncke G, Lauwerys RR, Roels HA, Celis HG, Claeys F, Dondeyne F, Fagard RH, Ide G, Lijnen PJ, Rondia D, Sartor F, Thijs LB, Amery AK. **1992.** Transfer of cadmium from a sandy acidic soil to man - a population study. *Environmental Research* **58:** 25-34.

Staessen JA, Lauwerys RR, Ide G, Roels HA, Vyncke G, Amery A. **1994.** Renal-function and historical environmental cadmium pollution from zinc smelters. *Lancet* **343:** 1523-1527.

Staessen JA, Roels HA, Vangronsveld J, Clijsters H, De Schrijver K, De Temmerman L, Dondeyne F, Van Hulle S, Wildemeersch D, Wilms L. **1995.** Preventiemaatregelen voor bodemverontreiniging met cadmium. *Tijdschrift Geneeskunde* **51:** 1387.

Staessen JA, Roels HA, Emelianov D, Kuznetsova T, Thijs L, Vangronsveld J, Fagard R. **1999.** Environmental exposure to cadmium, forearm bone density, and risk of fractures: prospective population study. *Lancet* **353:** 1140-1144.

Stephan UW, Scholz G. **1993.** Nicotianamine - mediator of transport of iron and heavy-metals in the phloem. *Physiologia Plantarum* **88:** 522-529.

Stern VO, Volmer M. **1919.** Über die ablingungszeit der fluoreszeng. *Physik Zeitschrift* **20:** 183-188.

Steudle E. **2000.** Water uptake by roots: effects of water deficit. *Journal of Experimental Botany* **51:** 1531-1542.

Steyn WJ, Wand SJE, Holcroft DM, Jacobs G. **2002.** Anthocyanins in vegetative tissues: a proposed unified function in photoprotection. *New Phytologist* **155:** 349-361.

Stiborova M, Doubravova M, Leblova S. **1986.** A comparative study of the effect of heavy metal ions on ribulose-1,5-Bisphosphate carboxylase and phosphoenolpyruvate carboxylase. *Biochemie und Physiologie der Pflanzen* **181:** 373-379.

Stohs SJ, Bagchi D. **1995.** Oxidative mechanisms in the toxicity of metal ions. *Free Radical Biology and Medicine* **18:** 321-336.

Strasser R.J., Srivastava A., Tsimilli-Michael M. 1999. Screening the vitality and photosynthetic activity of plants by the fluorescence transient. In: Behl R.K., Punia M.S., Lather B.P.S., eds. *Crop Improvement for Food Security*. Hisar, India: SSARM, 72-115.

Strasser BJ, Strasser RJ. **1995.** Measuring fast fluorescence transients to address environmental questions: the JIP test. In: Mathis P, ed. *Photosynthesis: from Light to Biosphere, vol. 5.* The Netherlands: Kluwer Academic Publisher, 977-980.

Strasser RJ, Srivastava A, Govindjee. **1995.** Polyphasic chlorophyll-alpha fluorescence transient in plants and cyanobacteria. *Photochemistry and Photobiology* **61:** 32-42.

Strasser RJ, Srivastava A, Tsimilli-Michael M. **2000.** The fluorescence transient as a tool to characterize and screen photosynthetic samples. In: Yunus M, Pathre U, Mohanty P, eds. *Probing Photosynthesis: Mechanisms, Regulation and Adaptation*. London: Taylor & Francis, 445-483.

Strasser RJ, Tsimilli-Michael M. **2001.** Stress in plants, from daily rhythm to global changes, detected and quantified by the JIP-Test. *Chimie Nouvelle (SRC)* **75:** 3321-3326.

Strasser RJ, Tsimilli-Michael M, Srivastava A. **2004.** Analysis of the fluorescence transient. In: Papageorgiou G, Govindjee, eds. *Chlorophyll Fluorescence: a Signature of Photosynthesis*. Dordrecht, The Netherlands: Springer, 321-362.

Studer D, Michel M, Wohlwend M, Hunziker EB, Buschmann MD. **1995.** Vitrification of articular-cartilage by high-pressure freezing. *Journal of Microscopy-Oxford* **179:** 321-332.

Suhita D, Raghavendra AS, Kwak JM, Vavasseur A. **2004.** Cytoplasmic alkalization precedes reactive oxygen species production during methyl jasmonate- and abscisic acid-induced stomatal closure. *Plant Physiology* **134:** 1536-1545.

Tarr M, Valenzeno DP. **2003.** Singlet oxygen: the relevance of extracellular production mechanisms to oxidative stress in vivo. *Photochemical & Photobiological Sciences* **2:** 355-361.

Telfer A. **2002.** What is beta-carotene doing in the photosystem II reaction centre? *Philosophical Transactions of the Royal Society of London Series B-Biological Sciences* **357:** 1431-1439.

Thomine S, Wang RC, Ward JM, Crawford NM, Schroeder JI. **2000.** Cadmium and iron transport by members of a plant metal transporter family in *Arabidopsis* with homology to Nramp genes. *Proceedings of the National Academy of Sciences of the United States of America* **97:** 4991-4996.

Torres MA, Dangl JL, Jones JDG. **2002.** *Arabidopsis* gp91(phox) homologues AtrbohD and AtrbohF are required for accumulation of reactive oxygen intermediates in the plant defense response. *Proceedings of the National Academy of Sciences of the United States of America* **99:** 517-522.

Trebst A. **2003.** Function of beta-carotene and tocopherol in photosystem II. *Zeitschrift fur Naturforschung C-A Journal of Biosciences* **58:** 609-620.

Tsay JM, Michalet X. **2005.** New light on quantum dot cytotoxicity. *Chemistry & Biology* **12:** 1159-1161.

Tsimilli-Michael M, Eggenberg P, Biro B, Koves-Pechy K, Voros I, Strasser RJ. **2000.** Synergistic and antagonistic effects of arbuscular mycorrhizal fungi and Azospirillum and Rhizobium nitrogen-fixers on the photosynthetic activity of alfalfa, probed by the polyphasic chlorophyll *a* fluorescence transient O-J-I-P. *Applied Soil Ecology* **15:** 169-182.

Tyystjarvi E, Koski A, Keranen M, Nevalainen O. **1999.** The Kautsky curve is a built-in barcode. *Biophysical Journal* **77:** 1159-1167.

Valentine JS, Wertz DL, Lyons TJ, Liou LL, Goto JJ, Gralla EB. **1998.** The dark side of dioxygen biochemistry. *Current Opinion in Chemical Biology* **2:** 253-262.

Van Breusegem F, Dat JF. **2006.** Reactive oxygen species in plant cell death. *Plant Physiology* **141:** 384-390.

Vangronsveld J, Clijsters H. **1994.** Toxic effects of metals. In: Farago ME, ed. *Plants and the chemical elements*. Weinheim: VCH Verlagsgesellshaft. 149-177

van Steveninck RFM, van Steveninck ME, Fernando DR, Edwards LB, Wells AJ. **1990.** Electron-probe X-ray microanalytical evidence for 2 distinct mechanisms of Zn and Cd binding in a Zn tolerant clone of *Lemna Minor* L. *Comptes Rendus de l Academie des Sciences Serie Iii-Sciences de la Vie-Life Sciences* **310:** 671-678.

Vatamaniuk OK, Mari S, Lu YP, Rea PA. **1999.** AtPCS1, a phytochelatin synthase from *Arabidopsis*: Isolation and in vitro reconstitution. *Proceedings of the National Academy of Sciences of the United States of America* **96:** 7110-7115.

Vatamaniuk OK, Bucher EA, Sundaram MV, Rea PA. **2005.** CeHMT-1, a putative phytochelatin transporter, is required for cadmium tolerance in *Caenorhabditis elegans*. *Journal of Biological Chemistry* **280:** 23684-23690.

Vazquez MD, Barcelo J, Poschenrieder C, Madico J, Hatton P, Baker AJM, Cope GH. **1992a.** Localization of zinc and cadmium in *Thlaspi Caerulescens* (Brassicaceae), a metallophyte that can hyperaccumulate both metals. *Journal of Plant Physiology* **140:** 350-355.

Vazquez MD, Poschenrieder C, Barcelo J. **1992b.** Ultrastructural effects and localization of low cadmium concentrations in bean roots. *New Phytologist* **120:** 215-226.

Verhoeven AS, Bugos RC, Yamamoto HY. **2001.** Transgenic tobacco with suppressed zeaxanthin formation is susceptible to stress-induced photoinhibition. *Photosynthesis Research* **67:** 27-39.

Vernoux T, Wilson RC, Seeley KA, Reichheld JP, Muroy S, Brown S, Maughan SC, Cobbett CS, Van Montagu M, Inze D, May MJ, Sung ZR. **2000.** The root meristemless1/cadmium sensitive2 gene defines a glutathione-dependent pathway involved in initiation and maintenance of cell division during postembryonic root development. *Plant Cell* **12:** 97-109.

Veselov D, Kudoyarova G, Symonyan M, Symonyan ST. **2003.** Effect of cadmium on ion uptake, transpiration and cytokinin content in wheat. *Bulgarian Journal of Plant Physiology* **special issue 2003:** 353-359.

Vitoria AP, Rodriguez APM, Cunha M, Lea PJ, Azevedo RA. **2003.** Structural changes in radish seedlings exposed to cadmium. *Biologia Plantarum* **47:** 561-568.

Vogeli-Lange R, Wagner GJ. **1990.** Subcellular localization of cadmium and cadmium-binding peptides in tobacco leaves - implication of a transport function for cadmium-binding peptides. *Plant Physiology* **92:** 1086-1093.

Vogeli-Lange R, Wagner GJ. **1996.** Relationship between cadmium, glutathione and cadmium-binding peptides (phytochelatins) in leaves of intact tobacco seedlings. *Plant Science* **114:** 11-18.

Waalkes MP. **2003.** Cadmium carcinogenesis. *Mutation Research* 107-120.

Wagner D, Przybyla D, Camp ROD, Kim C, Landgraf F, Lee KP, Wursch M, Laloi C, Nater M, Hideg E, Apel K. **2004.** The genetic basis of singlet oxygen-induced stress responses of *Arabidopsis thaliana*. *Science* **306:** 1183-1185.

Wagner GJ. **1993.** Accumulation of cadmium in crop plants and its consequences to human health. *Advances in Agronomy* **51:** 173-212.

Waisberg M, Joseph P, Hale B, Beyersmann D. **2003.** Molecular and cellular mechanisms of cadmium carcinogenesis. *Toxicology* **192:** 95-117.

Weber M, Harada E, Vess C, Roepenack-Lahaye E, Clemens S . **2004.** Comparative microarray analysis of *Arabidopsis thaliana* and *Arabidopsis halleri* roots identifies nicotianamine synthase, a ZIP transporter and other genes as potential metal hyperaccumulation factors. *Plant Journal* **37:** 269-281.

Welch RM. **1995.** Micronutrient Nutrition of Plants. *Critical Reviews in Plant Sciences* **14:** 49-82.

White PJ. **2000.** Calcium channels in higher plants. *Biochimica et Biophysica Acta-Biomembranes* **1465:** 171-189.

Williams LE, Pittman JK, Hall JL. **2000.** Emerging mechanisms for heavy metal transport in plants. *Biochimica et Biophysica Acta-Biomembranes* **1465:** 104-126.

Wójcik M, Tukiendorf A. **2004.** Phytochelatin synthesis and cadmium localization in wild type of *Arabidopsis thaliana*. *Plant Growth Regulation* **44:** 71-80.

Wójcik M, Tukiendorf A. **2005.** Cadmium uptake, localization and detoxification in *Zea mays*. *Biologia Plantarum* **49:** 237-245.

Wójcik M, Vangronsveld J, D'Haen J, Tukiendorf A. **2005.** Cadmium tolerance in *Thlaspi caerulescens* - II. Localization of cadmium in *Thlaspi caerulescens*. *Environmental and Experimental Botany* **53:** 163-171.

Xiang CB, Oliver DJ. **1998.** Glutathione metabolic genes coordinately respond to heavy metals and jasmonic acid in *Arabidopsis*. *Plant Cell* **10:** 1539-1550.

Xu XJ, Hu XY, Neill SJ, Fang JY, Cai WM. **2005.** Fungal elicitor induces singlet oxygen generation, ethylene release and saponin synthesis in cultured cells of *Panax ginseng* C. A. Meyer. *Plant and Cell Physiology* **46:** 947-954.

Zellnig G, Zechmann B, Perktold A. **2004.** Morphological and quantitative data of plastids and mitochondria within drought-stressed spinach leaves. *Protoplasma* **223:** 221-227.